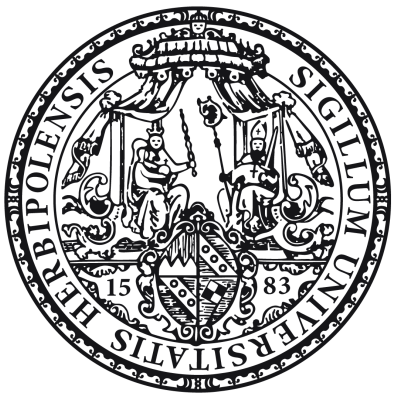

Multifunctional Hyaluronic Acid / Poly(glycidol) Hydrogels for Cartilage Regeneration Using Mesenchymal Stromal Cells

–

Multifunktionale Hyaluronsäure / Poly(glycidol) Hydrogele für die Knorpelregeneration mit Mesenchymalen Stromazellen

Dissertation zur Erlangung des naturwissenschaftlichen Doktorgrades der Graduate School of Life Sciences, Julius-Maximilians-Universität Würzburg, Klasse Biomedizin

Vorgelegt von
Thomas Böck
aus Schwäbisch Hall

Würzburg 2017

Eingereicht am: _____

Mitglieder des Promotionskomitees:

Vorsitzender: Prof. Dr. Thomas Dandekar

1. Betreuer: Prof. Dr. Torsten Blunk

2. Betreuer: Prof. Dr. Norbert Schütze

3. Betreuer: Dr. Jörg Teßmar

Datum des Promotionskolloquiums: _____

Doktorurkunden ausgehändigt am: _____

Contents

List of Figures

List of Tables

Part I

Introduction

Chapter 1

Introduction

1.1 Structure and Function of Cartilage

Native cartilage tissue accommodates solely one type of cell, the chondrocyte. According to the function and location in the human body, three types of cartilage tissues can be distinguished: hyaline cartilage, fibrocartilage, and elastic cartilage. Each type is composed of a specialized, characteristic extracellular matrix (ECM). Hyaline cartilage, in particular, articular cartilage is avascular and lacks neural and lymphatic supply, limiting thereby its capacity to heal and self-renew. Articular cartilage exhibits a zonal organization into a superficial, middle, deep and calcified zone. These zones differ in collagen organization, chondrocyte morphology and matrix composition (Figure 1.1) [1, 2]. This zonal-specific organization of collagens and their interaction with proteoglycans lead to the excellent viscoelastic shear stress response of articular cartilage [3]. Exemplarily, the compressive modulus of bovine articular cartilage changes significantly with depth from the articular surface and ranges from 0.079 MPa to 2.10 MPa [4]. These mechanical properties illustrate the main functions of articular cartilage which are, on the one hand, the protection of bone surfaces in joints, and on the other hand, to guarantee smooth and fluent joint movement in heavy weight bearing regions, such as hip or knee. Thus the ability of cartilage to resist high cyclic loadings, showing little or no signs of damage or durable deformation is unique [5].

Water is, with 60–80 %, the most abundant molecule in the ECM of articular cartilage and contributes mainly to the compression stability of this tissue. Collagen type II is the predominant protein, with 15–22 % in hyaline cartilage, and contributes through its network-like organization, facilitated by type IX and XI collagens, to the stiffness of cartilage [6]. With up to 10 % aggrecan, a proteoglycan, is the third most frequent

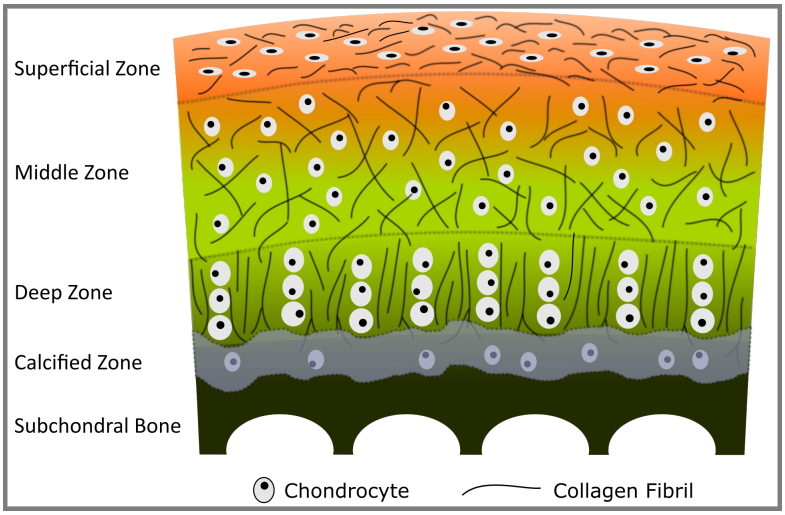

Figure 1.1: Schematic diagram showing the zonal organization and collagen structure of articular cartilage. Redrawn and simplified from references [1, 2].

molecule in the cartilage ECM and plays a key role in cartilage water balance. Owing to the highly negative charge of the attached glycosaminoglycans (GAG), aggrecan draws water into the cartilage ECM [2, 7]. The ability to form large multimolecular aggregates, together with hyaluronic acid (HA) and the link protein, aggrecan connects the ECM via a non-covalent mechanism and contributes significantly to the mechanical stability of articular cartilage [7, 8].

1.2 Cartilage Development

During cartilage development, an interplay of cellular interactions, growth factors, ECM remodeling and profound changes in cellular phenotype take place. In early limb development, cartilage formation is a major event and cells from the mesenchymal origin are recruited to the places of limb development [9–11]. In a first step, mesenchymal stromal cells (MSCs) begin to proliferate and condensate, establishing cell-cell interactions, among other things via N-cadherin signaling [12]. Additionally, type-specific integrins mediate cell-matrix interactions to newly produced ECM molecules, like collagen I and fibronectin [13, 14]. N-cadherin expression persists at the aggregating edge region of condensating cells and slightly diminishes in the differentiating center. When cells proceed towards a more differentiated state, N-cadherin expression is reduced [15]. Experimental evidence suggests that disruption of N-cadherin signaling during the condensation step of chondrogenesis leads to an inhibition of this process [16]. Transforming growth factor-β

(TGF-β)-mediated chondrogenesis of mesenchymal progenitor cells involves the coordinated cross-talk of N-cadherin, mitogen-activated protein kinase and Wnt signaling [17]. Similarly, complex interactions of the growth factors fibroblastic growth factor-2 (FGF-2), TGF-β and bone morphogenic proteins (BMP) and depending signaling cascades are essential during condensation phase [10, 12, 18]. Studies have shown that TGF-β is fundamental for the induction of chondrogenesis in the digits of the developing chick limb autopod, and together with BMPs, directs controlled cartilage development [19]. The addition of TGF-β1 as cell culture supplement facilitated MSC chondrogenesis reproducible and has been identified as a crucial factor for the sustainability of chondrogenic differentiation *in vitro* [20].

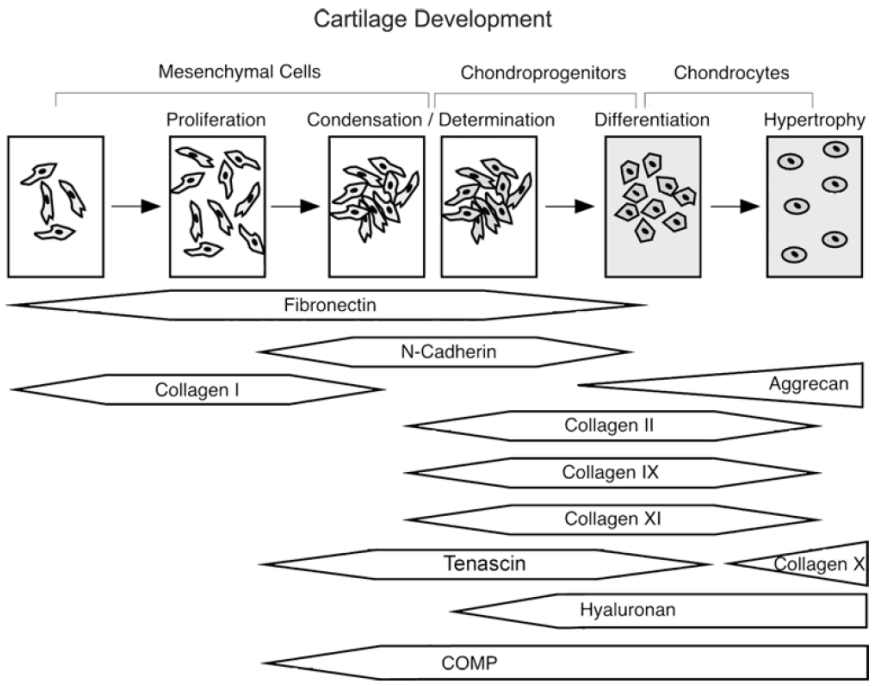

Figure 1.2: Schematic diagram showing the progression of mesenchymal stromal cells into chondrocytes, and the accompanying alterations in cell morphology and phenotype and in the structure and organization of the surrounding ECM. Reprinted from reference [12] with permission from John Wiley and Sons.

By committing to a chondroprogenitor state, the condensing cells begin to produce more cartilage-specific ECM components, e.g. collagen types II, IX and XI and also hyaluronic acid [12]. Concomitantly with increasing collagen II production, a shift in integrin expression patterns to a collagen type II-specific integrin occurs [14]. Furthermore, a key transcription factor of chondrogenesis, sex determining region Y-box 9 (Sox9),

is upregulated upon induction of chondrogenesis. The determining role of Sox9 in chondrogenesis has been shown for example as its expression predicts and correlates with the expression of *Col2a1* gene [21]. In a mouse model, the expression of Sox9 has been shown to be upregulated before the deposition of cartilage, suggesting that Sox9 is involved in initiating chondrogenic differentiation [22]. When the chondroprogenitor cells reach the differentiation state, becoming mature chondrocytes, the expression and production of the previously mentioned collagens reach their top level. Equally, aggrecan expression increases as chondrocytes differentiate and become hypertrophic [12]. As terminally differentiated chondrocytes become hypertrophic, their expression of articular cartilage-specific collagens decreases and the production of collagen X begins, a process that is accompanied by massive ECM remodeling. Finally, this phenotypical change leads to the formation of bone tissue which is a normal process during limb development, as well as bone morphogenesis (Figure 1.2 on page 5) [2, 9].

1.3 Clinical Approaches for the Treatment of Cartilage Defects

While generally, osteoarthritis can develop in any joint, it mainly affects the articular cartilage in hands, hips, knees and feet. Epidemiological studies conducted in the US show that 27 million people suffer from osteoarthritis [23]. The incidence of osteoarthritis correlates largely with advancing age. However, other risk factors remain elusive [23, 24].

Cartilage defects are graded routinely using the Outerbridge classification (Grade 0: normal cartilage, Grade I: cartilage with softening and swelling, Grade II: fissures on the cartilage surface that do not exceed 1.3 cm in diameter, Grade III: like grade II, but in an area with a diameter more than 1.3 cm, Grade IV: erosion of cartilage down to the subchondral bone) [25]. Patients with grade III and IV defects are often considered to need surgery [26, 27]. In the course of the last decades, various treatments for patients with articular cartilage defects have been developed, further improved and optimized. Broadly, these therapy concepts can be distinguished in cell-free and cell-based approaches.

1.3.1 Cell Sources for Cell-based Cartilage Tissue Engineering

The starting point of almost all cell-based cartilage tissue engineering approaches is the extraction of tissue from the patient, followed by isolation and *in vitro* expansion of the extracted chondrocytes. Subsequently, the expanded chondrocytes are seeded onto an appropriate scaffold and cultured *in vitro* for different periods of time (Table 1.1).

Finally, the tissue engineered constructs are implanted into the patients' cartilage defect. One major challenge almost all cell-based approaches are dealing with is the inevitable dedifferentiation of passaged chondrocytes. Along with dedifferentiation, it is known that chondrocytes change their rounded morphology to a more fibroblastic phenotype. Concomitantly, the expression and production of hyaline cartilage-specific ECM molecules, like type II collagen, decreases [28]. A general change in the gene expression profile can be seen for cultured chondrocytes, affecting e.g. BMP- and ERK-signaling [29]. Overall, the longer chondrocytes are kept under 2D culture conditions *in vitro*, the more they lose their chondrogenic potential [30]. Importantly, the chondrocyte supply in the body is very limited and the concerns regarding donor site morbidity must also be considered.

Thus, taking these issues with chondrocytes into account, mesenchymal stromal cells (MSCs) represent an alternative cell source for cell-based cartilage regeneration. MSCs can be gained in larger amounts from various sources of tissue, without the problem of donor site morbidity in the affected joint. MSCs can be isolated from adipose tissue [31], bone marrow [32], synovium [33], peripheral blood [34], etc. [35, 36]. Another advantage of MSCs is their pluripotency, enabling MSCs to differentiate into different lineages of cells. Besides being able to differentiate along the chondrogenic lineage [20, 32, 37], their multilineage differentiation potential allows MSCs to differentiate into several tissues, including adipose [32, 38, 39], bone [32, 40], muscle [41, 42], tendon [43, 44] and stroma [45, 46], making them a promising cell source for diverse tissue engineering approaches. Despite these favorable features, as of yet MSCs have not been used routinely in clinical tissue engineering approaches for the treatment of cartilage defects.

1.3.2 Scaffold-free Clinical Approaches

Current approaches aiming at the treatment of severe cartilage defects include for example bone marrow-stimulating microfracture, mosaicplasty with autologous or allogeneic osteochondral grafts [47], as well as cell-based autologous chondrocyte implantation (ACI), which was first reported by Brittberg in 1994 [48]. However, all of these surgical approaches do not result in sufficient healing of injured cartilage. While the level of patient satisfaction after microfracture treatment is high for several years [49], the formation of biomechanically insufficient fibrocartilage in the defect region leads still to unsatisfying long-term results [50, 51]. Compared to microfracture, mosaicplasty appears beneficial on pain release of patients in medium-term outcomes [52], yet a study by Bentley et al., in 2012, showed a high repair failure rate of 55 % for patients receiving mosaicplasty [53]. Another disadvantage of this method relates to the need for autologous

osteochondral grafts that have to be isolated from patients' remaining healthy tissue [47]. Thereby, additional defects are created in the already damaged joint, and hence donor site morbidity is enhanced. Another frequently used technique is ACI. Here, autologous chondrocytes are surgically harvested and subsequently expanded in cell culture *in vitro*. Finally, cells are re-implanted into the cartilage defect and covered with a periosteal flap in a second surgery [25]. Failure rates for this technique are in a low range, from 1.5–10 % [53, 54]. Mainly delamination and hypertrophy are reported [54]. Other studies showed that just 15–25 % of patients built up hyaline-like cartilage after surgery, while the defects in the remaining patients were filled with biochemically and mechanically less stable neo-cartilage [55, 56]. Since its introduction into the clinics, ACI has undergone many modifications to improve clinical outcomes. Besides the exchange of the periosteal flap with a collagen membrane [54], cell-carrying matrices are now being used to enhance mechanical integrity and to support tissue re-growth by the implanted chondrocytes (matrix-induced autologous chondrocyte implantation - MACI). These new strategies will be discussed in more detail in Section 1.3.3.

Scaffold-free approaches, like Chondrosphere® [57] and RevaFlex™ [58, 59], formerly named DeNovo NT®, have already shown their efficacy in clinical studies, however, long-term efficacy still needs to be evaluated. While Chondrosphere® uses autologous chondrocytes [57], RevaFlex™ applies allogenic, juvenile chondrocytes which are known for their superior proliferative and matrix production capabilities [60, 61]. Chondrosphere® constructs are spheroids consisting of chondrocytes, and their corresponding secreted matrix in a size ranging from 500 µm to 800 µm diameter which are afterwards injected into the defect site. RevaFlex™, on the other hand, is an up to 2.2 cm to 2.5 cm diameter sized disc-shaped chondrocyte-matrix construct that is cut into the desired size prior to implantation [62].

1.3.3 Cell- and Scaffold-based Clinical Approaches

Recently, Huang et al. extensively reviewed chondrocyte- and scaffold-based implants for cartilage repair that are currently used in clinical approaches [62]. The presently used products are, e.g. BioCart™II, Bioseed®-C, CaReS®, Cartipatch®, Hyalograft® C, INSTRUCT, NeoCart®, NOVOCART® 3D and MACI (Table 1.1).

The majority of the listed products follow the traditional concept of cartilage tissue engineering and are thus facing the issue of dedifferentiation of passaged chondrocytes (Section 1.3.1). Apart from the CaReS® and INSTRUCT systems, which use primary cells, all other products use chondrocytes at varying passage numbers (Table 1.1). While

INSTRUCT and CaReS® use primary cells, and circumvent the problem of chondrocyte dedifferentiation, they have the disadvantage of having only a limited number of cells, since the amount of healthy cartilage that is used for isolation of chondrocytes in the affected joint has to be kept low to avoid donor site morbidity.

Table 1.1: Overview of the currently used cell- and scaffold-based tissue engineered cartilage products and their scaffold material. Adapted in part from [62] with permission from Elsevier, for a more detailed listing please refer to the mentioned literature.

Product	Chondrocytes	Scaffold Material
BioCart™II	Autologous, unspecified passage	Freeze-dried fibrin/hyaluronic acid
Bioseed®-C	Autologous, unspecified passage	Polyglactin 910/poly-*p*-dioxanone, fibrin carrier
CaReS®	Autologous, primary	Type I collagen hydrogel
Cartipatch®	Autologous, up to P3	Agarose-alginate hydrogel
Hyalograft® C	Autologous, up to P3	Non-woven mesh of hyaluronic acid-based microfibers
INSTRUCT	Autologous, primary chondrocytes + bone marrow	Poly(ethylene oxide-terephthalate)/poly(butylene terephthalate) 3D printed scaffold
MACI	Autologous, P1–P3	Type I/III collagen scaffold from porcine peritoneum
NeoCart®	Autologous, unspecified passage	Honeycomb bovine type I collagen scaffold, collagen hydrogel carrier
NOVOCART® 3D	Autologous, P1	Bilayer type I collagen sponge containing chondroitin sulfate

Some of the currently available clinically used scaffolds are made of biopolymers, e.g. collagen type I and III, fibrin, hyaluronic acid, chondroitin sulfate and agarose. Additionally, synthetic polymers, like polyglactin 910/poly-*p*-dioxanone and poly(ethylene oxide-terephthalate)/poly(butylene terephthalate) (PEOT/PBT), are utilized (Table 1.1).

Most of the stated scaffolds are macroporous, except the rather microporous hydrogel-based scaffolds CaReS® and Cartipatch®. Due to their architecture, it is more challenging to distribute cells evenly throughout macroporous scaffolds. Hence, the seeding efficiency of this kind of scaffold needs to be laboriously optimized and has to be ensured with the help of special tools or material characteristics. In order to secure sufficient seeding with chondrocytes, for example, the biphasic NOVOCART® 3D system utilizes a cell-impermeable layer derived from bovine pericardium for cell retention [63]. Similarly, the MACI system exhibits an organization into two layers, with a more porous and a

denser layer to achieve satisfying seeding efficiencies [64]. In comparison, hydrogels, like Cartipatch® and CaReS®, are fairly easy to load with cells. Prior to gel casting, cells are resuspended in a gel solution or a buffer and are thereby homogeneously distributed throughout the gel. Thus, to ensure sufficient seeding, NeoCart® and Bioseed®-C use collagen [65] or low melting point-agarose [66] gels as cell carriers.

While some of the products mentioned above already have shown their general suitability in clinical trials, a Cartipatch® study showed that surgical outcomes were significantly worse after treatment compared to mosaicplasty for osteochondral defects of the femur [67]. Notably, Hyalograft® C and MACI are not any longer available on the market. Others, like INSTRUCT, BioCart™II or NeoCart®, do not provide sufficient long-term study data until today for a final evaluation [62]. By these facts, it becomes obvious that the presently employed clinical cartilage tissue engineering approaches are not yet sufficiently developed. They may rather serve as a good starting point since none of the previously mentioned scaffolds combines biomimetic cues together with the specific delivery of growth factors for cartilage tissue engineering.

1.4 Hydrogels for Cartilage Tissue Engineering

The application of hydrogels may more likely serve the needs for an efficient cell-based treatment of cartilage defects. Although hydrogels lack the mechanical properties of stiff scaffolds, the usage of this scaffold type has several advantages. Due to direct cell encapsulation, the seeding efficiency is high, and the seeding procedure is straightforward, resulting in a homogeneous cell distribution. Additionally, hydrogels can be used for the delivery of sensitive molecules (e.g. bioactive peptides, growth factors, and DNA) and the supply of encapsulated cells with oxygen, nutrients, and supplements is excellent since hydrogels exhibit a high permeability for liquids. Several, different materials in various modifications are currently used for cartilage tissue engineering approaches, highlighting the versatility of this concept. Apart from protein-, polysaccharide- or protein/polysaccharide-based hydrogels or chemically modified proteins and polysaccharides, also a vast amount of synthetic polymers or hybrids of biopolymers and synthetic polymers (composite hydrogels) are currently investigated (Table 1.2). Furthermore, it is easy to implement tissue-specific functionalizations with biomimetic peptides for cell adhesion, with growth factors, or with both, making them a promising material for tissue engineering approaches [68–72]. Therefore, the application of hydrogels will create opportunities to tailor scaffolds selectively for the needs of the chondrogenic niche.

Table 1.2: Overview of the currently used polymers for hydrogel-based cartilage tissue engineering. For reasons of simplicity, the variety of chemically modified polysaccharides and proteins that are also employed are not listed in this table [68–72].

Polysaccharide	Protein	Synthetic
Agarose	Collagen	Poly(ethylene glycol) derivatives
Alginate	Fibrin	Poly(2-hydroxyethyl methacrylate)
Chitosan	Silk	Poly(2-hydroxypropyl methacrylate)
Cellulose	Gelatin	Poly(N-isopropylacrylamide)
Chondroitin sulfate	Laminin	Poly(vinyl alcohol)
Dextran		
Gellan		
Hyaluronic acid		

Chondroitin sulfate: CS, Hyaluronic acid: HA, Poly(ethylene glycol): PEG, Poly(2-hydroxyethyl methacrylate): PHEMA, Poly(2-hydroxypropyl methacrylate): PHPMA, Poly(N-isopropylacrylamide): PNIPAm, Poly(vinyl alcohol): PVA.

1.4.1 Hyaluronic Acid-based Hydrogels for Cartilage Tissue Engineering

The materials listed in Table 1.2 are either permissive to MSC chondrogenesis, like agarose or PEG, or they directly support chondrogenesis by providing cartilage-specific cell attachment sites or by retaining growth factors in the hydrogel network. Most of the presently used materials are, however, not overly cartilage-specific, and lack cartilage-like ECM molecules and signals. In contrast to that, HA as an integral part of native cartilage inherently provides recognition sites for the cellular receptors CD44 [73] and CD168 (Receptor for Hyaluronan Mediated Motility: RHAMM) [74]. These features allow for MSC attachment and migration and may, therefore, be more favorable for cartilage tissue engineering approaches. Due to its excellent biocompatibility HA has been already used for the treatment of OA [75] and thermosensitive injectable hyaluronic acid copolymer hydrogels have been shown feasible for adipose tissue engineering [76]. Another important feature of HA is its high suitability for physical and chemical modifications, as mirrored by the use of thiol-, haloacetate-, dihydrazide-, aldehyde- and tyramine-modified HA for various tissue engineering approaches [77].

Photo-cross-linked methacrylated HA hydrogels are primarily used for cartilage tissue engineering. This kind of HA gel is prepared by adding a methacrylate group to the hyaluronic acid backbone followed by UV cross-linking [78, 79]. Burdick et al. were able to show that photoencapsulated fibroblasts in HA/poly(ethylene glycol) dimethacrylate (PEGDM) hydrogels remained viable under low macromer concentrations, while viability decreased gradually as the concentration of macromer was increased [80]. Composite gels

using fibrin and hyaluronic acid also exhibited a beneficial outcome for cartilage-like tissue formation by chondrocytes compared to pure fibrin gels [81]. A photo-cross-linked HA hydrogel, composed of the terminally modified cross-linker poly(ethylene glycol) diacrylate (PEGDA) and methacrylated (Me) HA (MeHA), displayed the general suitability of this material for MSC chondrogenesis. Compared to the biologically more inert PEGDA hydrogels, MSCs cultivated in MeHA gels showed enhanced chondrogenesis *in vitro* and *in vivo* [82].

Future strategies in cartilage tissue engineering, and thus for the development of materials and scaffolds for the treatment of cartilage defects, aim to recapitulate the native steps in cartilage development and to thereby achieve improved treatment options for cartilage injuries [83, 84]. Also, hydrogels that incorporate and combine cues of matrix-cell and cell–cell interactions, combined with the effect of locally administered growth factors delivery may enhance the chondrogenic potential of hydrogels.

1.4.2 Biomimetic Hydrogels for Cartilage Tissue Engineering

Apart from the generation of HA composite hydrogels, which combine the advantages of easily and controlled modifiable synthetic polymers such as PEG and derivatives of HA, the incorporation of bioactive peptides and growth factors has emerged as a powerful functionalization tool. The integration of peptides enables cell-induced degradation of hydrogels and improves the biocompatibility of hydrogels [68, 70, 71, 85]. PEG derivatives are frequently chosen for this approach, due to their hydrophilicity, excellent biocompatibility, and easy modifiability. In this way, modified PEG hydrogels are capable of supporting and guiding cell growth and differentiation appropriate for the desired tissue type [85].

One drawback in the use of pure PEG gels for tissue engineering approaches is their lack of cell-specific adhesion sites. Other limitations of both linear and branched PEG polymers arise due to their accessible sites of chemical modification, which are restricted to the distal endings of PEG polymer chains, making alternative polymers with similar characteristics (hydrophilic, biocompatible, chemically easily modifiable) but more functionalization sites desirable.

To overcome the bioinert related limitations of PEG, the cell adhesion sequence RGD, derived from fibronectin [86], is commonly used for surface modification of PEG-acrylate hydrogels to enhance biocompatibility [87, 88]. It could further be shown that incorporation of a cyclic RGD peptide enabled endothelial cells to adhere and spread on a PEGDA hydrogel. Cells grown on these gels showed elevated cell growth as compared

to linear RGD-modified hydrogels [87]. The introduction of the laminin-derived IKVAV [89] and YIGSR [90] peptide sequences into PEG hydrogels improved the function of β-cells [91] or permitted preadipocyte adherence and proliferation on a PEGDA scaffold [92]. Other cell-adhesive modifications used in hydrogels are for example the introduction of collagen I-derived peptides DGEA [93, 94], and GFOGER [95, 96]. MSCs photo-encapsulated in a collagen mimetic peptide-conjugated poly(ethylene oxide) diacrylate (CMP/PEODA) hydrogel produced higher glycosaminoglycan and collagen contents as compared to pure PEODA hydrogels after three weeks of *in vitro* culturing [97].

A cartilage ECM-specific peptide that has been incorporated into PEG hydrogels is the decorin-derived collagen II-binding sequence KLER. Interestingly, it was found that leucine-rich-repeat regions in decorin connect neighboring collagen molecules in the fibril, thus helping to stabilize and organize the collagen fibrils and direct fibrillogenesis in the cartilage ECM [98]. Incorporation of 1 mM RGD and 5 mM of KLER-peptide into 10% PEGDA hydrogels enhanced cartilage-specific matrix deposition relative to modification with 1 mM RGD and 5 mM of a scrambled LKRE-peptide [99].

As mentioned in Section 1.2 on page 4, MSC cell-cell interactions are established via N-cadherin molecules during the condensation phase and are crucial for initiating cartilage development [12]. By coupling 1 mM of a HAV peptide, which mimics the extracellular domain of N-cadherin [100], to the MeHA backbone of a photo-cross-linked hydrogel, Bian et al. demonstrated the positive effect of this peptide on chondrogenic differentiation of encapsulated MSCs, compared to a scrambled control [101].

Additionally, a way to design and shape hydrogels to behave more bioactive and bioresponsive can be achieved by the introduction of enzyme-sensitive peptide sequences which enable controlled degradation. By this, apart from the hydrolysis of ester linkages, which is relatively slow, photo-cross-linked PEGDA and thiol-ene hydrogels can be additionally tuned and customized with regard to their degradation rate. Such enzymatically degradable peptides are often sensitive to cell-secreted matrix metalloproteinases (MMPs) [102]. Notably, in a PEG hydrogel system, the introduction of a MMP-sensitive peptide and the GFOGER peptide improved the deposition of cartilage-specific ECM components and profoundly changed cytoskeletal morphology [96].

Another possibility to tailor hydrogels towards more biomimetic traits is to selectively control the application of bioactive molecules, e.g. growth factors, for cartilage tissue engineering. Several strategies have been established to administer growth factors, either as a shuttle for drug delivery into cartilage defect sites or tissue engineering approaches *in vitro* and *in vivo* [103–105]. In general, growth factors are mainly included based on three different concepts: a) Incorporation into microspheres for use as cell culture

supplements *in vitro* [106, 107] or by direct injection into the desired regeneration sites [108, 109]. b) Microsphere incorporation into scaffolds [110–113]. c) Direct tethering to scaffolds [114, 115]. For other possible protein delivery strategies using hydrogels, the reader is referred to an extensive review by Censi et al. [103].

As discussed above, growth factor modification of hydrogels is a potentially powerful tool to improve the regenerative potential of hydrogels *in vivo*. Thiol-Michael addition or thiol-ene click chemistry offers an elegant way to accomplish the covalent incorporation of growth factors into hydrogels and to thereby enhance their chondro-inductive capability. For example, polymers and proteins containing primary amine groups, such as TGF-β1, can easily be thiol-functionalized by reacting primary amines, which could be provided by the amino acid lysine, with 2-iminothiolane (Traut's reagent). The latent form of TGF-β1 has already been modified using Traut's reagent, and covalently incorporated into a HA hydrogel. Indeed, this incorporation resulted in increased chondrogenic activity of incorporated chondrocytes compared to negative controls [116]. Similarly, McCall et al. used Traut's reagent to incorporate TGF-β1 covalently into pure PEGDA hydrogels. Here, MSCs were encapsulated in hydrogels with and without tethered TGF-β1 and cultured *in vitro* for 21 days. MSCs cultured in gels with tethered TGF-β1 reached levels of chondrogenesis that were comparable to a positive control, cultured in medium containing soluble TGF-β1 [117]. The same research group obtained comparable results for encapsulated chondrocytes in a follow-up study [118]. So far, all experiments addressing the effect of covalently incorporated TGF-β1 on chondrogenesis solely compared the effect of tethered growth factor with the *in vitro* gold standard for chondrogenesis, soluble TGF-β1 in culture medium. Experiments comparing the effect of covalently bound growth factors with the impact of locally administered, but not covalently bound growth factors, however, have as of yet not been performed.

Collectively, PEG derivatives represent highly suitable polymers for the introduction of biological modifications into hydrogels. They are widely used as the basis for hydrogel generation, or in combination together with biopolymers in composite hydrogels since they are easily and highly modifiable [85]. However, due to their chemical nature and organization, the modifiability is limited to their terminal binding sites, compromising their ability to generate hydrogel networks, e.g. after peptide modification, which can just be overcome by an increase of initially used PEG molecules. Thus, more versatile, multi-functional surrogate polymers appear desirable, which may be used as an alternative basis or as cross-linker for the generation of hydrogels. Poly(glycidol)s (PG) might serve as such surrogate polymers since they are, like PEG, hydrophilic and water soluble, and possess excellent biocompatibility, rendering them promising synthetic polymers for biomedical

applications [119, 120]. Moreover, being a structural analog to PEG, PG additionally exhibits at each repeating unit a hydroxymethylene group that enables multifunctionalization [121, 122]. Exemplarily, linear PG with cross-linkable thiol-functionalized side-chains has been used successfully for hydrogel encapsulation of L929 mouse fibroblasts and showed high rates of viable cells [123]. Employing PG as a cross-linking polymer may provide a high cross-linking density and possibility for functionalization in comparison to linear and multi-arm PEG. However, despite these apparent favorable characteristics, PG so far has not been utilized in the context of cartilage regeneration. Therefore, the main point of the thesis was the biological evaluation of this versatile, multifunctional cross-linker, PG, in hydrogels for cartilage engineering. The application of side-chain-modified PG would enable to study the impact of multifunctional PG, together with incorporated biomimetic peptides and covalently tethered growth factors, in a hydrogel consisting of a natural polymer, e.g. hyaluronic acid, on MSC chondrogenesis.

Chapter 2

Goals of the Thesis

Over the last decades, many developments and novel therapeutic options for the treatment of cartilage defects emerged and improved the clinical outcome for patients. However, considering the currently available hydrogel-based treatments of defects, it becomes obvious that the research and development of clinically usable cartilage-specific materials are still at the very beginning [62]. Many different hydrogel-based approaches are in the pipeline and are intensively researched in laboratories, as already introduced in Section 1.4 on page 10, but new, highly modifiable polymers and materials appear desirable.

Therefore, the aim of the thesis was to initially establish a HA-based hydrogel system, cross-linked with a multifunctional polymer, PG, as an alternative to PEG. In comparison to PEG derivatives the utilization of PG as cross-linker could allow a higher cross-linking density and additional options for biomimetic functionalization. In spite of these advantages, PG has not yet been applied for cartilage engineering until now. Subsequently, biomimetic functionalization was either introduced by incorporation of biomimetic peptides or growth factors into the hydrogel. In a proof-of-principle experiment, the usability of the multifunctional polymer was evaluated in another hydrogel system. Finally, the effect of the zonal distribution of cells in a system consisting of two differently composed hydrogels was investigated in a pilot experiment.

Hence, the thesis can be divided into four major sections:

1. The establishment and optimization of a HA-based hydrogel system for MSC chondrogenesis, through variation of the cross-linker amount and the cross-linker type (PEG, PG).

2. The biomimetic functionalization of the PG-Acr cross-linked HA hydrogels with biomimetic peptides and growth factors and their extensive biological evaluation.

3. The investigation of the general suitability of a pure PG-based hydrogel system, consisting of a bioinert polymer for the evaluation of the effects of single biomimetic peptides on chondrogenesis.

4. The generation of a zonal hydrogel, employing HA and PG, for cartilage tissue engineering.

1. The establishment and optimization of a HA-based hydrogel system for MSC chondrogenesis, through variation of the cross-linker amount and the cross-linker type (PEG, PG).

In order to generate a suitable niche for chondrogenic differentiation of MSCs a commercially available thiol-modified HA (Glycosil®, HA-SH) [124, 125] was used as the basis for the hydrogels, since HA is an integral part of cartilage, and provides natural adhesion sites for MSCs. In the initial phase PEGDA, a frequently used PEG derivative with two terminal acrylates [85], served as cross-linker for HA-SH using Michael addition [124, 126]. After determination of the ideal PEGDA amount (Section 5.1.2), the effects of a 4-arm branched PEGTA on chondrogenesis regarding ECM deposition were evaluated qualitatively and quantitatively (Section 5.1.3). Since the main focus of the thesis was the introduction of a multifunctional, versatile cross-linker for MSC chondrogenesis for the generation of more complex HA-based hydrogels, the application of acrylate-modified PG (PG-Acr) as cross-linker was evaluated on histological and biochemical levels with regard to deposition of GAGs and collagens (Section 5.1.3).

2. The biomimetic functionalization of the PG-Acr cross-linked HA hydrogels with biomimetic peptides and growth factors and their extensive biological evaluation.

The influence of biomimetic functionalization on the chondrogenic potential of MSCs within PG-Acr cross-linked HA-SH gels (Glycosil®, HA-SH) was assessed next. For this purpose, the gels were initially functionalized with cysteine-modified peptides, by coupling peptides to PG-Acr, resembling cartilage ECM or by mimicking steps in cartilage development, by imitating cell-cell interactions. The HAV motif, a N-cadherin mimetic sequence, and the collagen II binding sequence KLER already have shown their potential to enhance MSC chondrogenesis in other studies [99, 101]. The cell adhesion sequence RGD was shown to have a positive impact on MSC viability in PEG-hydrogels [88]. Hence, the impact of these peptides on MSC chondrogenesis was investigated histologically and biochemically (Section 5.2.1).

Furthermore, growth factor modification with TGF-β1 may enhance the chondrogenic

and, thus, clinical potential of the newly developed materials. It has been demonstrated that co-delivery of chondrogenic factors and cells within hydrogels can be beneficial for induction of *in vivo* chondrogenesis of MSCs after implantation [111]. Usually, TGF-β1-supplemented medium is used during *in vitro* chondrogenesis of MSCs, and repeated administration of the growth factor with every change of medium is needed to generate robust chondrogenic differentiation of MSCs. The covalent incorporation of TGF-β1 would thereby eliminate this necessity. Thus, TGF-β1 was thiol-modified with Traut's reagent, and different amounts were covalently bound to the cross-linker PG-Acr and compared to gels in which TGF-β1 was merely mixed into (Section 5.2.2).

3. The investigation of the general suitability of a pure PG-based hydrogel system, consisting of a bioinert polymer for the evaluation of the effects of single biomimetic peptides on chondrogenesis.

In a proof-of-principle experiment, the general usability of pure PG gels for chondrogenic differentiation of MSCs, without the supportive background of HA, was investigated. This inert hydrogel system may enable the controlled investigation of the effects of single peptides. The gels were cross-linked by the utilization of UV-mediated thiol-ene reaction, and a cysteine-modified peptide was coupled to allyl-functionalized PG (P(AGE/G)), and simultaneously a thiolated PG (PG-SH) component was cross-linked with P(AGE/G). Again, the HAV motif was used as an example peptide to modify pure PG gels, while a scrambled peptide and an unmodified gel served as controls (Section 5.3).

4. The generation of a zonal hydrogel, employing HA and PG, for cartilage tissue engineering.

Within the European Union Seventh Framework Programme, under grant agreement n°309962, the HydroZONES consortium aims to develop bioactive hierarchical hydrogels as zonal implants for articular cartilage repair. Since resembling the zonal organization of cartilage is considered to be an important, though widely neglected design factor for hydrogels [127, 128], in this part of the thesis, the combination of a HA-containing bottom layer and a pure PG top layer as a combined zonal gel was evaluated. In a pilot experiment, two different thiol-ene UV cross-linked hydrogels were cast on top of each other, to investigate the feasibility of a zonal hydrogel. First, MSCs were encapsulated in a HA hydrogel (HA-SH_{FMZ} was cross-linked with P(AGE/G)) and subsequently MSCs encapsulated in a pure PG hydrogel, as introduced above, were layered on top of the HA gel (Section 5.4).

Part II

Materials and Methods

Chapter 3

Materials

3.1 Instruments

Table 3.1: Overview of used instruments.

Instrument	Manufacturer	Head Office
Accu-jet® pro	Brand	Wertheim, Germany
Analytical scale	Ohaus	Zürich, Switzerland
Analytical scale XA 105	Mettler-Toledo	Columbus, USA
Centrifuge Rotina 420 R	Hettich	Tuttlingen, Germany
Centrifuge SIGMA 1-14	SIGMA Laborzentrifugen GmbH	Osterode, Germany
CO_2 Incubator	IBS Integra Biosciences	Fernwald, Germany
Cryostat CM 3050S	Leica	Wetzlar, Germany
FluorChem FC2 Imager	Alpha Innotec	San Leandro, USA
Electrophoresis- and blotting chamber	Bio-Rad	München, Germany
Hemocytometer Neubauer	Paul Marienfeld GmbH	Lauda, Germany
Laminar flow box Typ-HS18	Heraeus	Hanau, Germany
Laminator	Severin	Sundern, Germany
Orbital shaker Unimax 1010	Heidolph	Schwabach, Germany
Mastercycler® Gradient	Eppendorf	Hamburg, Germany
Magnetic stirrer	VWR	Darmstadt, Germany
Microscope BX51/DP71 camera	Olympus	Hamburg, Germany
Microscope IX51/XC30 camera	Olympus	Hamburg, Germany

Table 3.1: Overview of used instruments: continued.

Instrument	Manufacturer	Head Office
Mini-PROTEAN® Tetra Cell System	Bio-Rad	München, Germany
MRX microplate reader	Dynatech Laboratories	Chantilly, USA
NanoDrop 2000c spectrophotometer	Thermo Scientific	Waltham, USA
pH-meter HI2210	Hanna Instruments	Kehl am Rhein, Germany
Pipettes Research® Plus	Eppendorf	Hamburg, Germany
Pipette multistep	Brand	Wertheim, Germany
PowerPac® basic power supply	Bio-Rad	München, Germany
Real-Time PCR Detection System CFX96T™	Bio-Rad	München, Germany
Tecan GENios pro spectrofluorometer	Tecan	Crailsheim, Germany
TissueLyser	Qiagen	Hilden, Germany
Thermomixer comfort MTP	Eppendorf	Hamburg, Germany
Thermomixer MHR 23	DITABIS	Pforzheim, Germany
Ultrasonic homogenizer SonoPlus	Bandelin	Berlin, Germany
UV hand lamp VL-4 with filter	Hartenstein	Würzburg, Germany
Vortex, IKA® MS3 basic	IKA®	Staufen, Germany
Water bath	Memmert	Schwabach, Germany

3.2 Consumables

Table 3.2: Overview of used consumables.

Consumable	Manufacturer	Head Office
Bottle top-filter Nalgene®	Thermo Scientific	Waltham, USA
Coverslip 24 mm × 60 mm	MENZEL	Braunschweig, Germany
Cryovials CryoPure 2.0 ml	Sarstedt	Nümbrecht, Germany

Table 3.2: Overview of used consumables: continued.

Consumable	Manufacturer	Head Office
Disposable forceps ratiomed	megro GmbH	Wesel, Germany
Falcon cell strainers 100 µm	BD Biosciences	Heidelberg, Germany
Hardshell PCR plates, 96-well, thin wall	Bio-Rad	München, Germany
Microseal® 'C' Film	Bio-Rad	München, Germany
Microtome blades	Feather	Osaka, Japan
6 & 12-well plates	Greiner Bio-One	Frickenhausen, Germany
96-well plate	TPP	Trasadingen, Switzerland
96-well plate black	Thermo Scientific	Waltham, USA
Parafilm	Pechiney	Chicago, USA
PAP pen liquid blocker	Sigma-Aldrich	München, Germany
PCR-strips 8 tubes 0.2 ml	Carl Roth GmbH	Karlsruhe, Germany
PD-Tips	Brand	Wertheim, Germany
Pipette filter tips	Sarstedt	Nümbrecht, Germany
Pipette tips	Starblab	Hamburg, Germany
Pipettes serological	Greiner Bio-One	Frickenhausen, Germany
pH indicator paper	Carl Roth GmbH	Karlsruhe, Germany
Polypropylene tubes 15 ml/50 ml	Greiner Bio-One	Frickenhausen, Germany
SafeSeal micro tubes 1.5 ml/2.0 ml	Sarstedt	Nümbrecht, Germany
Sample cup PE 2.5 ml	Hartenstein	Würzburg, Germany
Scalpels	Feather	Osaka, Japan
Super Frost® plus glass slide	R. Langenbrinck	Emmendingen, Germany
Syringe Filter Minisart® 0.2 µm	Sartorius AG	Göttingen, Germany
Syringes	BD Biosciences	Heidelberg, Germany
Tissue culture flasks T175	Greiner Bio-One	Frickenhausen, Germany

Table 3.2: Overview of used consumables: continued.

Consumable	Manufacturer	Head Office
Whatman® cellulose chromatography paper	Sigma-Aldrich	München, Germany
Whatman® nitrocellulose membrane	Sigma-Aldrich	München, Germany

3.3 Chemicals

If not stated otherwise in the Materials and Methods Section, all chemicals and reagents applied for the preparation of buffers and solutions were obtained from Applichem (Darmstadt, Germany), B. Braun AG (Melsungen, Germany), Carl Roth GmbH (Karlsruhe, Germany), Merck (Darmstadt, Germany) or Sigma-Aldrich (München, Germany).

Table 3.3: Overview of used chemicals.

Chemical	Manufacturer	Head Office
Amersham™ ECL™ Prime Western Blotting Detection Reagent	GE Healthcare	Freiburg, Germany
Ambion RNaseZAP	Life Technologies	Karlsruhe, Germany
Antibody diluent, Dako REAL™	Dako	Hamburg, Germany
Aqua ad iniectabilia	B. Braun	Melsungen, Germany
Brilliant III Ultra-Fast SYBR® Green QPCR Master Mix	Agilent	Santa Clara, USA
DAPI mounting medium ImmunoSelect®	Dianova	Hamburg, Germany
Dulbecco's Phosphate-buffered saline (PBS) (-)Ca^{2+}, (-)Mg^{2+}	Gibco® Life Technologies	Karlsruhe, Germany
Distilled water (DNAse/RNAse free)	Gibco® Life Technologies	Karlsruhe, Germany
ImProm-II™ reverse transcription system Kit	Promega	Madison, USA
Life/Dead Cell Staining Kit II	PromoKine	Heidelberg, Germany

Table 3.3: Overview of used chemicals: continued.

Chemical	Manufacturer	Head Office
Microplate BCA™ Protein Assay Kit	Thermo Scientific	Waltham, USA
Novex® sharp protein standard	Life Technologies	Karlsruhe, Germany
Papain	Worthingtion	Lakewood, USA
Photoinitiator Irgacure 2959	BASF	Ludwigshafen, Germany
Phosphate buffered saline (Dulbecco A) tablets	Thermo Scientific	Waltham, USA
Proteinase K (Digest-All 4)	Life Technologies	Karlsruhe, Germany
Terralin Liquid® disinfectant	Schülke	Norderstedt, Germany
Tissucol Duo S 0.5 mL Immuno	Baxter	Deerfield, USA
Tissue-Tek® O.C.T. compound	Sakura Finetek	Zoeterwonde, Netherlands
Traut‘s reagent (2-iminothiolane)	Thermo Scientific	Waltham, USA
TRIzol® Reagent	Life Technologies	Karlsruhe, Germany
0,25% Trypsin-EDTA	Life Technologies	Karlsruhe, Germany

3.4 Antibodies

Table 3.4: Overview of used primary antibodies.

Antibody	Type/Source	Application/Dilution	Manufacturer
Anti-Aggrecan	Monoclonal IgG mouse	IHC 1:300	Thermo Scientific (Clone 969D4D11)
Anti-Collagen I	Polyclonal IgG rabbit	IHC 1:800 WB 1:1000	Abcam (ab34710)
Anti-Collagen II	Monoclonal IgG mouse	IHC 1:100 WB 1:250	Acris (Clone II-4C11)
Anti-Collagen X	Monoclonal IgG mouse	IHC 1:200	eBioscience (Clone X53)
Anti-GAPDH	Monoclonal IgG mouse	WB 1:1000	Merck (Clone 6C5)

Table 3.5: Overview of used secondary antibodies.

Antibody	Type/Source	Application/Dilution	Manufacturer
Alexa Fluor 488 anti-rabbit	Polyclonal IgG goat	IHC 1:400	Dianova (711-545-152)
Cy3 anti-mouse	Polyclonal IgG donkey	IHC 1:500	Dianova (715-165-150)
HRP anti-rabbit	Polyclonal IgG goat	WB 1:2000	Dako (P0448)
HRP anti-mouse	Polylonal IgG mouse	WB 1:1000	Dako (P0161)

3.5 Primers

Table 3.6: Overview of used qPCR primers.

Gene	Gene Symbol	Unique Assay ID	Manufacturer
Aggrecan	*ACAN*	qHsaCID0008122	Bio-Rad
Collagen I	*COL1A1*	qHsaCED0043248	Bio-Rad
Collagen II	*COL2A1*	qHsaCED0001057	Bio-Rad
Collagen X	*COL10A1*	qHsaCED0043992	Bio-Rad
GAPDH	*GAPDH*	qHsaCED0038674	Bio-Rad
TGF-β receptor 1	*ALK-5*	qHsaCID0009475	Bio-Rad
Sox9	*SOX9*	qHsaCED0021217	Bio-Rad

3.6 Peptides

All peptides were purchased from Genecust (Ellange, Luxemburg).

Table 3.7: Overview of biomimetic peptide sequences, their applied doses, and their biological function as they were introduced into the PG-Acr cross-linked HA-SH or pure PG hydrogels.

Peptide Sequence	Molarity [mM]	Biological Function
Ac-HAVDIGGGC	1, 2.5	Natural N-cadherin mimetic peptide sequence
Ac-AGVGDHIGC	1, 2.5	Scrambled N-cadherin mimetic peptide sequence
CGKLERG	5	Natural collagen type II binding site from decorin protein
CGLKREG	5	Scrambled collagen type II binding site from decorin protein
CGRGDSG	1	Cell adhesion sequence from fibronectin protein that is recognized by integrins

3.7 Hydrogel Components

Glycosil®: Commercially available thiolated hyaluronic acid (HA-SH; GS222, ESI BIO, Alameda, USA).

$HA\text{-}SH_{FMZ}$: Thiolated hyaluronic acid was synthesized at the Department for Functional Materials in Medicine and Dentistry (FMZ), University Hospital Würzburg with a M_n=1.58 MDa and 58% SH-functionality ($HA\text{-}SH_{FMZ}$; AK Groll, Würzburg, Germany).

PEGDA: Commercially available linear 2-arm poly(ethylene glycol) acrylate (PEGDA; MW=3400 Da; GS710, Glycosan Biosystems, Salt Lake City, USA).

PEGTA: Commercially available 4-arm poly(ethylene glycol) acrylate (PEGTA; MW=10 000 Da; A7068, JenKem Technology USA, Plano, USA).

PG-Acr: Linear acrylate-modified poly(glycidol) was synthesized at the FMZ with a M_n=4200 Da and 20% acrylate-functionality (PG-Acr; AK Groll, Würzburg, Germany).

P(AGE/G): Linear allyl-modified poly(glycidol) was synthesized at the FMZ with a M_n=4760 Da and 10% allyl-functionality (P(AGE/G); AK Groll, Würzburg, Germany).

PG-SH: Linear thiolated poly(glycidol) was synthesized at the FMZ with a M_n=5320 Da and 20% SH-functionality (PG-SH; AK Groll, Würzburg, Germany).

3.8 Cell Culture Media

Proliferation medium: Dulbecco's Modified Eagle's Medium/Ham's F-12 (DMEM/F12; ThermoFisher, MA) supplemented with 10% fetal bovine serum (FBS) and 1% penicillin-streptomycin (PS; 100 U/mL penicillin, 0.1 mg/mL streptomycin ThermoFisher, MA), and 5 ng/mL basic fibroblast growth factor (bFGF; BioLegend, London, UK).

Cryopreservation medium: Proliferation medium, supplemented with 10% DMSO.

Chondrogenic medium:	Dulbecco's Modified Eagle's Medium high glucose 4.5 g/L (DMEM) supplemented with 1% ITS+ Premix (Corning; NY), 40 µg/mL L-proline, 50 µg/mL L-ascorbic acid 2-phosphate sequimagnesium salt hydrate, 0.1 µM dexamethasone, 1 mM sodium pyruvate, 1% PS, and 10 ng/mL transforming growth factor-β1 (TGF-β1; BioLegend, London, UK).

3.9 Buffers and Solutions

Citric acid buffer:	25 g citric acid monohydrate, 6 mL glacial acid, 60 g sodium acetate trihydrate, 17 g NaOH, bring volume to 500 mL with ddH_2O. Add 100 mL ddH_2O, and 150 mL 2-propanol. Adjust carefully to pH 6, and store at 4 °C under toluene.
Chloramine T solution:	141 mg chloramine T, 8 mL citric acid buffer, and 1 mL 2-propanol.
DAB solution:	1.5 g p-dimethylamino-benzaldehyde (DAB), 6 mL 2-propanol, and 2.6 mL 60% perchloric acid.
DMMB solution:	16 mg dimethylmethylene blue (DMMB) is dissolved for 16 h in 5 mL absolute ethanol. Afterwards, it is added to a prepared NaCl-glycine solution, consisting of 900 mL ddH_2O, 3.04 g glycine, 2.37 g NaCl. Adjust to pH 3.0 and and bring volume to 1 L with ddH_2O.
Papain digestion buffer:	20 mL PBE buffer, 17 mg L-cysteine, 2 U/mL papain, and sterilize with a 0.2 µm syringe-filter.
PBE buffer:	6.53 g Na_2HPO_4, 6.48 g NaH_2PO_4, 10 mL 500 mM EDTA in 900 mL ddH_2O. Adjust to pH 6.5 and bring volume to 1 L with ddH_2O and sterilize with a 0.2 µm bottle top-filter.
PBS:	10 PBS (Dulbecco A) tablets in 1 L ddH_2O.
PBST:	0.1% Tween® 20 in 1 x PBS
Resolving gel buffer:	1 M Tris, adjust to pH 8.8
Running buffer:	25 mM Tris, 192 mM glycine, 0.1% SDS

Stacking gel buffer:	0.5 M Tris-HCl, adjust to pH 6.8
TEN buffer:	0.1 M NaCl, 1 mM EDTA, 10 mM Tris, adjust to pH 7.4
Transfer buffer:	25 mM Tris, 192 mM, 10% methanol
WB blocking solution:	5% nonfat dried milk powder in PBST

Chapter 4

Methods

4.1 Isolation of MSCs

Human bone marrow-derived mesenchymal stromal cells (MSCs) were isolated from surgically removed cancellous bone of patients undergoing total hip arthroplasty, with written informed consent from all patients (57 years to 77 years), and as approved by the local ethics committee. Cells were collected by repeated washing of bone debris and marrow in PBS, then centrifuged (300 *g*, 10 min), resuspended in proliferation medium, and seeded into T175 cm^2 flasks. Non-adherent cells were removed after two or three days by carefully washing with PBS, subsequently adherent cells were propagated to a subconfluent level at 37 °C, 5% CO_2 in proliferation medium. For cryopreservation of MSCs, 10% DMSO was added to the proliferation medium. For passaging, 0.25% trypsin-EDTA was used, and cells seeded at a density from 3000 cells/mL to 5000 cells/mL in T175 cm^2 flasks. Prior to hydrogel encapsulation, the cells were propagated up to passage 2 or 3.

4.2 Generation of Hydrogels

4.2.1 HA Hydrogels Generated by Michael Addition

For cell encapsulation 1.0 mL of sterile water was added to a Glycosil® (HA-SH) vial, containing 10 mg of thiol-modified hyaluronic acid. Afterwards, the HA-SH was allowed to dissolve completely for up to 45 min at RT on a horizontal shaker. The PEG and PG cross-linker solutions were prepared in PBS at concentrations as stated in Table 4.1 on the next page, and sterile-filtered with a 0.2 µm syringe-filter immediately prior to use.

Prior to cross-linking, MSCs at passage 2 or 3 were carefully resuspended in the

HA-SH solution, next the required amount of cross-linker was added and mixed with the cell suspension at a final concentration of 20.0×10^6 MSCs/mL. For this purpose, the cross-linker solutions were used in a 1:4 volume ratio with the HA-SH solution (i.e., 1.0 mL HA-SH solution with 0.25 mL cross-linker solution). Subsequently, 40 µL of the final hydrogel precursor solution was filled into a glass ring (⌀ 5 mm), and allowed to gel for 30 min at 37 °C, 5% CO_2. Hydrogel-encapsulated cells were cultured for up to 21 d in chondrogenic medium, supplemented with TGF-β1 or in medium w/o TGF-β1, as negative control.

Table 4.1: Overview of cross-linker concentrations used for the cross-linking of HA-SH hydrogels by Michael addition.

Cross-Linker	Stock Solution [mg/mL]	Final Conc. [wt%]
PEGDA	5.0	0.1
PEGDA	10.0	0.2
PEGDA	20.0	0.4
PEGDA	50.0	1.0
PEGDA	100.0	2.0
PEGTA	29.4	0.6
PG-Acr	29.4	0.6

Biomimetic Functionalization with Peptides

Various amounts of different biomimetic peptides (concentrations and peptide sequences are stated in Table 3.7 on page 29) were covalently bound to PG-Acr for 1 h at 37 °C. For cell encapsulation, MSCs at passage 2 or 3 were resuspended in the HA-SH solution prior to cross-linking, and subsequently mixed with the peptide-modified PG-Acr solution, leading to a final concentration of 20.0×10^6 MSCs/mL. Unmodified 0.6% PG-Acr HA-SH hydrogels served as controls. Cell-laden PG-Acr cross-linked HA-SH hydrogel solutions were polymerized for 30 min at 37 °C, 5% CO_2, and afterwards chondrogenic medium, supplemented with TGF-β1, was added and constructs were cultured for up to 21 d. Unmodified hydrogels cultured in medium w/o TGF-β1 served as negative control.

Biomimetic Functionalization with Growth Factors

TGF-β1 was reacted with Traut's reagent, using a molar ratio of 4:1 of Traut's reagent to TGF-β1, for 1 h at RT in PBS. Afterwards, various doses of thiolated TGF-β1 (final concentrations in the hydrogels: 10 nM, 50 nM, and 100 nM) were coupled to PG-Acr for

1 h at 37 °C. An additional PG-Acr solution, containing 100 nM of TGF-β1 w/o Traut's reagent (TGF-β1 w/o Traut) modification was prepared, and subsequently compared to the TGF-β1-coupled group.

Prior to cross-linking, MSCs at passage 2 or 3 were resuspended in the HA-SH solution, and TGF-β1-modified PG-Acr was added to the HA-SH cell suspension at a final concentration of 20.0×10^6 MSCs/mL. Finally, 40 µL of the HA-SH hydrogel solution was filled into a glass ring (⌀ 5 mm), and polymerized for 30 min at 37 °C, 5% CO_2. Hydrogel-encapsulated cells were cultured for up to 21 d in chondrogenic medium, w/o soluble TGF-β1. Unmodified 0.6% PG-Acr HA-SH hydrogels served as controls, and were cultured in chondrogenic medium either supplemented with TGF-β1 or in medium w/o TGF-β1, as negative control.

4.2.2 Thiol-ene Clickable Poly(glycidol) Hydrogels

Pure Poly(glycidol) Hydrogels

For cell encapsulation 15 wt% (7.5 wt% P(AGE/G) and 7.5 wt% PG-SH) hydrogel solutions, containing 0.05 wt% photoinitiator Irgacure, were prepared. Additional to an unmodified hydrogel, the hydrogels were either functionalized with a 1 mM HAV peptide sequence or with 1 mM of the corresponding scrambled peptide sequence (Table 3.7 on page 29). Prior to cross-linking, MSCs at passage 2 were resuspended at a concentration of 20.0×10^6 MSCs/mL in the hydrogel precursor solution, and filled into a glass ring (⌀ 5 mm). Afterwards, the hydrogel precursor solution was UV irradiated with an UV hand lamp VL-4 at 365 nm for 10 min (∼1 mW/cm^2). The MSC containing hydrogels were cultured for up to 21 d in chondrogenic medium, supplemented with TGF-β1.

Zonal Hydrogels

A PG-based hydrogel system was used to form layered constructs. The zonal hydrogels were formed by sequential photo-polymerization. Initially, 45 µL of a 10 wt% (5,6 wt% HA-SH_{FMZ} and 4,4 wt% P(AGE/G)) hydrogel precursor solution, containing 0.05 wt% Irgacure and 20.0×10^6 MSCs/mL passage 3 MSCs were filled into a silicone mold (⌀ 6 mm), and UV irradiated with an UV hand lamp VL-4 at 365 nm for 5 min (∼1 mW/cm^2) to form a bottom layer. The hydrogel top layer of the zonal constructs was generated as described above. 15 µL of a 15 wt% (7.5 wt% P(AGE/G) and 7.5 wt% PG-SH) hydrogel precursor solution, containing 0.05 wt% Irgacure, were prepared with 20.0×10^6 MSCs/mL passage 3 MSCs, and UV irradiated with an UV hand lamp VL-4 at 365 nm for 10 min (∼1 mW/cm^2).

Tissucol Duo S 0.5 mL Immuno served as basis for the generation of fibrin hydrogel controls. For the preparation of cell-laden fibrin hydrogels, the thrombin component was diluted 1:50 and the fibrinogen component 1:15 with PBS. MSCs were resuspended in the diluted fibrinogen solution, and equal volumes (1:1) of diluted thrombin and cell-containing fibrinogen were mixed to a total volume of 60 µL, containing 20.0×10^6 MSCs/mL and allowed to polymerize for 30 min at 37 °C, 5% CO_2.

The MSC containing zonal constructs were cultured afterwards for 28 d in chondrogenic medium, supplemented with TGF-β1. Equally cultured fibrin hydrogels served as a control.

4.3 Cell Viability Assay

The cell viability of the gel-encapsulated cells was assessed using a Live/Dead cell staining kit. Images were routinely taken 2 d, 10 d and 21 d after cell encapsulation, in section 5.4 at 1 d and 28 d. Gels were initially washed with PBS and afterwards immediately stained by incubation in a staining solution (4 µM ethidium homodimer III (EthD-III), 2 µM calcein acetoxymethyl ester (Calcein-AM)) for 45 min. Subsequently, constructs were washed with PBS, and top view images were captured with a fluorescence microscope (Microscope BX51/DP71 camera).

4.4 Cryosectioning

The hydrogels were removed from chondrogenic medium, washed with PBS for 15 min, then fixed in 3.7 % PBS buffered formalin for 60 min, washed again in PBS for 15 min and finally incubated in O.C.T. overnight at 4 °C. On the next day constructs were transferred into cryomolds, embedded in O.C.T., frozen with liquid nitrogen, and stored at −80 °C until used.

The frozen, embedded gels were sectioned using a cryostat (Leica CM 1850) at −20 °C. 8 µm longitudinal-sections were cut for each construct, collected on Super Frost® plus glass slides, and stored at RT until stained.

4.5 Histology and Immunohistochemistry

4.5.1 Histology

Cryosections of the constructs were either stained for glycosaminoglycans with safranin O, or for collagens using picrosirius red.

Briefly, sections were first hydrated for 1 min, afterwards sequentially immersed for 5 min in Weigert's hematoxylin, 5 min under running tap water, 4 min in 0.02 % fast green, 10 sec in 1 % acetic acid, and 6 min in 0.1 % safranin O, dehydrated in an alcohol series up to xylene, mounted with Entellan® and images were captured with a microscope (Microscope BX51/DP71 camera) [129].

For picrosirius red staining, sections were hydrated for 1 min, then sequentially immersed for 8 min in Weigert's hematoxylin, 10 min under running tap water, 60 min in 0.1 % picrosirius red, washed in two changes of acidified water for 5 min, dehydrated in an alcohol series, cleared in xylene, and finally mounted with Entellan® and images were captured with a microscope (Microscope BX51/DP71 camera) [130].

4.5.2 Immunohistochemistry

Cryosections were initially rehydrated and antigen retrieval was performed for all antibodies, using Proteinase K (Digest-All 4) for 10 minutes at room temperature. Slides were washed three times in PBS for 3 min and all sections were blocked with 1 % bovine serum albumin (BSA) in PBS for 30 min at room temperature. Primary antibodies were diluted in Antibody diluent Dako REAL, and incubated overnight in a humidified chamber at room temperature. Primary antibodies for aggrecan, collagen type I, II and X were used at dilutions as stated in Table 3.4 on page 28. Slides were afterwards washed three times in PBS for 3 min. The secondary antibodies were diluted in Antibody diluent Dako REAL as stated in Table 3.5 on page 28 and incubated in the dark for 60 min. Finally, slides were washed three times in PBS for 3 min, and after drying, mounted with DAPI mounting medium ImmunoSelect® and images were captured with a fluorescence microscope (Microscope BX51/DP71 camera).

4.6 Biochemical Analysis

4.6.1 Papain Digestion

Prior to biochemical analysis, the hydrogels were digested using papain. Therefore, the hydrogels were removed from medium, at indicated time points, and washed two times

in PBS for 10 min, transferred into 2 mL SafeSeal micro tubes, and 500 µL of sterile PBE-cysteine buffer was added. Afterwards, the gels were homogenized at 25 Hz for 5 min, with a TissueLyser. Subsequently, 500 µL of PBE-cysteine buffer containing papain 3 U/mL was added to the homogenized PBE/hydrogel solution, and incubated for 10 h to 16 h at 60 °C. The digested samples were stored at −20 °C until used in biochemical assays.

4.6.2 DNA Assay

For DNA content measurement, a solution of Hoechst 33258 DNA intercalating dye was used [131]. Therefore, 10 µL of papain digested samples were added to 200 µL of a Hoechst 33258 dye solution and the DNA quantification was carried out with the Tecan GENios pro spectrofluorometer at 340 nm and 465 nm, using salmon testis as standard.

4.6.3 GAG Assay

The amount of sulfated glycosaminoglycans (GAGs) was measured as chondroitin sulfate using the dimethylmethylene blue (DMMB) assay adapted to 96-well plate format [132]. Therefore, 10 µL of papain digested samples were added to 40 µL of PBE-cysteine buffer and finally 200 µL DMMB solution were added and the GAG amount was determined spectrophotometrically at 525 nm with the MRX microplate reader, using bovine chondroitin sulfate as standard.

4.6.4 Collagen Assay

The hydroxyproline content was determined spectrophotometrically after acid hydrolysis and reaction with p-dimethylamino-benzaldehyde (DAB) and chloramine T. The hydroxyproline assay was adapted to 96-well plate format [133]. Therefore, 100 µL of 36% HCl were added to 100 µL of papain digested samples, and hydrolyzed for 16 h at 105 °C. Afterwards, HCl was allowed to evaporate, and pellets were resuspended in 500 µL ddH_2O. For quantification, 50 µL chloramine T solution, and 50 µL DAB solution were added to 100 µL of the water resuspended samples, and quantification was carried out with the MRX microplate reader at 570 nm, using L-hydroxyproline as standard. The amount of total collagen was calculated using a hydroxyproline to collagen ratio of 1:10 [134].

4.7 Quantitative Real-time PCR Analysis

Total RNA from hydrogel encapsulated MSCs was isolated after 5 d, 10 d, 15 d and 21 d of *in vitro* culture using TRIzol reagent. The RNA was transcribed into first-strand cDNA using the ImProm-II™ reverse transcription system Kit. The Brilliant III Ultra-Fast SYBR® Green QPCR Master Mix was used for quantitative real-time polymerase chain reaction (qRT-PCR) analysis with a Real-Time PCR Detection System CFX96T™. qRT-PCR was performed using the following cycling protocol:

Table 4.2: qRT-PCR cycling protocol.

Step	Temperature	Time	Number of Cycles
Activation	95 °C	3 min	1
Denaturation	95 °C	5 sec	40
Annealing/extension	60 °C	30 sec	
Melt curve	65 °C to 95 °C (0.5 °C increments)	5 sec /step	1

qRT-PCR was employed with commercially available primer pairs as stated in Table 3.6 on page 29. The mRNA expression levels of all genes were normalized to the expression of the housekeeping gene GAPDH of 2D samples from day 0, and the increase in expression levels was determined using the $2^{-\Delta\Delta CT}$ method.

4.8 Protein Isolation

A modified protocol for isolation and extraction of proteins out of TRIzol reagent, following RNA extraction, was used [135]. The TRIzol-chloroform fractions from hydrogel samples were stored at −20 °C until used for protein isolation. Briefly, after the precipitation of DNA, the proteins were precipitated by the addition of isopropanol after 10 min at RT. Subsequently, the samples were centrifuged (12000 g, 10 min, 4 °C), and the supernatant was discarded. Afterwards, the protein pellets were washed three times with 0.3 M guanidine hydrochloride solution. In each step, samples were strongly shaken, incubated 20 min at RT, and centrifuged (7500 g, 10 min, 4 °C). After the last washing step absolute ethanol was added, and samples were again incubated 20 min at RT, and centrifuged (7500 g, 10 min, 4 °C). Next, the supernatant was carefully removed and 1:1 buffer was added to the protein pellets, followed by 5 cycles sonication and 30 sec incubation on ice, to dissolve proteins. Pulse power was adjusted to 90 %. Finally, the samples were centrifuged (3200 g, 10 min, 4 °C) to sediment insoluble material. The supernatant was

transferred to a fresh reaction tube and was stored at −80 °C prior to BCA assay and SDS-PAGE.

4.9 Western Blot

Total protein content was determined by spectroscopic quantification using the Microplate BCA™ Protein Assay Kit according to manufacturer's instructions. 10 µg of each sample was loaded on a polyacrylamide gel for separating the proteins by sodium dodecyl sulfate polyacrylamide gel electrophoresis (SDS-PAGE).

4.9.1 SDS-PAGE

10 µg of the isolated proteins were separated by SDS-PAGE on 8% polyacrylamide gels (Tables 4.3 and 4.4), and 10 µL Novex® sharp protein standard was used for the size determination of separated proteins. The proteins were separated with the Mini-PROTEAN® Tetra Cell System, by applying constant amperage of 50 mA.

Table 4.3: Composition of 8% separating gels.

Components	Volume for two gels
30% acrylamide	4.1 mL
1M TRIS pH 8.8	5.7 mL
10% SDS	150.0 µL
H_2O	4.9 mL
10% APS	150.0 µL
TEMED	7.5 µL

Table 4.4: Composition of stacking gels.

Components	Volume for two gels
30% acrylamide	0.9 mL
0.5M TRIS-HCL pH 6.8	1.5 mL
10% SDS	60.0 µL
H_2O	3.4 mL
10% APS	60.0 µL
TEMED	6.0 µL

4.9.2 Transfer of Proteins

The separated proteins were transferred to a nitrocellulose membrane by tank blotting, using the Bio-Rad Mini-PROTEAN® Tetra Cell System, by applying constant amperage of 300 mA for 1 h.

4.9.3 Immunodetection of Proteins

After the transfer of the proteins to the nitrocellulose membrane, membranes were blocked by incubating the membrane in WB blocking solution on an orbital shaker for 1 h at RT. The primary antibody was diluted as stated in Table 3.4 on page 28 in blocking solution, added to the membrane and incubated overnight at 4 °C. Next, the primary antibody was removed, and the membrane washed three times in PBST for 10 min on an orbital shaker. The corresponding HRP-conjugated secondary antibody was diluted as stated in Table 3.5 on page 28, added to the membrane, and incubated for 1 h at RT. Afterwards, the membrane was washed three times in PBST for 10 min. Finally, the immunoreactive proteins were detected by chemiluminescence using the Amersham™ ECL™ Prime Western Blotting Detection Reagent with the FluorChem FC2 Imager. The expression of proteins was quantified by the determination of density values using Fiji software [136].

4.10 Statistics

Statistical analysis was performed using GraphPad Prism, Version 6.0 (GraphPad Software, La Jolla, USA). Results are presented as mean values ± standard deviation (SD). Statistical significance was assessed by either multiple t tests followed by Holm-Sidak post-hoc test, or by two-way analysis of variance (ANOVA) followed by Tukey's post-hoc test, as appropriate. The statistical significance level was set with a significance level of $p<0.05$.

Part III

Results

Chapter 5

Results

5.1 Hyaluronic Acid Hydrogels Cross-linked with Poly(eythylene Glycol) or Poly(glycidol) Derivatives

In this section thiolated hyaluronic acid (Glycosil®, HA-SH) was cross-linked with acrylate-modified poly(ethylene glycol)s (PEG) and poly(glycidol)s (PG) using Michael addition at physiological pH (Figure 5.1).

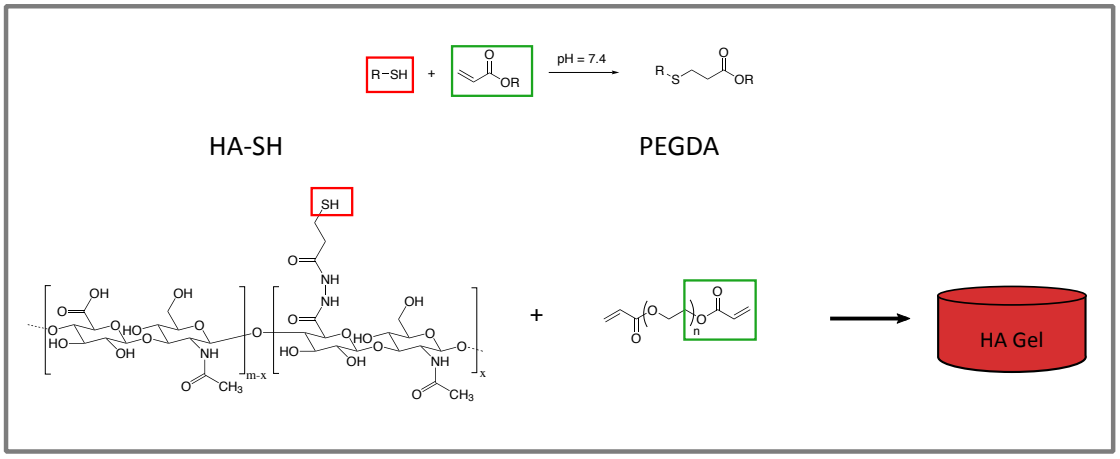

Figure 5.1: Cross-linking scheme of Michael addition. Thiolated HA (Glycosil®, HA-SH) was cross-linked with PEGDA to form a HA-SH gel.

1. First, the general material suitability for chondrogenesis of MSCs within PEGDA cross-linked HA-SH hydrogels was assessed (Section 5.1.1 on the next page).
2. Subsequently, the HA-SH hydrogel composition was optimized (Section 5.1.2 on page 48).

3. Finally, in order to find the best HA-SH hydrogel formulation for further experiments, different cross-linkers were evaluated step by step (Section 5.1.3 on page 53).

5.1.1 General Material Suitability for MSC Chondrogenesis

To confirm the general material suitability of thiolated HA (Glycosil®, HA-SH) for MSC chondrogenesis, it was cross-linked with 0.4 % poly(ethylene glycol) diacrylate (PEGDA). The prepared hydrogels were seeded with 20.0×10^6 MSCs/mL, and cells were differentiated for 21 days in chondrogenic differentiation medium. A group cultured in medium w/o TGF-β1 served as a negative control (no chondrogenesis, Neg. Ctr.).

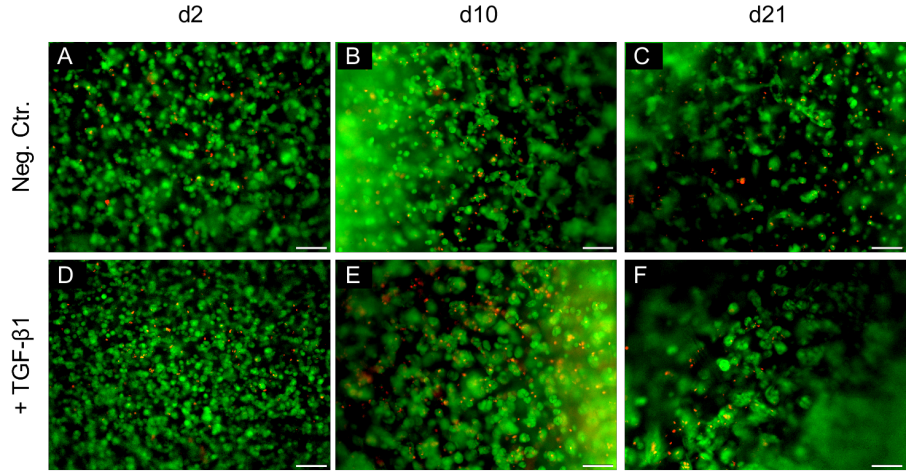

Figure 5.2: Cell viability of MSCs encapsulated in HA-SH gels cross-linked with 0.4 % PEGDA, seeded with 20.0×10^6 MSCs/mL, after 2, 10 and 21 days of chondrogenic differentiation. Viable cells were labeled green with calcein-AM, and dead cells were labeled red with EthD-III; scale bars represent 100 µm.

The evaluation of the Live/Dead assay showed in both groups good cell viability over the 21 days culturing period and a homogeneous distribution of cells (Figure 5.2).

Chondrogenic differentiation of MSCs was shown by staining of GAGs with safranin O, and for the presence of the extracellular matrix (ECM) components collagen I and collagen II using immunofluorescence. MSCs cultured in TGF-β1 containing medium showed an increase in cell-associated safranin O staining from day 10 to 21 (Figure 5.3, C–D), while the Neg. Ctr. group exhibited no safranin O staining (Figure 5.3, A–B). A signal for collagen I could be detected in both groups, with increasing signal in a time-dependent manner in the group +TGF-β1 (Figure 5.3, G–H). In the Neg. Ctr. group

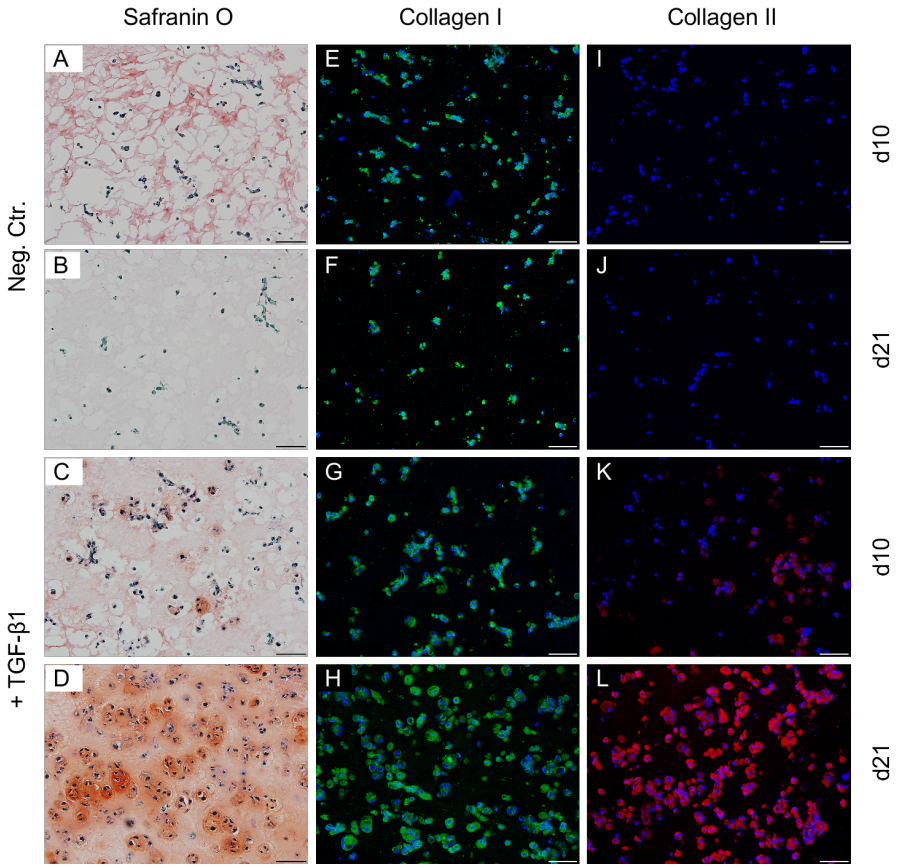

Figure 5.3: Histological and immunohistochemical staining of MSCs encapsulated in HA-SH gels cross-linked with 0.4 % PEGDA, seeded with 20.0×10^6 MSCs/mL, after 10 and 21 days of chondrogenic differentiation. Longitudinal sections were stained for deposition of GAGs with safranin O and collagen I (green) or collagen II (red) to show ECM development. Nuclei (blue) were counterstained with DAPI; scale bars represent 100 µm.

no signal for collagen II was detectable (Figure 5.3, I–J). The group +TGF-β1 showed increasing deposition of collagen II from day 10 to 21 (Figure 5.3, K–L). Herewith, the general suitability for chondrogenic differentiation of MSCs within the HA-SH gels was demonstrated.

5.1.2 Variation of PEGDA Cross-linker Concentrations

Next, the influence of varying cross-linker concentrations on basic handling characteristics in cell culture, mechanical stability, storage modulus and the impact on chondrogenic differentiation of MSCs within the HA-SH gels was assessed. A group without TGF-β1 served as a negative control for not proceeding chondrogenesis (0.4% PEGDA, Neg. Ctr.).

Therefore, different concentrations of PEGDA, in the range of 0.1%–2.0%, were used to prepare MSC-seeded HA-SH gels (Table 5.1). Gels cast with low concentrations of PEGDA, 0.1% and 0.2 %, shrunk during cell culture period and were difficult to handle, e.g. while routinely changing cell culture medium. Moreover, the distribution of cells within these gels was not homogeneous (Figure 5.4 A, B). Gels that were cross-linked with higher concentrations of PEGDA maintained their shape, were easy to handle and showed a homogeneous cell distribution (Figure 5.4 C–E). The storage modulus increased with increasing PEGDA concentrations from 8 ± 5 Pa (0.1%) up to 762 ± 191 Pa (2.0%). MSCs were able to differentiate chondrogenically in all differently concentrated HA-SH gels (Table 5.1). Concerning cell viability, no differences between the different PEGDA concentrations could be observed (data not shown).

Table 5.1: Handling and physicochemical characteristics of PEGDA cross-linked HA-SH hydrogels. ⋆(unpublished data by Verena Schill (Department for Functional Materials in Medicine and Dentistry (FMZ), University Hospital Würzburg)). Data are presented as means ± standard deviation (n=3)

	HA-SH PEGDA Hydrogels				
Polymer Concentration [%]	0.1	0.2	0.4	1.0	2.0
Handling in Cell Culture	unstable	unstable	stable	stable	stable
Volume Stability	shrink	shrink	stable	stable	stable
Storage Modulus [Pa]⋆	8 ± 5	65 ± 18	218 ± 37	394 ± 140	762 ± 191
Chondrogenesis	yes	yes	yes	yes	yes

Focusing on ECM deposition in the differently cross-linked HA-SH gels, lower concentrated gels (0.1%–0.4%) showed a more continuous distribution of GAGs in the safranin O staining (Figure 5.4, F–H) and of collagens in the picrosirius red staining (Figure 5.4, K–M). Gels with higher amounts of PEGDA (1.0% and 2.0%) exhibited a

more pronounced pericellular location of these ECM molecules (Figure 5.4 I, J, N, O).

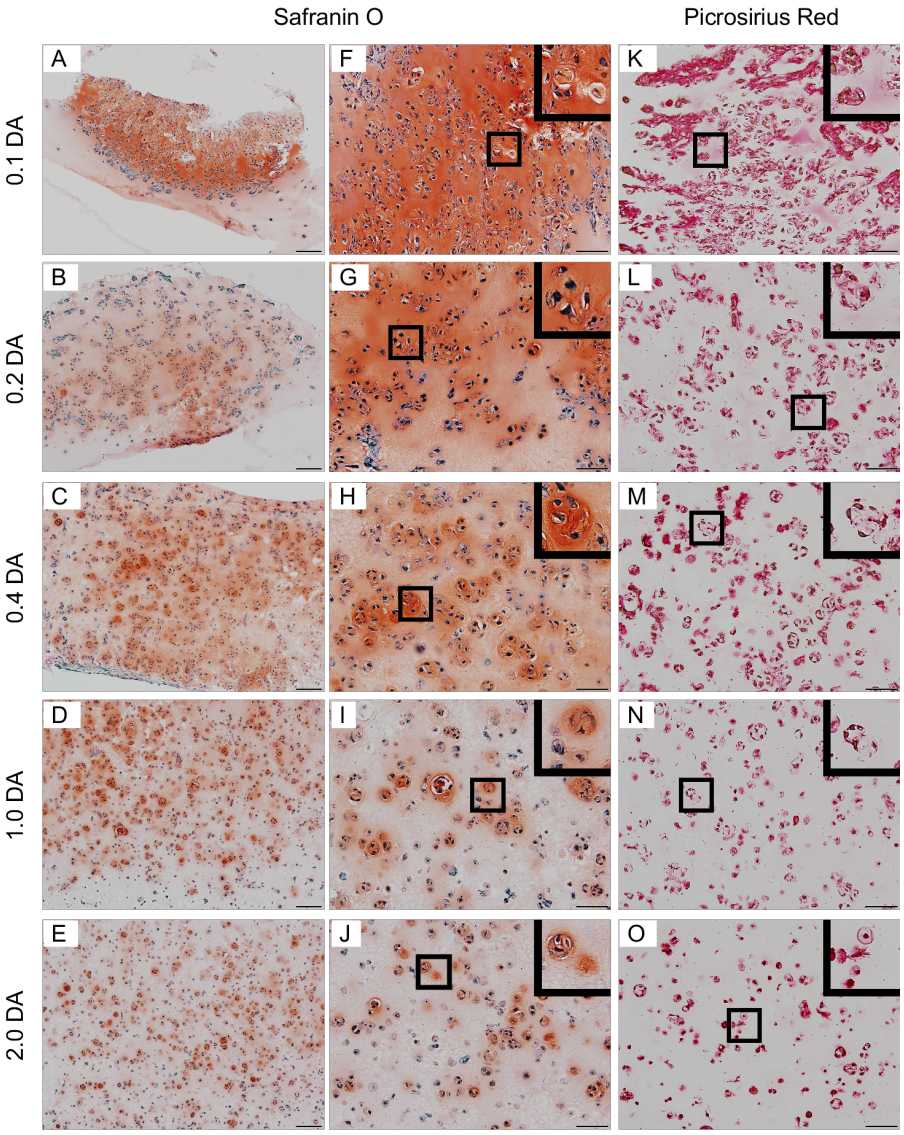

Figure 5.4: Histological staining of the HA-SH hydrogels cross-linked with varying PEGDA concentrations, seeded with 20.0×10^6 MSCs/mL, after 21 days of chondrogenic differentiation. Longitudinal sections were stained for deposition of GAGs with safranin O and collagens with picrosirius red; scale bars represent 100 µm. The black boxes show a selected image section in higher magnification in the upper right corner.

Biochemical evaluation of total DNA, GAG and collagen amount was used to determine quantitative differences between the hydrogels with varying amounts of PEGDA. The quantification of DNA amount showed enhanced proliferation in all gels on day 10 and

21 compared to Neg. Ctr., except for the 0.1% PEGDA gel on day 10 (Figure 5.5, A). Determination of total GAG and collagen showed that all chondrogenically induced HA-SH gels produced large amounts of these ECM components. Just the total amounts on day 21 in the 0.1% PEGDA gel were smaller compared to all other concentrated PEGDA hydrogels (Figure 5.5, B, D). This observation was not longer detectable when GAG and collagen were normalized to DNA amount (Figure 5.5, C, E).

A glance on the immunohistochemical (IHC) staining of the gels with the lower PEGDA concentrations (0.1%–0.4%) showed for collagen I and collagen II a strong pericellular signal, and also deposition of these ECM components throughout the hydrogels (Figure 5.6, A–C, F–H). In the gels with 1.0% and 2.0% PEGDA the area of pericellular signal became smaller, and no incorporation into the gel matrix was visible (Figure 5.6, D, E, I, J). Aggrecan, on the other hand, was spread in all gels over the whole gel area, but to a lesser extent in the 1.0% and 2.0% PEGDA gels with a more pronounced pericellular staining (Figure 5.6, K–O).

Taking all observations into account, 0.4% PEGDA gels were chosen as a basis for further investigation and optimization of HA-SH hydrogels. While there were no detectable quantitative differences regarding GAG or collagen amount between the different amounts of PEGDA used for cross-linking of the HA-SH hydrogels (Figure 5.5), a qualitative difference in ECM deposition in the gel matrix could be noticed. becoming lesser and more pericellular pronounced in the higher concentrated gels in a dose-dependent manner (Figures 5.4 and 5.6). With 0.4% PEGDA concentration the gels were still stable and good to handle in cell culture, but also the distribution and deposition of synthesized ECM was more extensive than compared to the higher PEGDA concentrations of 1.0% and 2.0%.

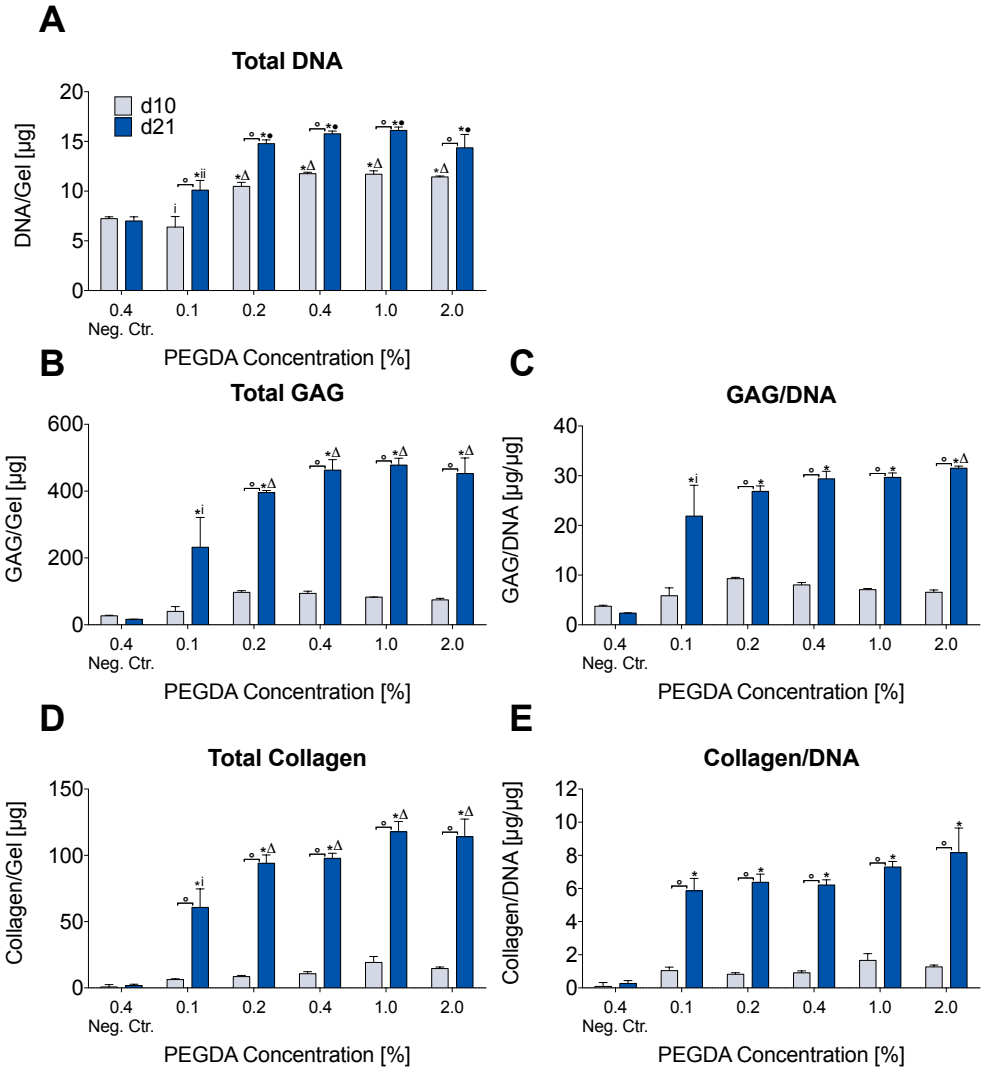

Figure 5.5: Effect of varying PEGDA concentrations of the prepared HA-SH hydrogels on total DNA amount (A) as well as total GAG (B) and collagen (D) per gel or normalized to DNA amount (C, E) after 10 and 21 days of chondrogenic differentiation. Data are presented as means ± standard deviation (n=3). Statistically significant differences between gels prepared with different PEGDA concentrations and control gels w/o TGF-β1 at the same time point are denoted with ($\star$) $p<0.05$, groups with a common (i) are statistically different to groups with a (Δ) $p<0.05$, groups with a common (ii) are statistically different to groups with a ($\bullet$) $p<0.05$. Statistically significant differences between time points within a group are denoted with ($\circ$) $p<0.05$. Representative results of one of two independent experiments are shown.

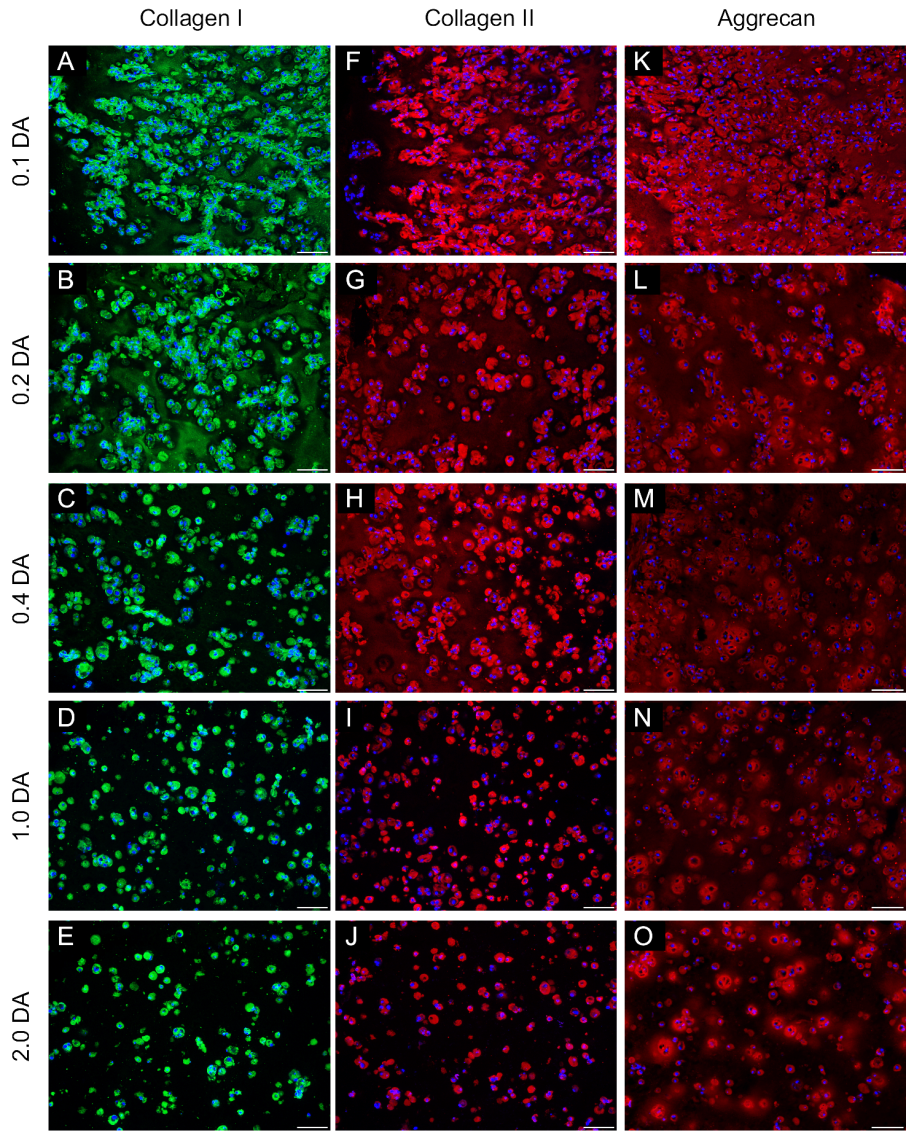

Figure 5.6: Immunohistochemical staining of MSCs encapsulated in HA-SH hydrogels cross-linked with varying PEGDA concentrations, seeded with 20.0×10^6 MSCs/mL, after 21 days of chondrogenic differentiation. Staining for collagen I (green), collagen II (red) and aggrecan (red) shows ECM development. Nuclei (blue) were counterstained with DAPI; scale bars represent 100 µm.

5.1.3 Variation of the Hydrogel Cross-linker

The variation of the hydrogel cross-linker from poly(ethylene glycol) diacrylate (PEGDA) to poly(ethylene glycol) tetraacrylate (PEGTA) or the even higher acrylate modified poly(glycidol)-acrylate (PG-Acr) to cross-link the thiolated hyaluronic acid (Glycosil®, HA-SH) (Figure 5.7), may result in a change of general mechanical and handling characteristics or cell behavior in the differently cross-linked HA-SH hydrogels.

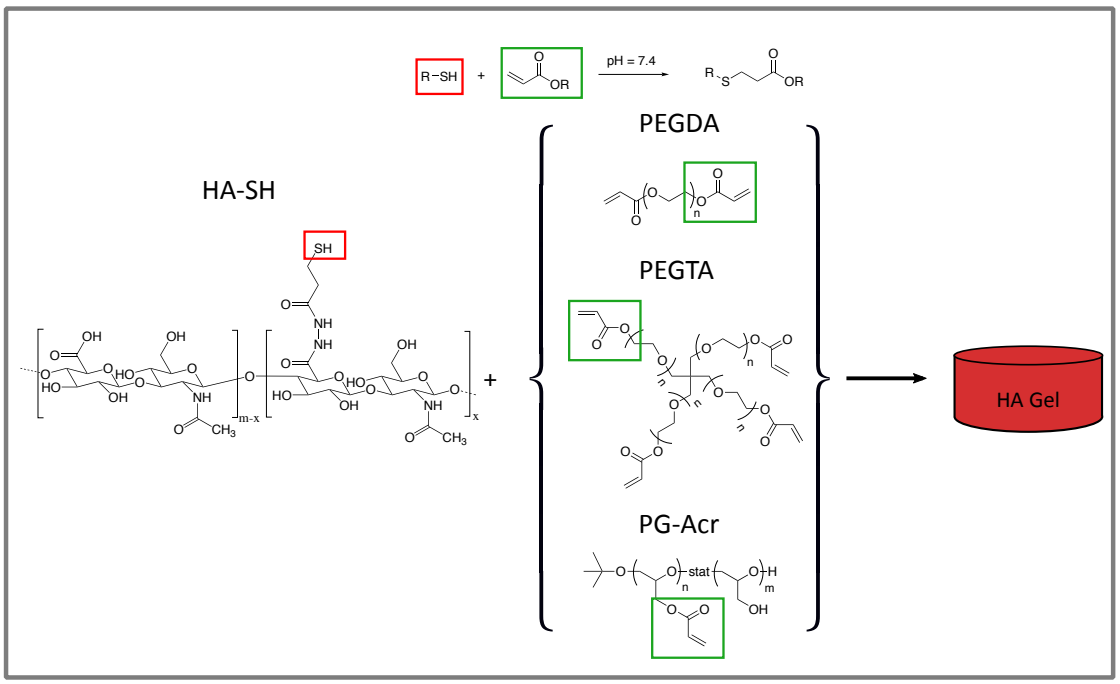

Figure 5.7: Cross-linking scheme of HA-SH hydrogels cross-linked with different cross-linkers by Michael addition. Thiolated HA (Glycosil®, HA-SH) was cross-linked either with PEGDA, PEGTA and PG-Acr to form a HA-SH gel.

Hence, different concentrations of different cross-linkers were used to generate HA-SH hydrogels. While the change from 0.4% PEGDA to 0.6% PEGTA resulted in a far higher storage modulus, from 218 ± 37 Pa up to 1643 ± 469 Pa, the theoretical amount of acrylate groups in both gels stayed the same (Figure 5.8). On the other hand, the switch to 0.6% PG-Acr resulted in a softer gel (604 ± 241 Pa) compared to a 0.6% PEGTA cross-linked gel, but with an approximately 5-fold higher number of acrylate groups, as the final concentration of cross-linker in the hydrogels was equal (Figure 5.8).

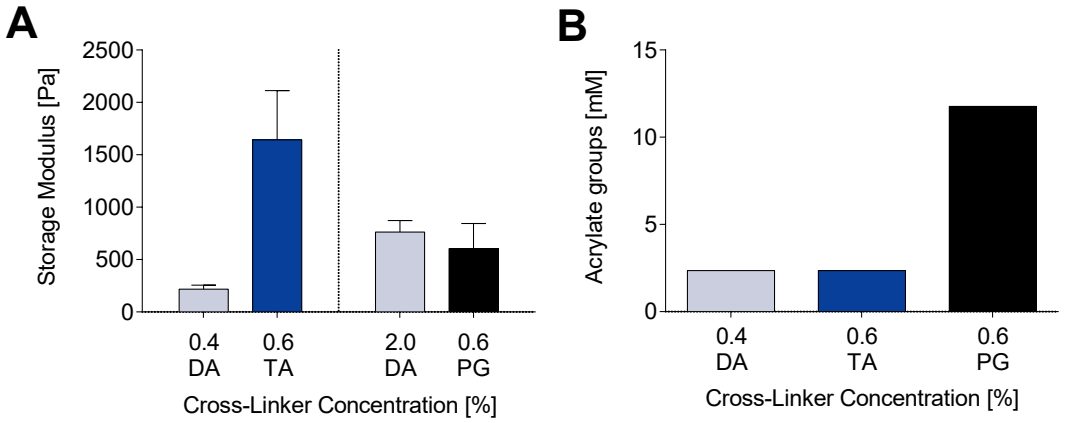

Figure 5.8: Storage Modulus of the HA-SH gels cross-linked with different cross-linkers, e.g. PEGDA, PEGTA or PG-Acr to form a HA-SH gel (unpublished data by Verena Schill (FMZ, University Hospital Würzburg)).

Hydrogels Cross-linked with PEGDA and PEGTA

To investigate possible differences in the chondrogenesis of MSCs in HA-SH hydrogels cross-linked with either 0.4% PEGDA or 0.6% PEGTA, the corresponding hydrogels were seeded with 20.0×10^6 MSCs/mL, and differentiated for 21 days in chondrogenic differentiation medium. A group cultured in medium w/o TGF-β1 served as a negative control (no chondrogenesis, (Neg. Ctr.)).

The chondrogenic differentiation of MSCs was shown by staining of GAGs with safranin O, or by using immunofluorescence to detect the ECM components collagen I and collagen II. Gels of both cross-linker groups exhibited a strong safranin O staining on day 21 (Figure 5.9, D, G), while the Neg. Ctr. group showed, as expected, no safranin O staining (Figure 5.9, A). Collagen I was present in both cross-linker groups on day 21, with a slightly stronger signal in the 0.4% PEGDA group (Figure 5.9, E, H). In the Neg. Ctr. group only a pericellular signal for collagen I and no signal for collagen II was detectable (Figure 5.9, B–C). The 0.4% PEGDA group showed a slightly higher deposition of collagen II on day 21 throughout the gel matrix compared to the 0.6% PEGTA gels (Figure 5.9, F, I). Regarding cell viability, no differences between the PEGTA and PEGDA cross-linked gels could be detected during the 21 days culturing period (data not shown).

To analyze possible quantitative differences between 0.4% PEGDA and 0.6% PEGTA hydrogels, total DNA, GAG and collagen amount was measured. Determination of total

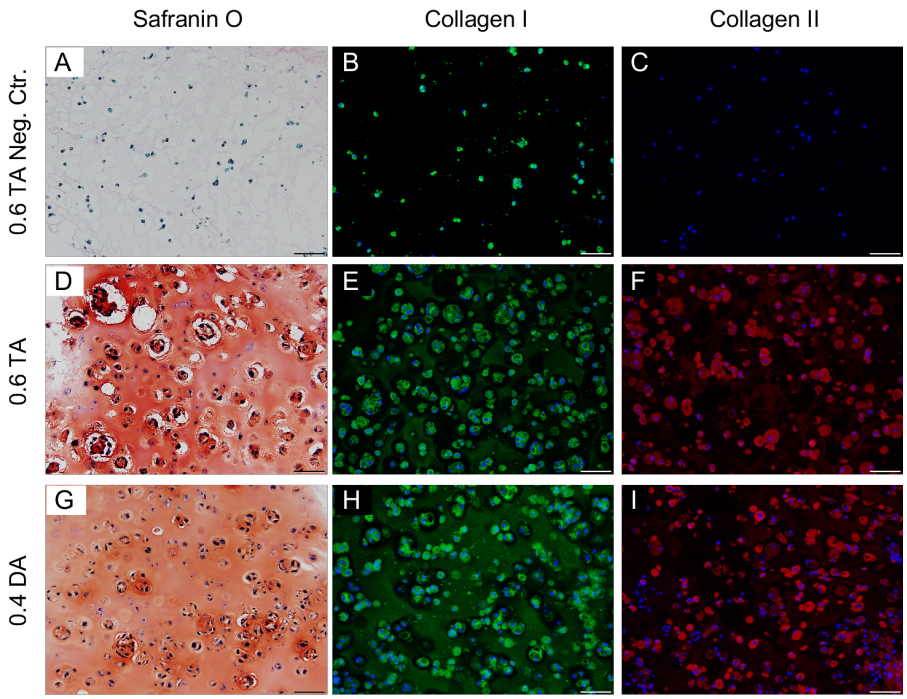

Figure 5.9: Histological and immunohistochemical staining of MSCs encapsulated in HA-SH hydrogels cross-linked either with 0.4% PEGDA or 0.6% PEGTA, seeded with 20.0×10^6 MSCs/mL, after 21 days of chondrogenic differentiation. Longitudinal sections were stained for deposition of GAGs with safranin O and collagen I (green) or collagen II (red) to show ECM development. Nuclei (blue) were counterstained with DAPI; scale bars represent 100 µm.

DNA showed significantly higher amounts of DNA for both groups on day 10 and 21 compared to the Neg. Ctr., but no differences between both cross-linkers (Figure 5.10, A). Analysis of GAG and collagen, either total or normalized to DNA, showed a significant increase on day 21 compared to the Neg. Ctr., but no changes depending on the cross-linker type (Figure 5.10, B–E).

In summary, no major differences in quality or quantity of MSC chondrogenesis, when using either 0.4% PEGDA or 0.6% PEGTA to cross-link the HA-SH, could be observed (Figures 5.9 and 5.10).

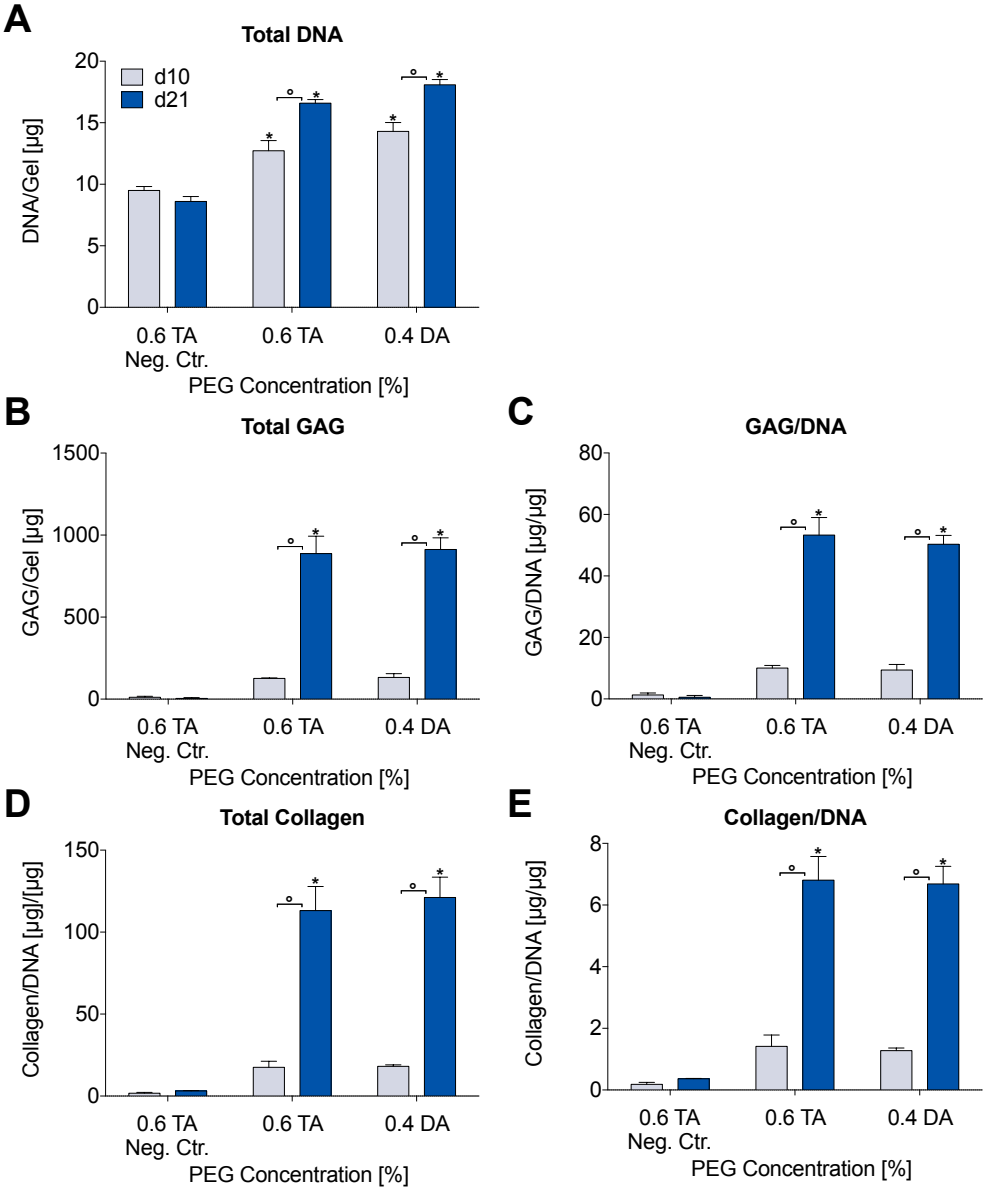

Figure 5.10: Effect of varying cross-linker on MSCs encapsulated in HA-SH hydrogels either cross-linked with 0.4% PEGDA or 0.6% PEGTA, on total DNA amount (A) as well as total GAG (B) and collagen (D) per gel or normalized to DNA amount (C, E) after 10 and 21 days of chondrogenic differentiation. Data are presented as means ± standard deviation (n=3). Statistically significant differences between gels prepared with different cross-linkers and control gels w/o TGF-β1 at the same time point are denoted with (⋆) $p<0.05$. Statistically significant differences between time points within a group are denoted with (∘) $p<0.05$. Representative results of one of two independent experiments are shown.

Hydrogels Cross-linked with PEGTA and PG-Acr

In the following experiments, the chondrogenic differentiation of MSCs in HA-SH hydrogels cross-linked either with 0.6% PEGTA or 0.6% PG-Acr was analyzed. The hydrogels were seeded with 20.0×10^6 MSCs/mL and chondrogenically differentiated for 21 days. Regarding cell viability, no differences between the PEGTA and PG-Acr cross-linked gels could be seen during the 21 day period of chondrogenic differentiation (data not shown).

Visualization of MSC chondrogenesis by staining for GAGs with safranin O showed for the 0.6% PEGTA hydrogel a more pericellularly pronounced staining, while GAGs in the 0.6% PG-Acr hydrogel seemed to be more evenly distributed (Figure 5.11 A, D). A similar staining pattern could be observed by using immunofluorescence for collagen I and collagen II. In the 0.6% PG-Acr HA-SH hydrogel both collagens were more evenly distributed, whereas the signals in the 0.6% PEGTA gels were more restricted to an area close to the nuclei (Figure 5.11 B, C, E, F).

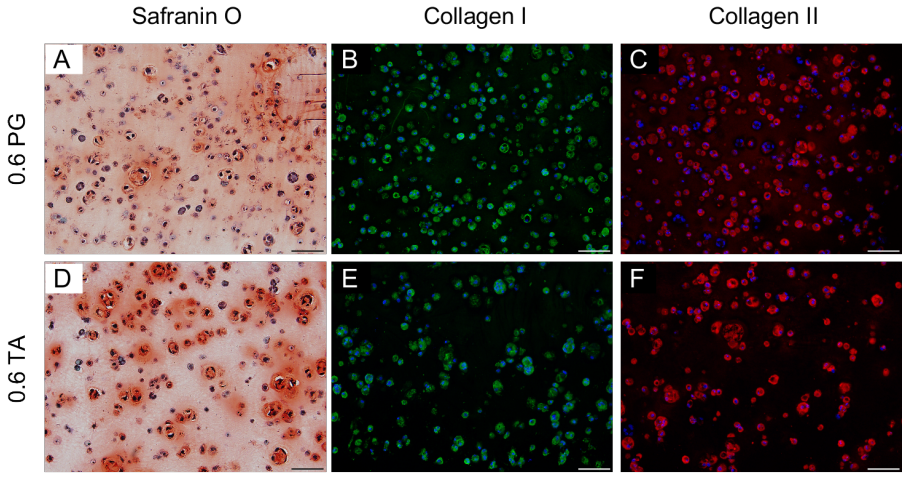

Figure 5.11: Histological and immunohistochemical staining of MSCs encapsulated in HA-SH hydrogels either cross-linked with 0.6% PEGTA or 0.6% PG-Acr, seeded with 20.0×10^6 MSCs/mL, after 21 days of chondrogenic differentiation. Longitudinal sections were either stained for deposition of GAGs with safranin O and collagen I (green) or collagen II (red) to show ECM development. Nuclei (blue) were counterstained with DAPI; scale bars represent 100 µm.

Quantification of total DNA led to no significant differences between both groups (Figure 5.12, A). Analysis of GAG production, either total or normalized to DNA, showed a clear increase on day 21 compared to day 10, but no considerable differences between 0.6% PEGTA (22.4 ± 3.2 µg/µg) and 0.6% PG-Acr (19.1 ± 1.8 µg/µg) (Figure 5.12, B–C). Interestingly, determination of total collagen and collagen/DNA showed a distinct increase for the PG-Acr cross-linked gels (9.2 ± 0.3 µg/µg) compared to the PEGTA cross-linked

gels (5.4 ± 0.6 µg/µg) on day 21 (Figure 5.12, D–E).

Considering all observations (ECM deposition, increase in acrylate groups), PG-Acr was chosen as the most favorable cross-linker for further experiments, in order to address the influence of biomimetic functionalization, either by incorporation of biomimetic peptides or growth factors into the HA-SH hydrogels.

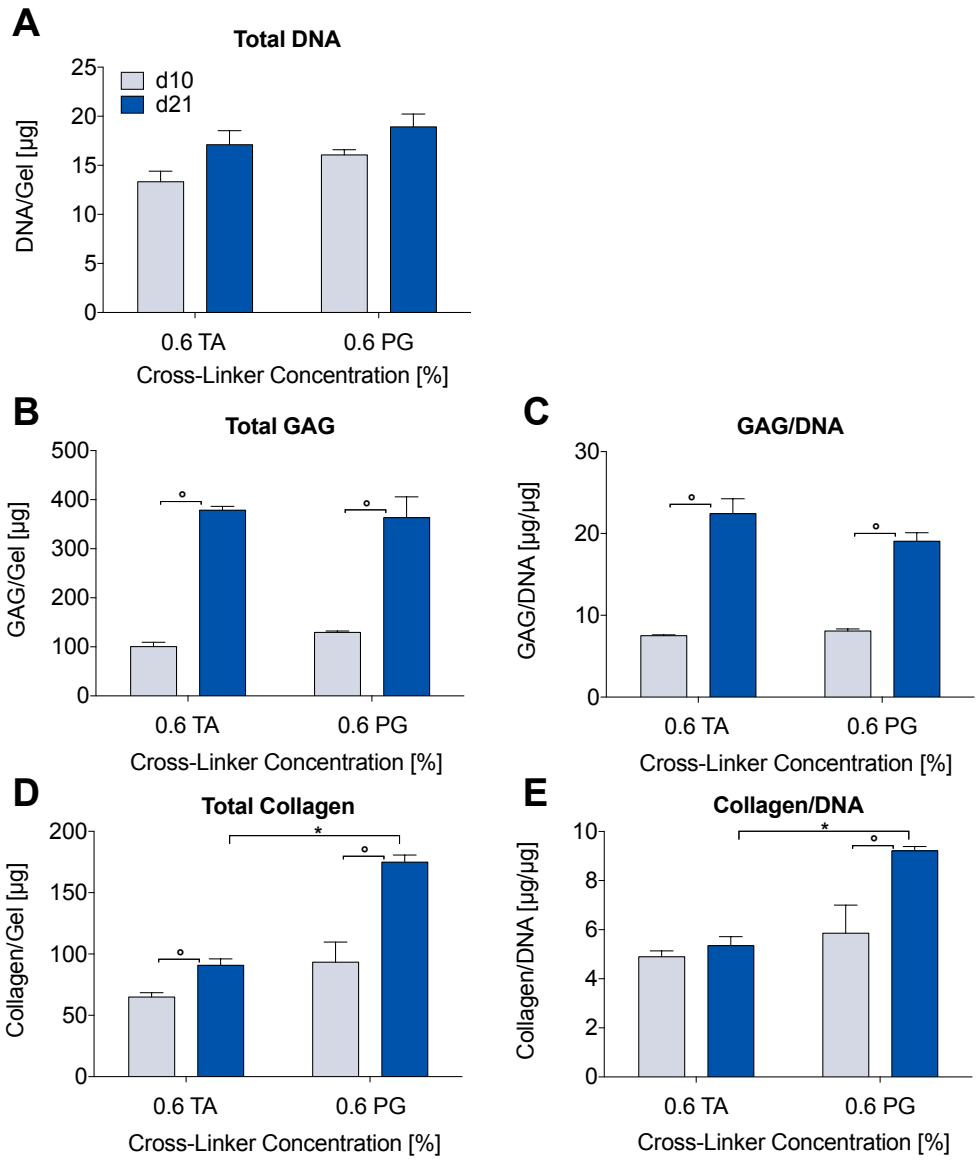

Figure 5.12: Effect of varying cross-linker on MSCs encapsulated in HA-SH hydrogels either cross-linked with 0.6% PEGTA or 0.6% PG-Acr, on total DNA amount (A) as well as total GAG (B) and collagen (D) per gel or normalized to DNA amount (C, E) after 10 and 21 days of chondrogenic differentiation. Data are presented as means ± standard deviation (n=3). Statistically significant differences between gels prepared with different cross-linkers are denoted with a line and a ($\star$) $p<0.05$. Statistically significant differences between time points within a group are denoted with ($\circ$) $p<0.05$.

5.2 Biomimetic Functionalization of Hyaluronic Acid Hydrogels

In order to improve the general chondrogenic and potentially the clinical performance of the developed PG-Acr cross-linked HA-SH gels, the gels underwent various types of biomimetic functionalization. The gels were either functionalized with peptides to resemble the natural cartilage ECM in more depth or to mimic the natural development of cartilage, by imitating e.g. cell-to-cell contact with a N-cadherin mimetic peptide. Additionally, the gels were covalently modified with the growth factor TGF-β1, which may enhance the clinical potential of the developed hydrogels.

5.2.1 Biomimetic Functionalization with Peptides

For the biomimetic functionalization of the developed HA-SH hydrogels cysteine-modified peptides were initially bound to the cross-linker poly(glycidol)-acrylate (PG-Acr) using Michael addition. In a second step, the peptide-modified PG-Acr was used to cross-link thiolated HA (Glycosil®, HA-SH) (Figure 5.13).

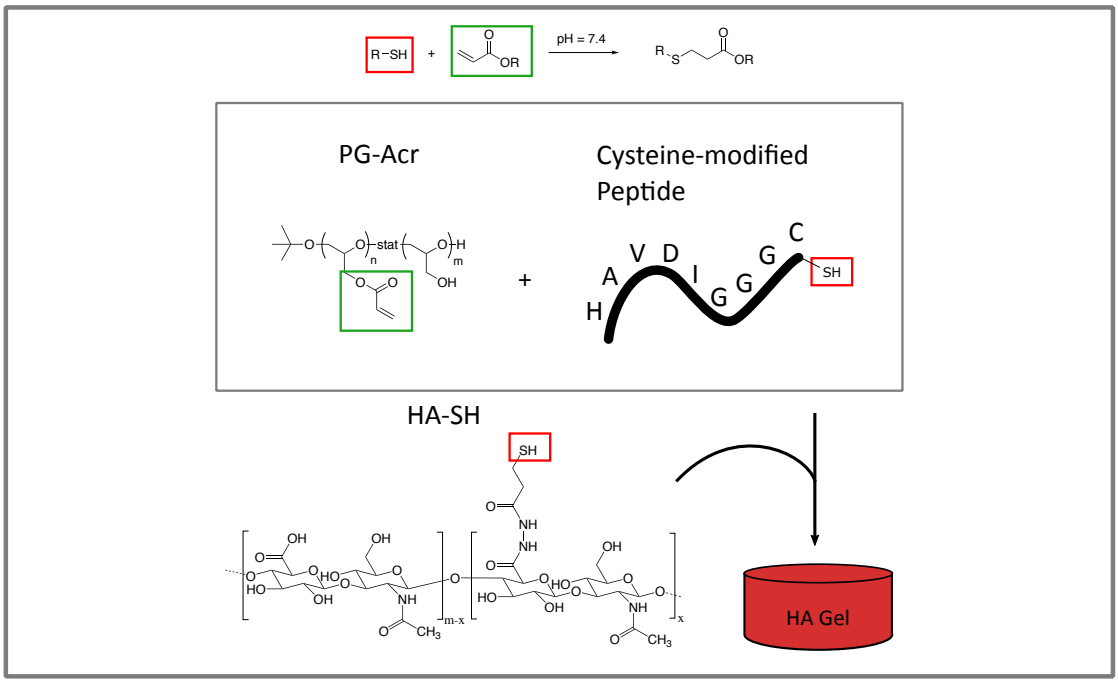

Figure 5.13: Cross-linking scheme of the biomimetic functionalization with peptides by using Michael addition. First, cysteine-modified peptides were bound to the cross-linker PG-Acr. In a second step, thiolated HA (Glycosil®, HA-SH) was cross-linked with the peptide-modified cross-linker.

For the biomimetic functionalization, only peptide sequences were used that were

already reported to promote chondrogenesis of MSCs in hydrogels (Table 5.2).

Table 5.2: Overview of peptide sequences and their biological function that were introduced into the PG-Acr cross-linked HA-SH hydrogels.

Peptide Sequence	Biological Function
Ac-HAVDIGGGC	Natural N-cadherin mimetic peptide sequence
Ac-AGVGDHIGC	Scrambled N-cadherin peptide sequence
CGKLERG	Natural collagen type II binding site from decorin protein
CGLKREG	Scrambled collagen type II binding site from decorin protein
CGRGDSG	Cell adhesion sequence from fibronectin protein that is recognized by integrins

The applied peptide concentrations based on other studies that incorporated these peptides into other gel systems [99, 101] (Table 3.7 on page 29).

HA-SH hydrogels were cross-linked with the peptide-modified PG-Acr, seeded with 20.0×10^6 MSCs/mL, and underwent chondrogenic differentiation for 21 days. Groups without any peptide modification served either as an unmodified control (Unmod. Ctr.) or as a negative control in which TGF-β1 was left out (Neg. Ctr.). Regarding cell viability, no significant differences could be seen for all investigated gels during the 21 day culturing period (data not shown).

In general, the control gels exhibited the usual staining patterns. Unmod. Ctr. gels showed a clear GAG staining with safranin O, which was not apparent in the Neg. Ctr. (Figure 5.14, A–B). In both gels a collagen I signal could be observed, that was more prominent and extensive in the Unmod. Ctr. gels (Figure 5.14, G–H). A staining of collagen II, on the other hand, was only detectable in the Unmod. Ctr. (Figure 5.14, M–N).

Compared to the Unmod. Ctr. gels, peptide modification with 1.0 mM HAV and 1.0 mM Scr showed no differences in safranin O staining for GAGs (Figure 5.14, C–D). The staining for collagen type I and II showed a stronger, more evenly distributed ECM signal in 1.0 mM HAV and Scr peptide-modified gels (Figure 5.14, I–J and O–P). 2.5 mM HAV modification, on the other hand, led to a significant decrease in staining for GAGs and collagen II, while the collagen I staining was affected to a lesser extent. Furthermore, peptide modification with 2.5 mM Scr yielded staining for the ECM components comparable to the Unmod. Ctr. (Figure 5.14, E–F, K–L and Q–R).

Modification with 5 mM KLER, 5 mM Scr peptide and 1 mM RGD yielded weaker safranin O staining of GAGs in comparison to the Unmod. Ctr. (Figure 5.15, C–E). Also immunofluorescence staining for collagen I and collagen II was weaker and less prominent

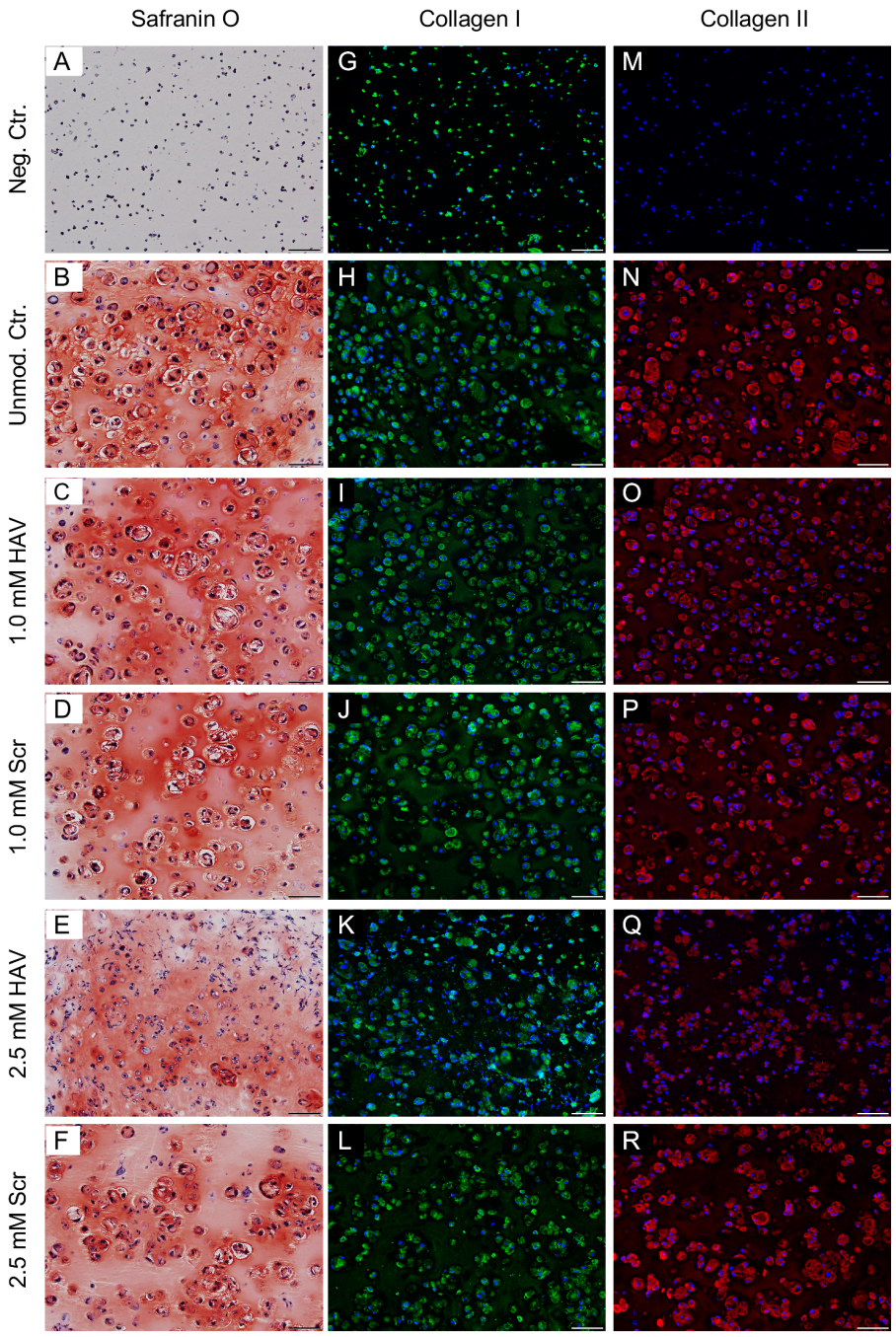

Figure 5.14: Histological and immunohistochemical staining of MSCs encapsulated in 1.0 mM HAV, Scr and 2.5 mM HAV, Scr peptide-modified HA-SH hydrogels cross-linked with 0.6% PG-Acr, seeded with 20.0×10^6 MSCs/mL, after 21 days of chondrogenic differentiation. Longitudinal sections were stained for deposition of GAGs with safranin O and collagen I (green) or collagen II (red) to show ECM development. Nuclei (blue) were counterstained with DAPI; scale bars represent 100 µm.

in these peptide-modified gels (Figure 5.15, H–J, M–O).

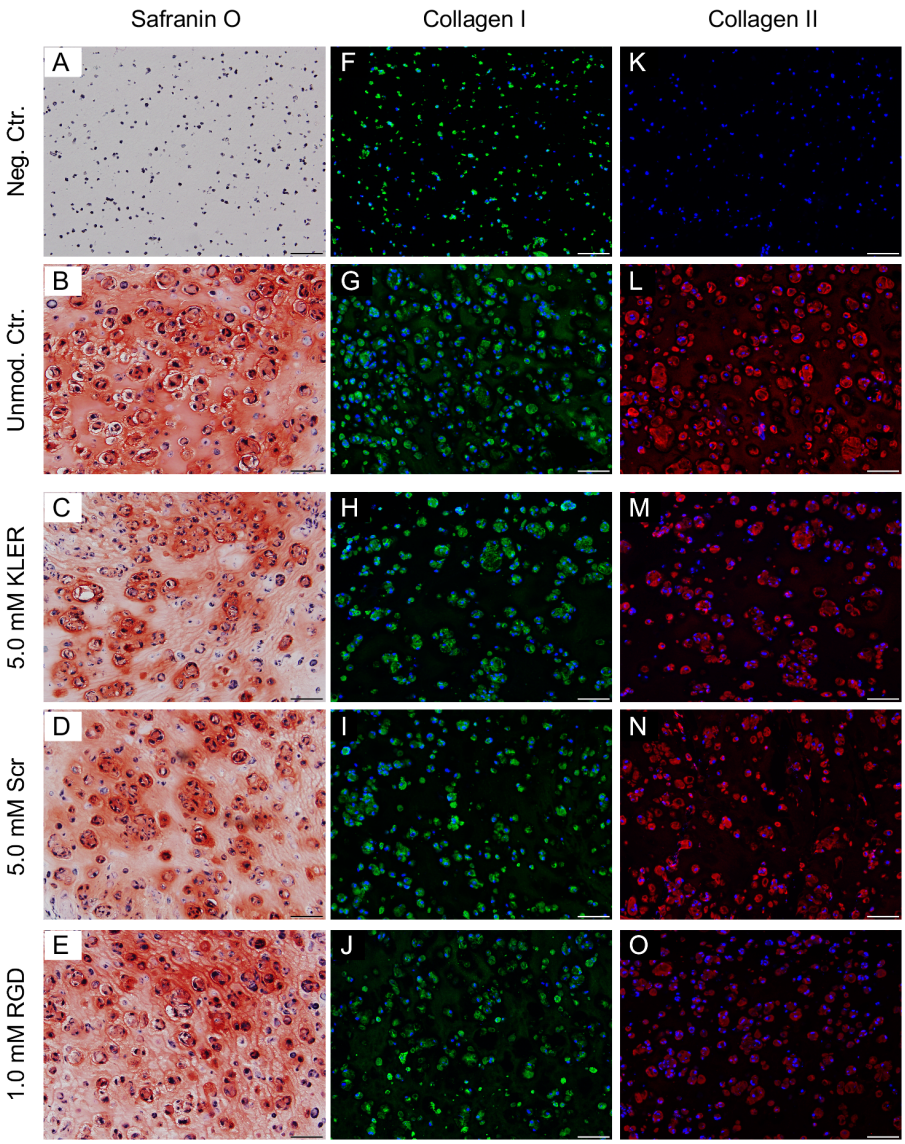

Figure 5.15: Histological and immunohistochemical staining of MSCs encapsulated in 5.0 mM KLER, Scr and 1.0 mM RGD peptide-modified HA-SH hydrogels cross-linked with 0.6% PG-Acr, seeded with 20.0×10^6 MSCs/mL, after 21 days of chondrogenic differentiation. Longitudinal sections were stained for deposition of GAGs with safranin O and collagen I (green) or collagen II (red) to show ECM development. Nuclei (blue) were counterstained with DAPI; scale bars represent 100 µm.

Interestingly, the determination of DNA amount showed on day 10 a significantly lower DNA amount in the Unmod. Ctr. gels compared to all other chondrogenically

induced gels. This difference did not persist until day 21, at this time the Unmod. Ctr. reached comparable DNA values (Figure 5.16, A). While the analysis of total GAG amount showed increased levels in the 1.0 mM HAV- (960.6 ± 59.5 µg/gel) and its corresponding 1.0 Scr-modified gels (1047.6 ± 97.0 µg/gel) compared to the Unmod. Ctr. group (832.2 ± 42.6 µg/gel), the GAG/DNA values of these groups reached similar levels at day 21. The 2.5 mM HAV- (21.4 ± 2.3 µg/µg), 5.0 mM KLER- (32.1 ± 3.6 µg/µg), Scr- (31.6 ± 2.9 µg/µg), and 1.0 mM RGD-modified gels (27.1 ± 2.1 µg/µg) gained substantially lower GAG/DNA quantities after 21 days of chondrogenic differentiation compared to Unmod. Ctr. gels (43.3 ± 4.5 µg/µg; Figure 5.16, B–C).

Remarkably, the 1.0 mM HAV- (12.6 ± 1.3 µg/µg) and Scr-modified hydrogels (12.6 ± 2.1 µg/µg) produced the highest amounts of collagen compared to all other gels at day 21, e.g., Unmod. Ctr. gels (9.5 ± 1.3 µg/µg). On the other hand, seemed peptide modification with 1.0 mM RGD (5.1 ± 0.5 µg/µg) to suppress collagen production notably on day 21 (Figure 5.17, A–B).

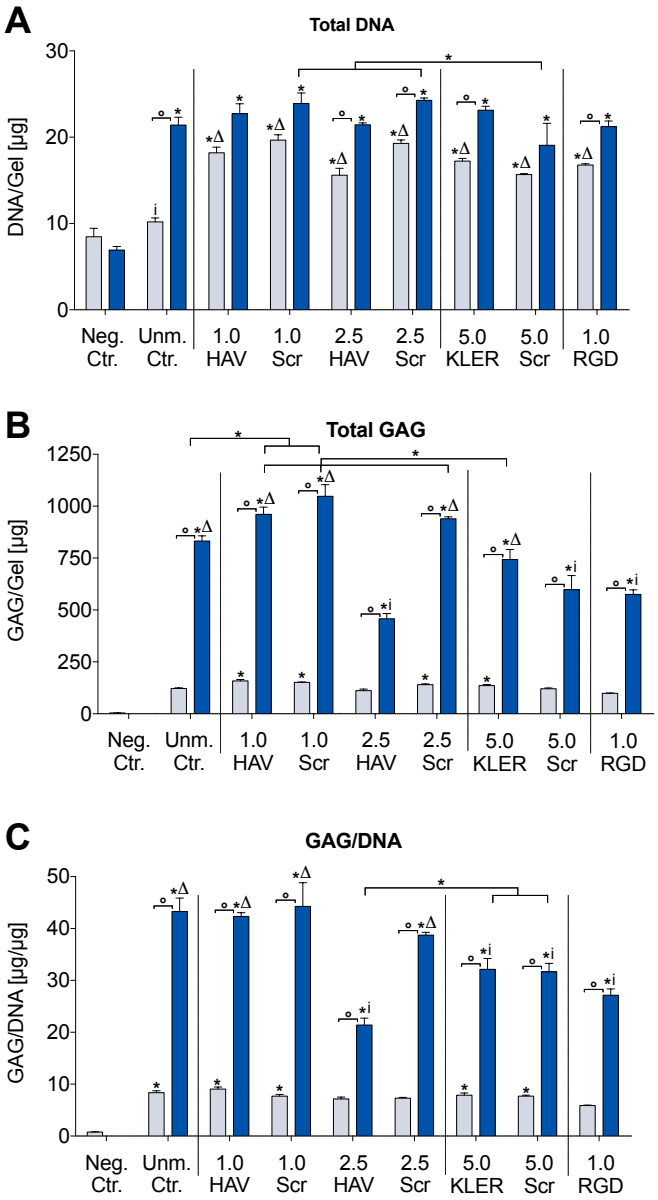

Figure 5.16: Effect of peptide modification on MSCs encapsulated in HA-SH hydrogels cross-linked with 0.6% PG-Acr, regarding total DNA amount (A), total GAG per gel (B) or normalized to DNA amount (C) after 10 and 21 days of chondrogenic differentiation. Numbers on the x-axis represent mM peptide concentrations. Data are presented as means ± standard deviation (n=3). Statistically significant differences between gels prepared with different peptides and control gels w/o TGF-β1 at the same time point are denoted with ($\star$) $p<0.05$, groups with a common (i) are statistically different to groups with a (Δ) $p<0.05$, additional significant differences between differently modified gels are indicated with a line and a ($\star$) $p<0.05$. Statistically significant differences between time points within a group are denoted with ($\circ$) $p<0.05$. Representative results of one of two independent experiments are shown.

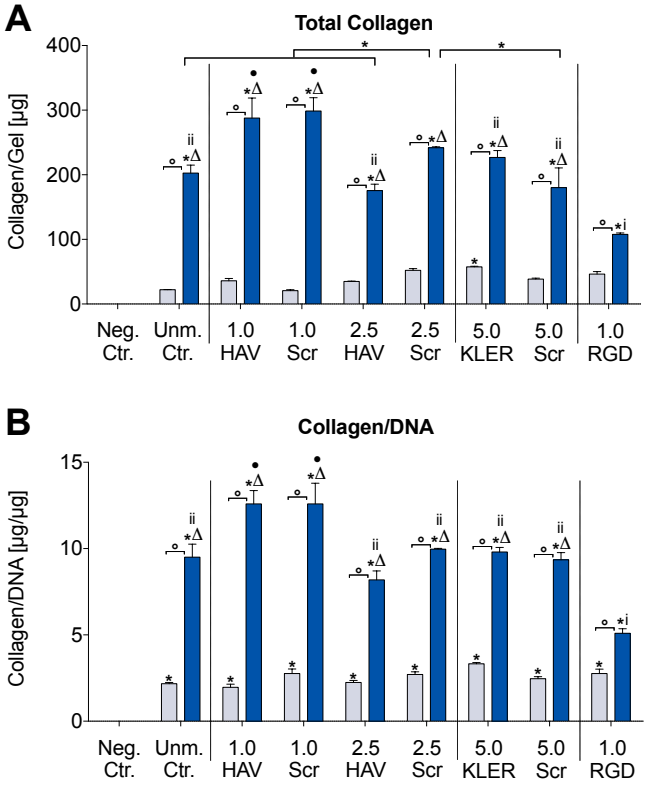

Figure 5.17: Effect of peptide modification on MSCs encapsulated in HA-SH hydrogels cross-linked with 0.6% PG-Acr, regarding total collagen amount per gel (A) or normalized to DNA amount (B) after 10 and 21 days of chondrogenic differentiation. Numbers on the x-axis represent mM peptide concentrations. Data are presented as means ± standard deviation (n=3). Statistically significant differences between gels prepared with different peptides and control gels w/o TGF-β1 at the same time point are denoted with ($\star$) $p<0.05$, groups with a common (i) are statistically different to groups with a (Δ) $p<0.05$, groups with a common (ii) are statistically different to groups with a ($\bullet$) $p<0.05$, additional significant differences between differently modified gels are indicated with a line and a ($\star$) $p<0.05$. Statistically significant differences between time points within a group are denoted with ($\circ$) $p<0.05$. Representative results of one of two independent experiments are shown.

5.2.2 Biomimetic Functionalization with Growth Factors

In order to include growth factor functionalization into the developed HA-SH hydrogels, TGF-β1 was first thiol-functionalized using Traut's reagent. In the next step thiol-functionalized TGF-β1 was bound to the cross-linker poly(glycidol)-acrylate (PG-Acr) by Michael addition. Subsequently, growth factor-modified PG-Acr was used to cross-link thiolated hyaluronic acid (Glycosil®) and thus the HA-SH gels were generated.

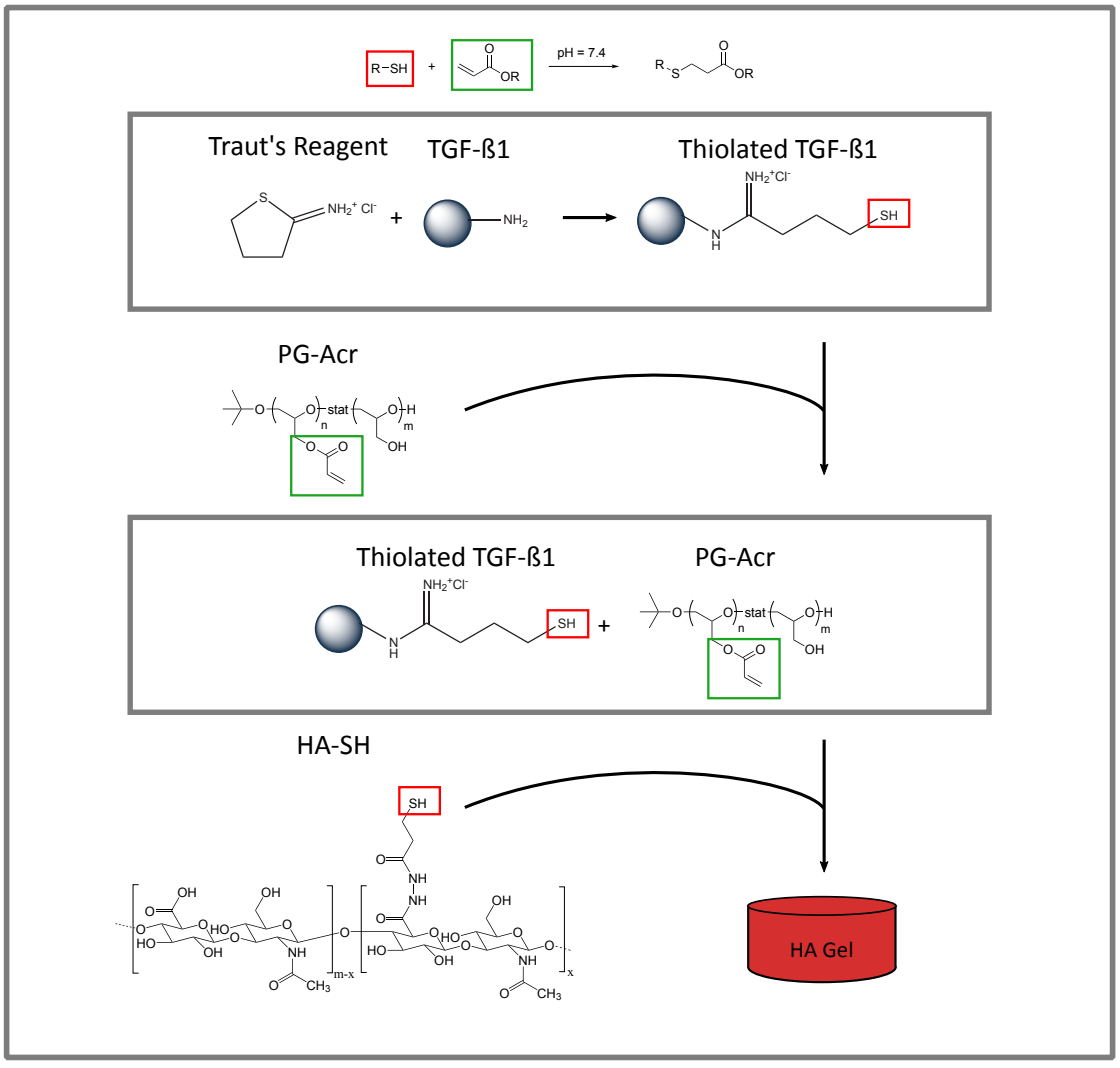

Figure 5.18: Cross-linking scheme of the biomimetic functionalization with TGF-β1 by using Michael addition. First, TGF-β1 was thiol-functionalized with Traut's reagent and then coupled to the cross-linker PG-Acr. Subsequently, thiolated HA (Glycosil®, HA-SH) was cross-linked with growth factor-modified cross-linker.

In the following experiments, TGF-β1 was covalently bound to PG-Acr and different amounts of TGF-β1 were incorporated into HA-SH gels in order to examine the effects of incorporated TGF-β1: 10, 50 and 100 nM (10, 50 and 100 nM TGF-β1 Traut). A group in which 100 nM TGF-β1 was merely mixed into the gels served as control, i.e., without thiol-functionalization of TGF-β1, and thus, without covalent binding (100 nM TGF-β1). A group cultured in medium without TGF-β1 served as a negative control (w/o TGF-β1). Gels that were cultured in TGF-β1-supplemented medium (addition with each medium change, standard concentration: 10 ng/µl) served as a standard control for *in vitro* chondrogenesis of MSCs (TGF-β1 Medium). The hydrogels were seeded with 20.0×10^6 MSCs/mL, and differentiated chondrogenically for 21 days *in vitro*.

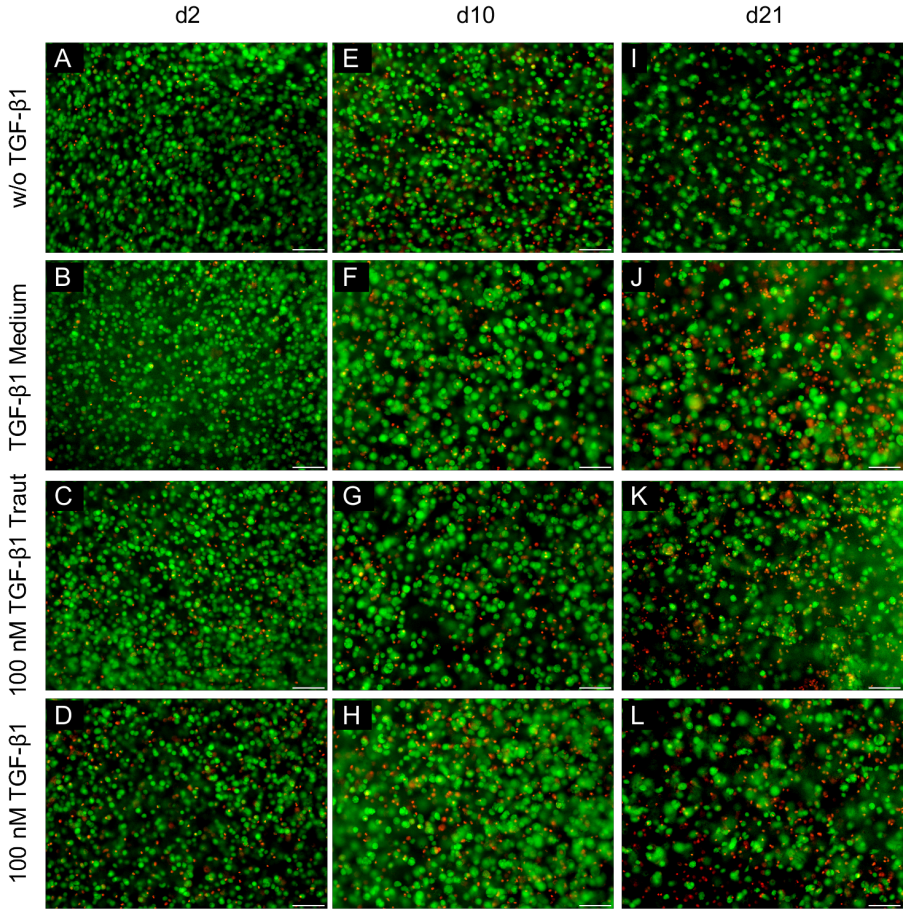

Figure 5.19: Cell viability of MSCs encapsulated in growth factor-laden HA-SH hydrogels, seeded with 20.0×10^6 MSCs/mL, after 2, 10 and 21 days of chondrogenic differentiation. Viable cells were labeled green with calcein-AM, and dead cells were labeled red with EthD-III; scale bars represent 100 µm.

All groups exhibited high amounts of viable cells during the 21 days culturing period. No considerable differences between the different amounts of tethered TGF-β1, and dosage forms of TGF-β1 could be seen (Figure 5.19; data for 10 and 50 nM TGF-β1 Traut not shown).

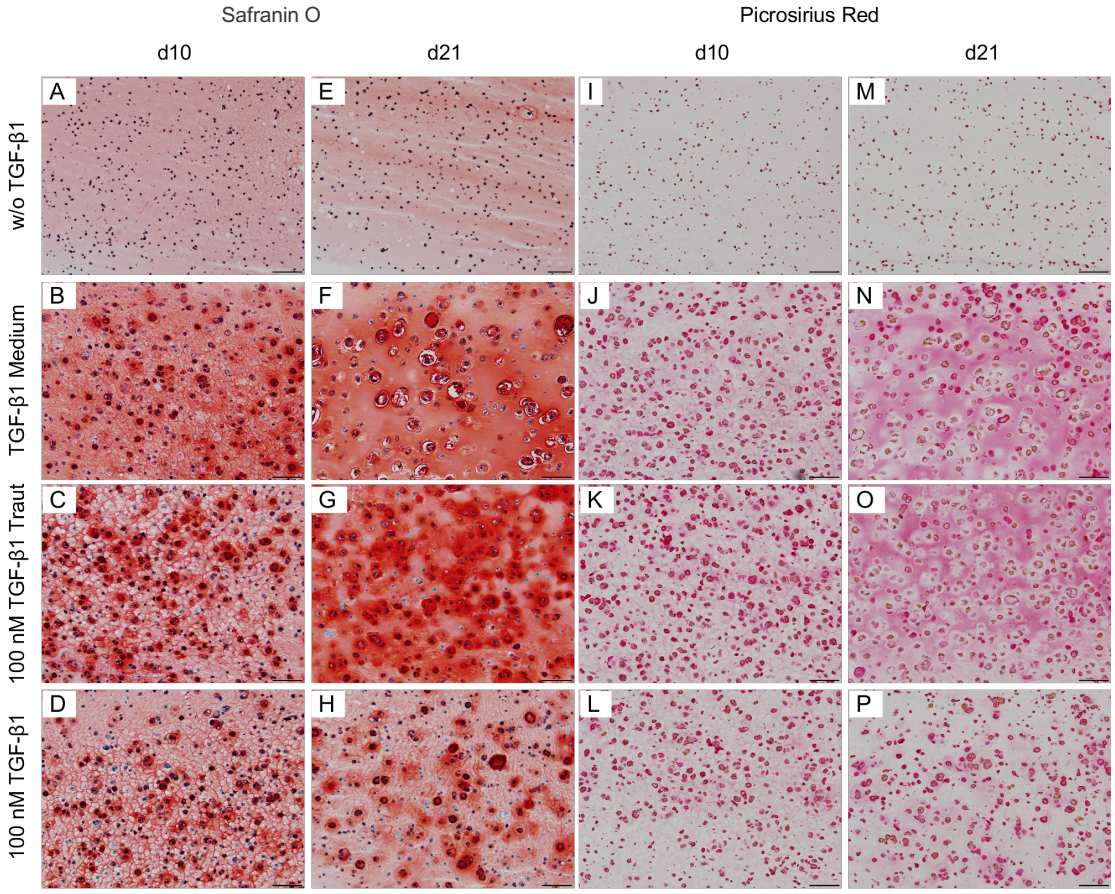

Figure 5.20: Histological staining of MSCs encapsulated in growth factor-laden HA-SH hydrogels cross-linked with 0.6% PG-Acr, seeded with 20.0×10^6 MSCs/mL, after 10 and 21 days of chondrogenic differentiation. Longitudinal sections were stained for deposition of GAGs with safranin O and collagens with picrosirius red; scale bars represent 100 µm.

MSCs cultured in gels w/o TGF-β1 showed, as expected, no cell-associated safranin O staining for GAGs, while the general collagen deposition was restricted to pericellular regions (Figure 5.20, A, E, I, M). In the TGF-β1 Medium group, a strong and increasingly uniform GAG staining could be seen. The 100 nM TGF-β1 Traut gels exhibited a comparable GAG signal on day 10, which appeared to be superior on day 21, but more pericellularly pronounced. Hydrogels in which 100 nM TGF-β1 was merely mixed into demonstrated a clearly lesser extent of GAG deposition at both time points (Figure 5.20,

B–D, F–H). Picrosirius red staining showed comparable collagen deposition patterns in the TGF-β1 Medium and 100 nM TGF-β1 Traut gels on day 10. After 21 days, the collagen staining in both groups became more extensive, while the TGF-β1 Medium group showed a more pericellular pronounced and overall stronger signal compared to 100 nM TGF-β1 Traut group. On the other hand, showed the 100 nM TGF-β1 gels mainly pericellular signals at both time points (Figure 5.20, J–L, N–P). Results for the 10 nM Traut group were comparable to gels cultured w/o TGF-β1, while gels in the 50 nM TGF-β1 Traut group produced only neglectable amounts of GAG and collagen (data for 10 and 50 nM TGF-β1 Traut not shown).

The biochemical quantification of DNA amount showed that gels cultured w/o TGF-β1 or when modified with 10 and 50 nM TGF-β1 did not proliferate from day 10 to 21. In contrast to that, gels cultured in TGF-β1 Medium and the group with 100 nM TGF-β1 Traut nearly doubled their DNA content on day 21 compared to the control group w/o TGF-β1. The DNA levels of the 100 nM TGF-β1 group were also increased, compared to gels w/o TGF-β1, but were lower than in the TGF-β1 Medium and 100 nM TGF-β1 Traut groups (Figure 5.21, A).

The results of the GAG/DNA amount showed only a insignificant proteoglycan production for gels cultured w/o TGF-β1 and in the 10 nM TGF-β1 Traut group. Therefore, the concentration of 10 nM TGF-β1 was not sufficient to induce a noticeable GAG production. The 50 nM TGF-β1 Traut group exhibited only on day 21 indications of GAG production, but still on a low level (4.8 ± 2.5 µg/µg). The 100 nM TGF-β1 Traut group produced already large GAG amounts after 10 days (10.7 ± 1.1 µg/µg), and significant higher amounts after 21 days (26.6 ± 2.3 µg/µg), especially in comparison to gels of the 100 nM TGF-β1 group. Gels in which 100 nM TGF-β1 was just mixed into, reached considerable lower levels at both time points compared to the Traut-modified group (day 10: 3.8 ± 0.6 µg/µg, day 21: 13.0 ± 2.7 µg/µg). On the other hand, the standard control, TGF-β1 Medium, already showed a significant increase in GAG production at day 10 (10.8 ± 0.1 µg/µg) that became even bigger at day 21 (17.2 ± 3.1 µg/µg), but it was surprisingly significant lower than in the 100 nM TGF-β1 Traut group. The total GAG production per gel resembled the GAG/DNA findings to a large extent, whereby the 100 nM TGF-β1 Traut group clearly produced the highest amounts at day 21 (485.6 ± 73.0 µg/gel) (Figure 5.21, B, C).

The hydroxyproline assay was performed to determine the production of total collagen and showed mainly similar tendencies as the DMMB assay, e.g. gels cultured w/o TGF-β1 produced the lowest amounts of collagen/DNA at both time points again. The main differences observed by determination of collagen were thereby that now the TGF-β1 Medium group reached the highest levels after 21 days of *in vitro* chondrogenesis

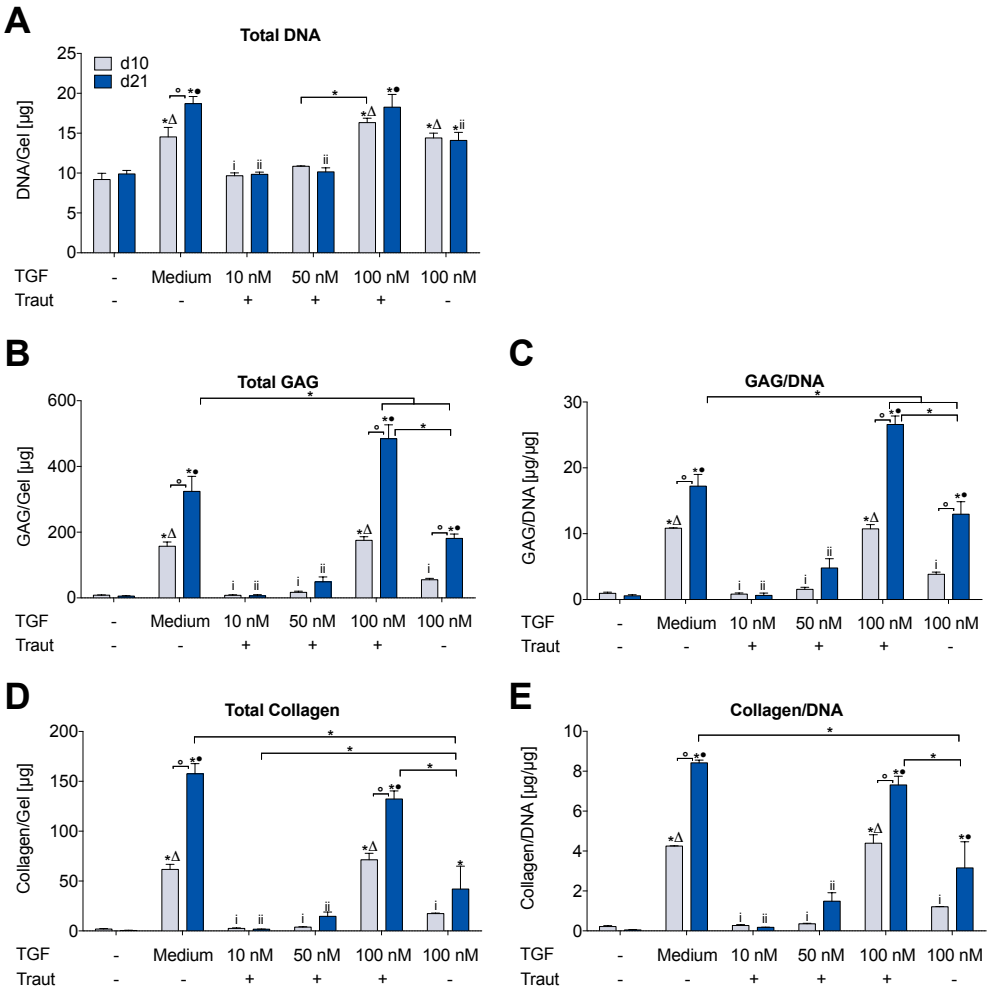

Figure 5.21: Effect of growth factor modification on MSCs encapsulated in HA-SH hydrogels cross-linked with 0.6% PG-Acr, regarding total DNA amount (A) as well as total GAG (B) and collagen (D) per gel or normalized to DNA amount (C, E) of hydrogels after 10 and 21 days of chondrogenic differentiation. Data are presented as means ± standard deviation (n=3). Statistically significant differences between different TGF-β1-modified and control gels w/o TGF-β1 at the same time point are denoted with (⋆) $p<0.05$, groups with a common (i) are statistically different to groups with a (Δ) $p<0.05$, groups with a common (ii) are statistically different to groups with a (•) $p<0.05$, additional significant differences between differently modified gels are indicated with a line and a (⋆) $p<0.05$. Statistically significant differences between time points within a group are denoted with (○) $p<0.05$. Representative results of one of three independent experiments are shown.

($8.4 \pm 0.2\,\mu g/\mu g$). But not to a significantly higher extent when compared to the 100 nM TGF-β1 Traut modified gels ($7.3 \pm 0.8\,\mu g/\mu g$). In total, the TGF-β1 Medium treated gels produced with $157.7 \pm 17.5\,\mu g$/gel the highest levels of collagen per gel after 21 days (Figure 5.21, D, E). This increase in collagen production was already seen in the picrosirius red staining in the TGF-β1 Medium gels compared to the 100 nM TGF-β1 Traut gels at day 21 (Figure 5.20, N, O), and thus was reflected in hydroxyproline assay.

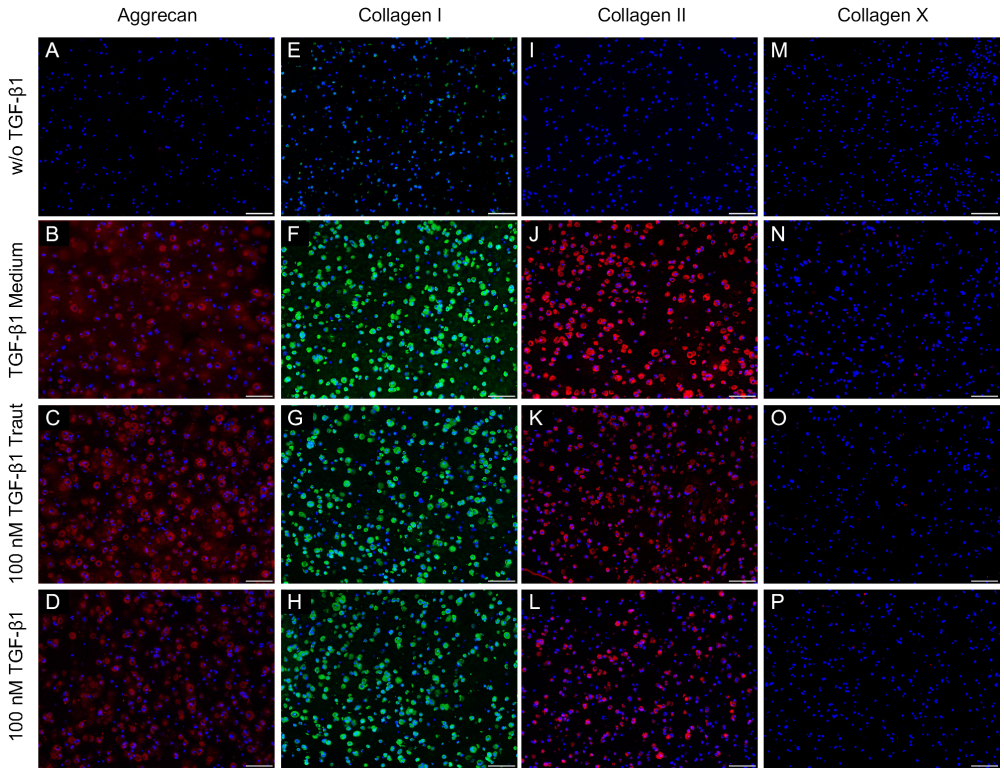

Figure 5.22: Immunohistochemical staining of MSCs encapsulated in growth factor-laden HA-SH hydrogels cross-linked with 0.6% PG-Acr, seeded with 20.0×10^6 MSCs/mL, after 10 days of chondrogenic differentiation. Longitudinal sections were stained for collagen I (green), aggrecan, collagen II and collagen X (red) to show ECM development. Nuclei (blue) were counterstained with DAPI; scale bars represent 100 µm.

Immunohistochemistry (IHC) at day 10 showed that gels cultured w/o TGF-β1 lacked in the production of cartilage-specific ECM components, like aggrecan and collagen type II. Gels cultured with 100 nM TGF-β1 Traut or in the TGF-β1 Medium group exhibited already at day 10 distinct and equal aggrecan signals. The aggrecan signal in 100 nM TGF-β1 group was clearly weaker (Figure 5.22, A–D). Regarding type I collagen, gels cultured w/o TGF-β1 produced just low amounts in the pericellular region, whereas the other three groups seemed to deposit comparable higher amounts of collagen I into the gel

matrix (Figure 5.22, E–H). Additionally, produced gels that were cultured w/o TGF-β1, as expected, no type II collagen. The strongest and most prominent staining for type II collagen exhibited gels cultured in the TGF-β1 Medium group. In the 100 nM TGF-β1 Traut group the overall signal was weaker and less pronounced in the pericellular region. Compared to this, the 100 nM TGF-β1 group showed less signal in total, but a more intense pericellular staining in comparison to the Traut-modified group (Figure 5.22, I–L). Analysis of the hypertrophy marker collagen X showed no signal at the early stage of chondrogenic differentiation in all investigated groups (Figure 5.22, M–P; data for 10 and 50 nM TGF-β1 Traut not shown).

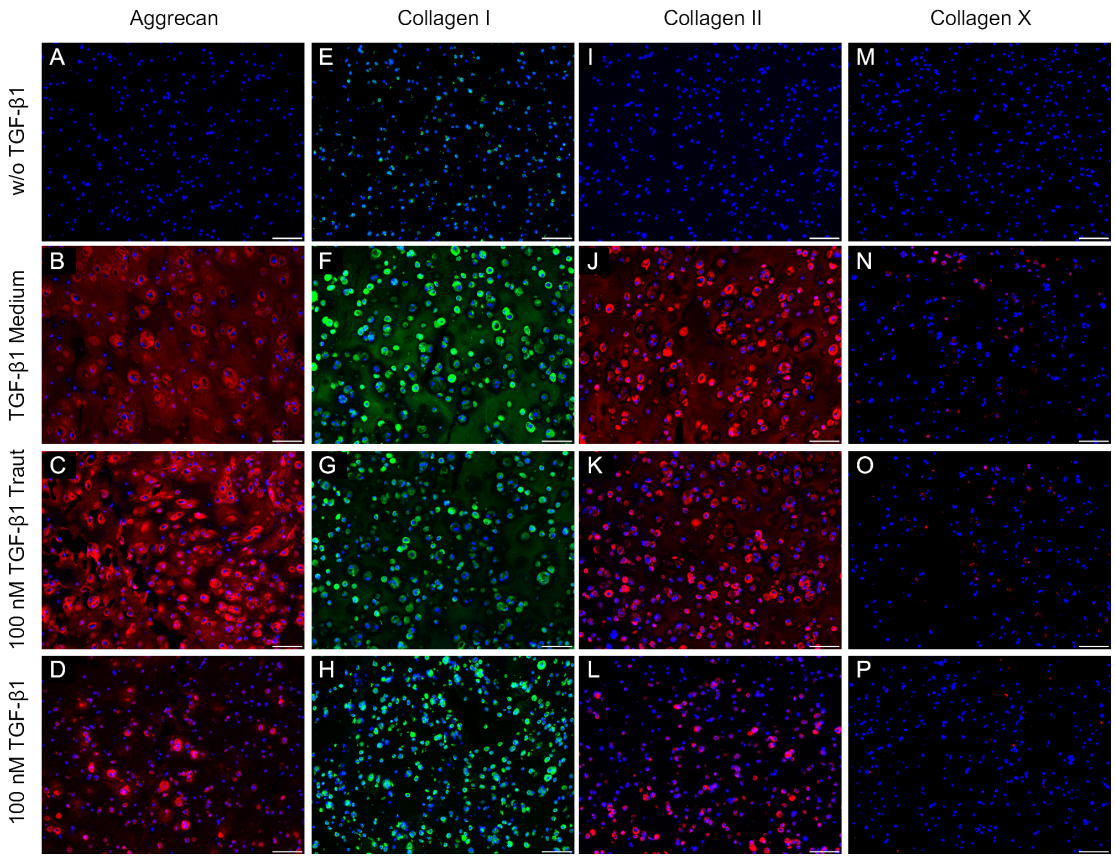

Figure 5.23: Immunohistochemical staining of MSCs encapsulated in growth factor-laden HA-SH hydrogels cross-linked with 0.6% PG-Acr, seeded with 20.0×10^6 MSCs/mL, after 21 days of chondrogenic differentiation. Longitudinal sections were stained for collagen I (green), aggrecan, collagen II and collagen X (red) to show ECM development. Nuclei (blue) were counterstained with DAPI; scale bars represent 100 µm.

At day 21, gels cultured w/o TGF-β1 exhibited, as expected, no signals for aggrecan, type II collagen, and type X collagen, while the type I collagen signal was restricted

only to pericellular regions (Figure 5.23, A, E, I, M). The strongest, most intensive and spread aggrecan staining showed the 100 nM TGF-β1 Traut group. TGF-β1 Medium gels presented an extensive staining over the entire gel, but with no clear pericellular signal. On the other hand, the 100 nM TGF-β group demonstrated some clear pericellular signals, but in total the fewest and weakest aggrecan signals (Figure 5.23, B–D). Gels of the TGF-β1 Medium group deposited collagen I into the gel and showed strong pericellular signals. The type I collagen signal in the 100 nM TGF-β1 Traut was well distributed over the gel section but to a lesser extent. Compared to this, the 100 nM TGF-β1 gels showed rather strong pericellular signals (Figure 5.23, F–H). The most prominent pericellular staining and the most extended deposition of collagen type II into the gel was achieved by the TGF-β1 Medium group. The 100 nM TGF-β1 Traut demonstrated a dimmer pericellular signal and a less pronounced deposition into the gel. In contrast to that, the group with 100 nM TGF-β1 showed several pericellular stainings, but no incorporation into the gel matrix (Figure 5.23, J–L). While the TGF-β1 Medium group and the 100 nM TGF-β1 Traut group showed some, but very rarely signals for collagen X, the 100 nM TGF-β1 gels showed hardly any collagen X signals (Figure 5.23, N–P; data for 10 and 50 nM TGF-β1 Traut not shown).

The time course for gene expression profiles of *COL1A1* which is upregulated in the early chondensation phase of chondrogenesis and usually decreases during cartilage development, the chondrogenic marker genes *COL2A1*, *ACAN*, *SOX9*, *ALK-5* (TGF-β receptor 1), and *COL10A1* as marker for beginning of osteogenic differentiation were assessed using qRT-PCR. *COL1A1* expression increased initially until day 15 in the 100 nM TGF-β1 Traut and the 100 nM TGF-β1 group compared to the TGF-β1 Medium group, but decreased at day 21 as chondrogenesis prolonged (Figure 5.24, A). Expression profiles of the chondrogenic marker genes *COL2A1*, *ACAN* and *SOX9*, were clearly upregulated at day 15 and 21 in the TGF-β1 Medium, 100 nM TGF-β1 Traut and 100 nM TGF-β1 groups compared to the negative control group w/o TGF-β1, which expressed only very low levels of the chondrogenic marker genes (Figure 5.24, B–D). At day 21 the 100 nM TGF-β1 Traut showed even a significantly upregulation of *COL2A1*, *ACAN* and *SOX9*, compared to the other chondrogenically induced groups. The expression of *ALK-5*, the receptor mediating TGF-β1 signaling to the Smad-dependent pathway, was significantly upregulated in the 100 nM TGF-β1 Traut group at day 15 and 21, and in the TGF-β1 Medium group after 15 days of *in vitro* culture (Figure 5.24, F). The expression of the osteogenic and hypertrophic marker gene *COL10A1* was also elevated in all chondrogenically induced groups, in comparison to the gels cultured w/o TGF-β1 at later points in time. The 100 nM TGF-β1 Traut group showed a significant upregulation

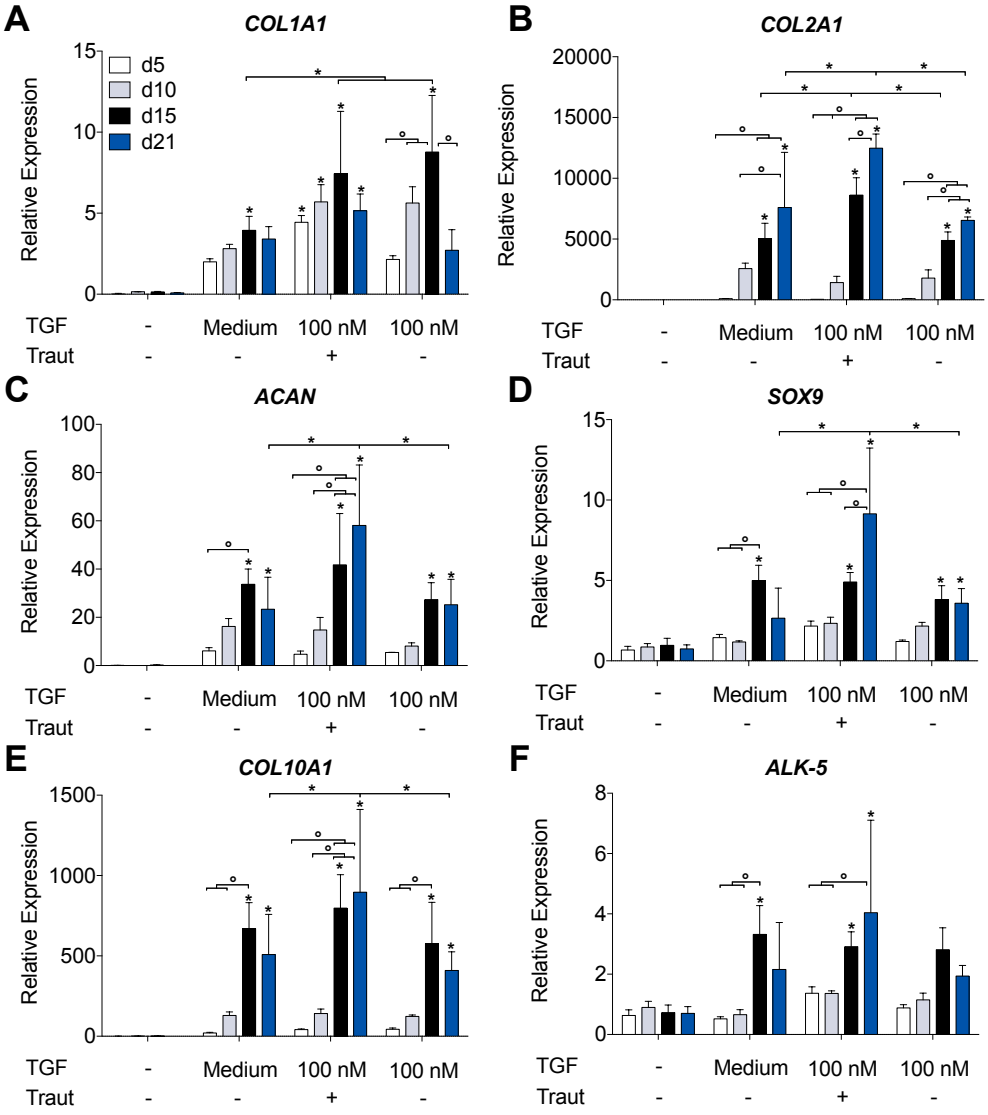

Figure 5.24: Effect of growth factor modification on MSCs encapsulated in HA-SH hydrogels on the time course of gene expression after 5, 10, 15 and 21 days of MSC chondrogenesis, determined by qRT-PCR. Gene expression levels were normalized to the housekeeping gene *GAPDH* and the obtained values were further normalized to expression levels at day 0. Data are presented as means ± standard deviation (n=3). Statistically significant differences between different TGF-β1-modified and control gels w/o TGF-β1 at the same time point are denoted with (⋆) $p<0.05$. Additional significant differences between differently modified gels are indicated with a line and a (⋆) $p<0.05$. Statistically significant differences between time points within a group are denoted with (∘) $p<0.05$. Representative results of one of two independent experiments are shown.

of *COL10A1* at 21 day of differentiation in contrast to the TGF-β1 Medium and the

100 nM TGF-β1 group (Figure 5.24, E).

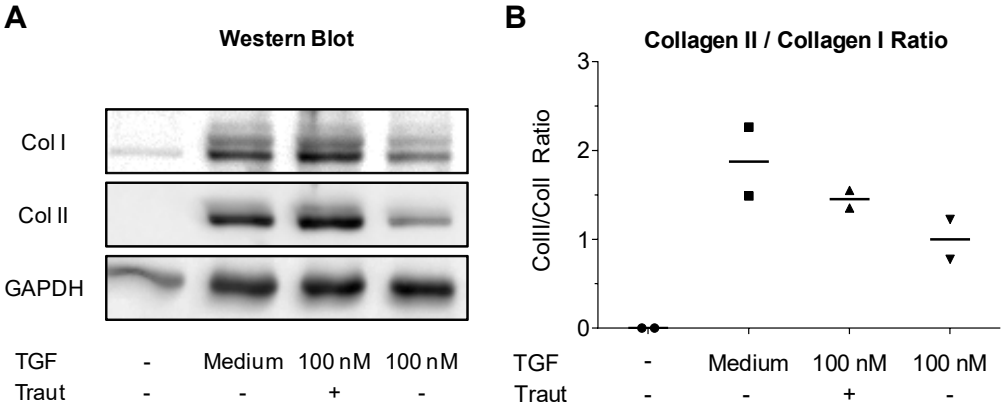

Figure 5.25: Effect of growth factor modification on MSCs encapsulated in HA-SH hydrogels, regarding protein production after 21 days of chondrogenic differentiation, shown by Western Blot analysis. Antibodies against ECM molecules collagen I and collagen II were used, GAPDH was used as loading control (A). Collagen I and collagen II protein expression was densitometrically analyzed using Fiji, and a ratio was calculated. The results are stated in the graph. The ratio for 100 nM TGF-β1 was set to 1, and the results of the other groups are shown in relation (n=2)(B).

Another approach to evaluate the quality of chondrogenesis was to measure the amount of protein expression of type I and type II collagen, using Western Blot analysis.

Here, Western Blot analysis showed clearly that gels cultured w/o TGF-β1 produced no collagen II, as well as a lower protein expression of collagen I and the loading control GAPDH in general. MSCs encapsulated within gels of the 100 nM TGF-β1 Traut group seemed to produce more collagen II and collagen I, when compared to the TGF-β1 Medium group. Compared to both other chondrogenically induced groups, the protein bands for type I and type II collagen in the 100 nM TGF-β1 group appeared distinctly weaker in total (Figure 5.25, A). Comparing 100 nM TGF-β1 Traut group with the 100 nM TGF-β1 mixed group, the Traut group not only showed distinctly stronger signals for type I and type II collagens, moreover, it appeared as if also the ratio of collagen II/collagen I was slightly increased (Figure 5.25, B).

In summary, the covalent incorporation of 100 nM TGF-β1 using Traut's reagent led to a distinctly improved chondrogenic differentiation compared to the group in which 100 nM TGF-β1 was merely mixed into gels. While, with regard to collagens, advantages for the TGF-β1 Medium were detected (Figures 5.21 to 5.23 and 5.25), with regard to GAG production and gene expression profiles the 100 nM TGF-β1 Traut group appeared even superior to the standard TGF-β1 Medium group (Figures 5.20, 5.21, 5.23 and 5.24).

5.3 Biomimetic Functionalization of Pure Poly(glycidol) Hydrogels

In the following section, the general material suitability for chondrogenic differentiation and the effect of biomimetic functionalization of pure poly(glycidol) (PG) hydrogels without the supportive background of hyaluronic acid was analyzed. The gels were cross-linked by the utilization of UV-initiated thiol-ene reaction, in a first proof-of-principle experiment. A cysteine-modified peptide was coupled to allyl-modified PG (P(AGE/G)) and simultaneously thiolated PG (PG-SH) was cross-linked with P(AGE/G), as shown in Figure 5.26.

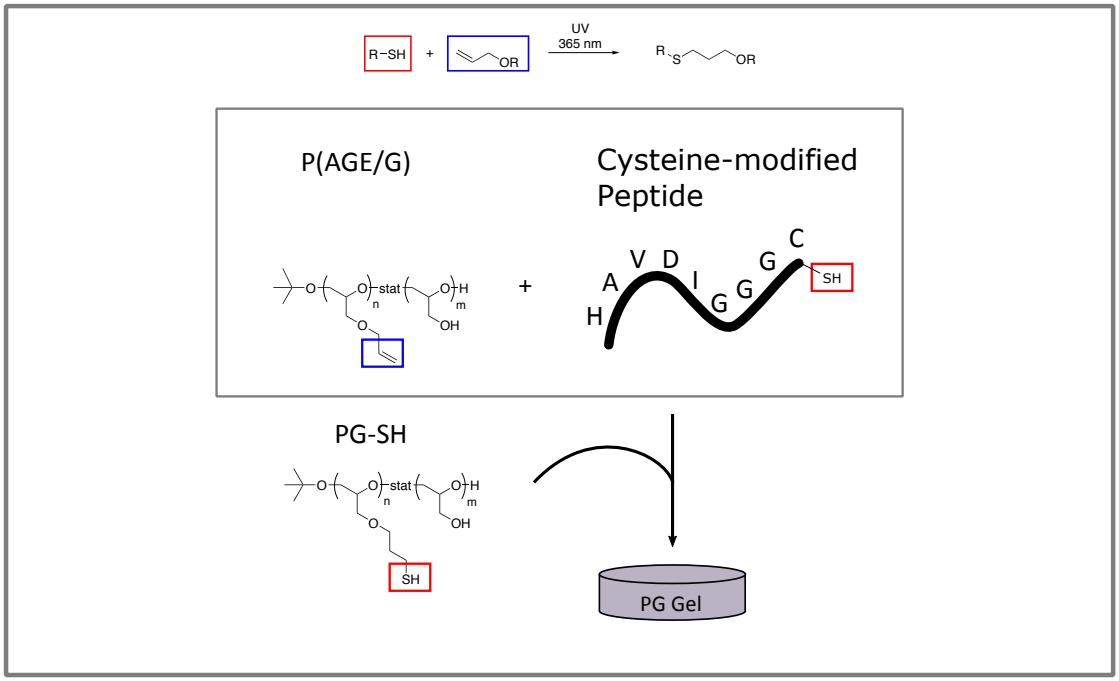

Figure 5.26: Cross-linking scheme of the generation of UV-cross-linked pure PG hydrogels by using thiol-ene reaction. The gels were modified with a N-cadherin mimetic peptide sequence. The cysteine-modified peptide is coupled in a one-step procedure to P(AGE/G) and, at the same time, PG-SH is cross-linked with the peptide-modified P(AGE/G).

The pure PG gels were seeded with 20.0×10^6 MSCs/mL, and differentiated chondrogenically for 21 days. The hydrogels were either modified with 1.0 mM HAV or the related scrambled motif (Scr) (Table 5.2 on page 61). In a third group, the PG gel without any peptide modification served as a unmodified control (Unmod. Ctr.).

With regard to cell viability, the HAV and Scr modification of PG gels improved the number of viable cells compared to unmodified gels already after two days of culturing

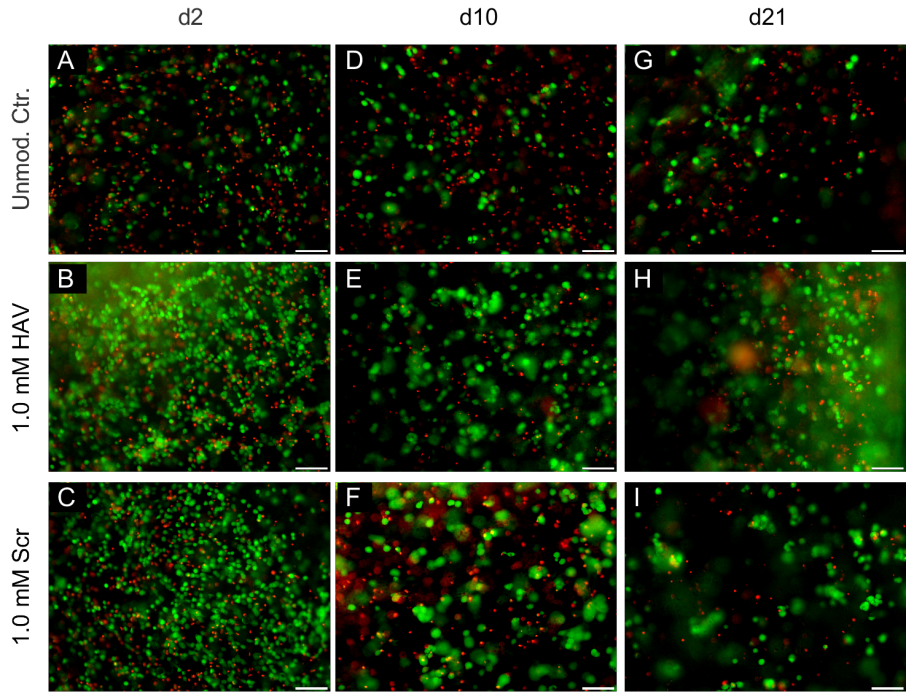

Figure 5.27: Cell viability of MSCs encapsulated in peptide-modified or unmodified pure PG hydrogels, seeded with 20.0×10^6 MSCs/mL, after 2, 10 and 21 days of chondrogenic differentiation. Viable cells were labeled green with calcein-AM, and dead cells were labeled red with EthD-III; scale bars represent 100 µm.

(Figure 5.27, A–C). The highest number of viable cells were observed in 1.0 mM HAV-modified gels at day 10 and day 21 (Figure 5.27, D–I).

Chondrogenesis of MSCs was visualized by staining of GAGs with safranin O, and by IHC for the presence of ECM components collagen I, collagen II and aggrecan. MSCs cultured in HAV-modified PG gels showed the most, but mainly pericellular-associated staining of GAGs at day 10. Unmodified gels exhibited only marginal safranin O staining (Figure 5.28, A–C). Similar staining patterns could be seen for aggrecan (Figure 5.28, D–F). Compared to the two other groups, HAV modification of gels led to the strongest staining for collagen I and II, while no clear differences in collagen signals could be seen between unmodified and Scr-modified gels (Figure 5.28, G–L).

After 21 days the differences between the three groups became more obvious. HAV-modified gels demonstrated the strongest GAG signal, with a significant deposition into the gel matrix. Deposition of GAGs in Scr-modified gels was as well more pronounced compared to unmodified gels (Figure 5.29, A–C). The same relation was found for aggrecan staining (Figure 5.29, D–F). The strongest signals for collagen I and collagen II were also found in HAV-modified gels. The scrambled modified gels again showed enhanced signals for both types of collagens compared to unmodified gels (Figure 5.29, G–L).

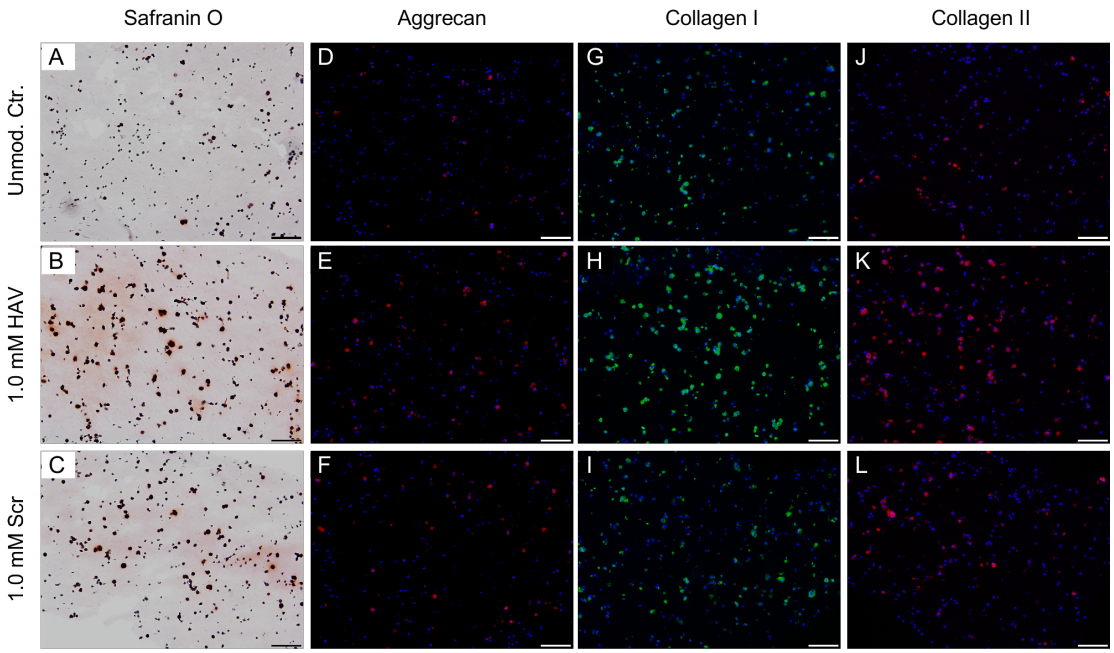

Figure 5.28: Histological and immunohistochemical staining of MSCs encapsulated in peptide-modified and unmodified pure PG hydrogels, seeded with 20.0×10^6 MSCs/mL, after 10 days of chondrogenic differentiation. Longitudinal sections were stained for deposition of GAGs with safranin O, collagen I (green), collagen II and aggrecan (red) to show ECM development. Nuclei (blue) were counterstained with DAPI; scale bars represent 100 µm.

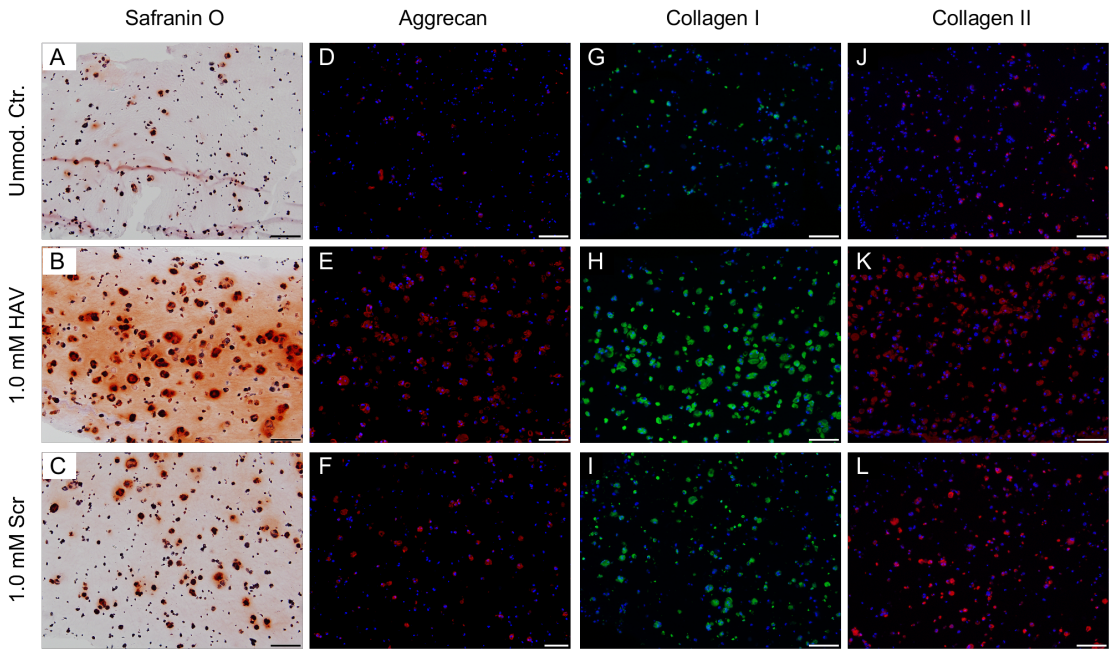

Figure 5.29: Histological and immunohistochemical staining of MSCs encapsulated in peptide-modified and unmodified pure PG gels, seeded with 20.0×10^6 MSCs/mL, after 21 days of chondrogenic differentiation. Longitudinal sections were stained for deposition of GAGs with safranin O, collagen I (green), collagen II and aggrecan (red) to show ECM development. Nuclei (blue) were counterstained with DAPI; scale bars represent 100 µm.

The quantification of DNA amount showed that the cell number in the unmodified control gels cells decreased from day 10 ($6.8 \pm 1.0\,\mu g$/gel) to day 21 ($2.8 \pm 0.8\,\mu g$/gel), while it remained stable in HAV- and Scr-modified gels (Figure 5.30, A). The 1.0 mM HAV-modified gels showed a significant increase of GAG/DNA amount at day 10 and 21 compared to unmodified PG gels. In comparison to the Scr-modified gels ($8.3 \pm 0.2\,\mu g/\mu g$), the GAG/DNA content in the 1.0 mM HAV gels ($14.4 \pm 2.5\,\mu g/\mu g$) was significantly elevated after 21 days. The same pattern and differences could be seen for collagen/DNA amount on day 21 of chondrogenic differentiation (HAV: $8.7 \pm 2.2\,\mu g/\mu g$, Scr: $4.1 \pm 1.2\,\mu g/\mu g$) (Figure 5.30, B–E).

In this proof-of-principle experiment, the obtained histological, immunohistochemical, and biochemical data correlated very well and showed the general suitability of pure PG gels for the analysis of single peptide effects on chondrogenesis of MSCs.

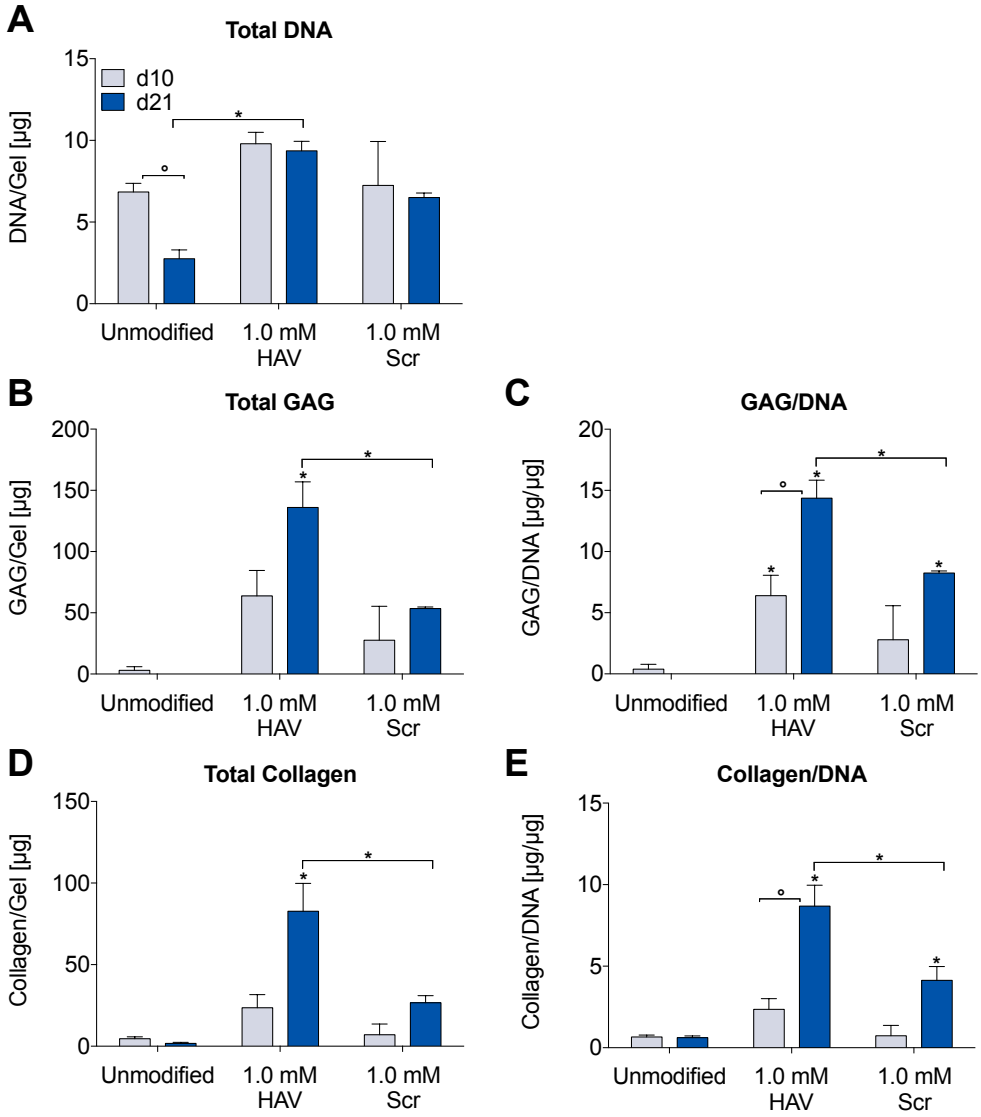

Figure 5.30: Effect of peptide modification on MSCs encapsulated in pure PG hydrogels, regarding total DNA amount (A) as well as total GAG (B) and collagen (D) per gel or normalized to DNA amount (C, E) after 10 and 21 days of chondrogenic differentiation. Data are presented as means ± standard deviation (n=3). Statistically significant differences between modified and unmodified control gels at the same time point are denoted with ($\star$) $p<0.05$, additional significant differences between differently modified gels are indicated with a line and a ($\star$) $p<0.05$. Statistically significant differences between time points within a group are denoted with ($\circ$) $p<0.05$.

5.4 Zonal Gels - Combination of HA Gels and PG Gels

In this section, the feasibility of zonal gels for chondrogenic differentiation of MSCs was assessed in a preliminary experiment, as part of the HydroZONES project. Therefore, first, a hydrogel bottom layer consisting of HA-SH_{FMZ} and P(AGE/G) was cross-linked based on UV-initiated thiol-ene reaction. Both hydrogels were seeded again with 20.0×10^6 MSCs/mL. Subsequently, a smaller top layer hydrogel, analog to the pure PG hydrogel in Section 5.3, was cast and cross-linked on top of the HA-layer (Figure 5.31). HA-SH_{FMZ} bottom zone hydrogels were cross-linked by thiol-ene click-chemistry between HA-SH_{FMZ} and P(AGE/G). PG top zone hydrogels, generated by cross-linking of PG-SH and P(AGE/G), were cast on top of the HA-SH gels. Constructs were differentiated chondrogenically for 28 days *in vitro*. MSCs encapsulated in fibrin gels served, according to the HydroZONES guidelines, as a control group.

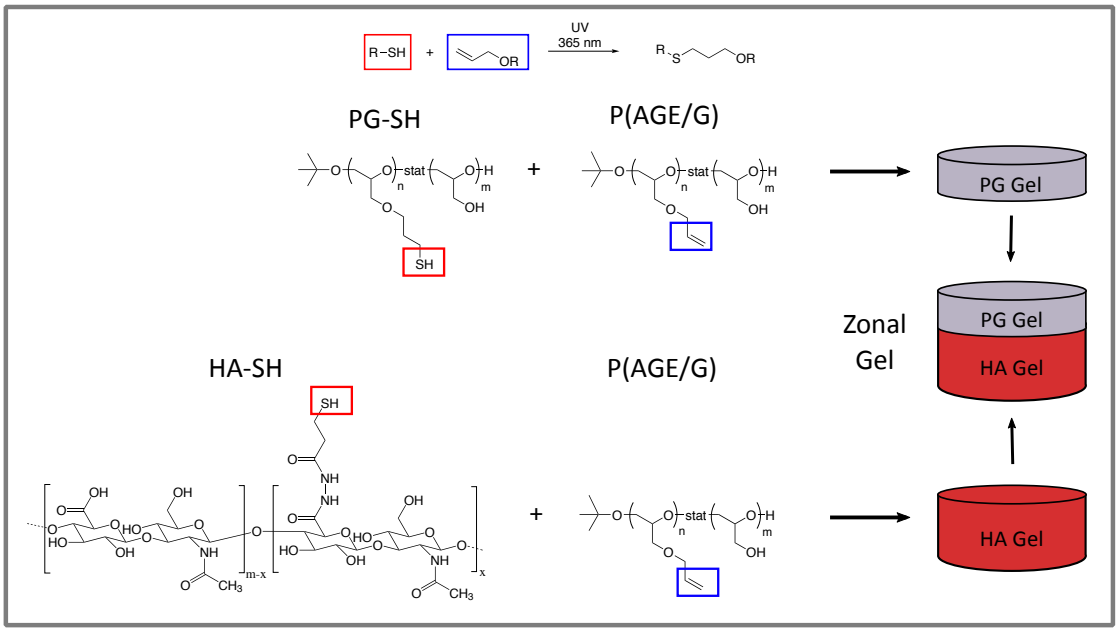

Figure 5.31: Cross-linking scheme of the generation of UV-cross-linked zonal hydrogels by using thiol-ene reaction. First, a bottom layer consisting of HA-SH_{FMZ} and P(AGE/G) was cross-linked. Subsequently, a pure PG gel (PG-SH and P(AGE/G)) top layer was cast on the HA-SH_{FMZ} containing bottom layer.

During the 28 day culturing period zonal gels kept their shape, were good to handle, and the top zone and the bottom zone gels stuck together and did not separate, while fibrin gels shrank.

Considering cell viability, the number of dead cells increased from day 1 to 28 in zonal

and fibrin control gels. (Figure 5.32 **a**). The number of dead cells in the PG-SH top-layer seemed to be a bit higher compared to the HA-SH_{FMZ} gel on the bottom after 28 days (Figure 5.32, **a** D–E). The border between the PG-SH top zone and the HA-SH_{FMZ} bottom zone could be seen very good in specially prepared longitudinal sections of the zonal gels. Thereby, the zonal organization and cellular distribution within the zonal gels was illustrated and showed no significant differences between both zones (Figure 5.32, **b**).

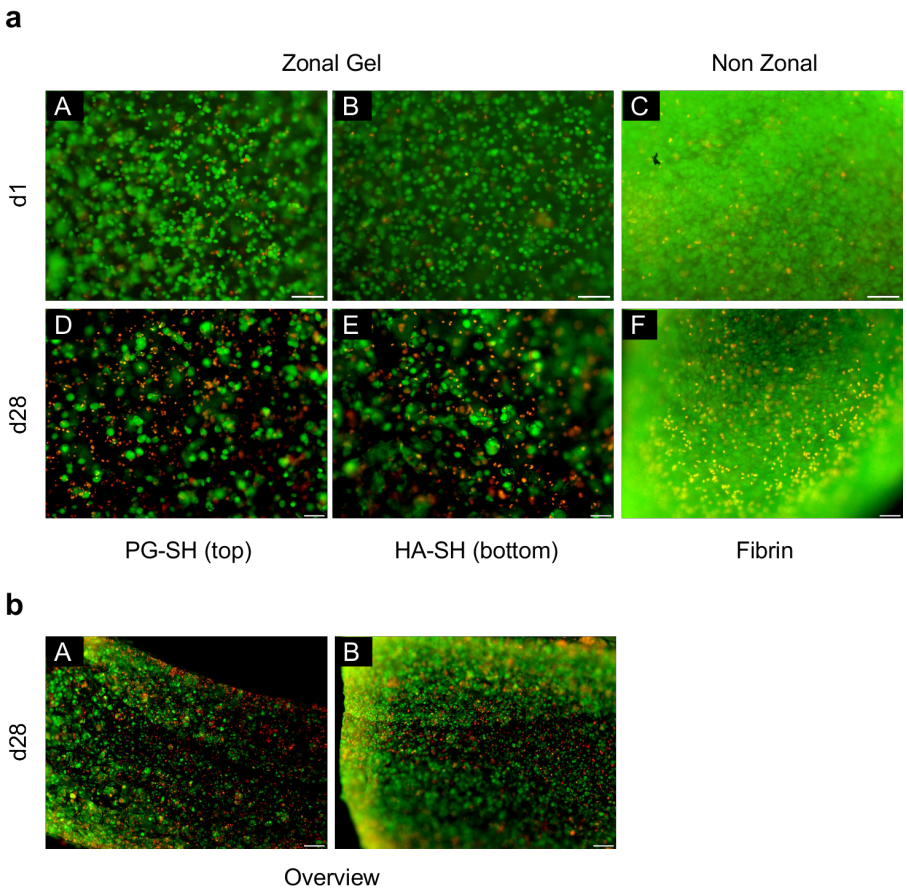

Figure 5.32: Cell viability of MSCs encapsulated in zonal and fibrin hydrogels, seeded with 20.0×10^6 MSCs/mL. Viable cells were labeled green with calcein-AM, and dead cells were labeled red with EthD-III. **a** After 1 and 28 days of chondrogenic differentiation; scale bars represent 100 µm. **b** Longitudinal sections after 28 days of chondrogenic differentiation; scale bars represent 200 µm.

The chondrogenic differentiation of MSCs was shown by staining of GAGs with safranin O, and with IHC for the presence of the ECM components collagen I and collagen II. In the overview image of the safranin O staining, the zonal organization became

very obvious. The PG-SH top layer exhibited a significantly lower, pinkish background staining, while the HA-SH_{FMZ} bottom layer showed a stronger background staining, and was all over stained in reddish color. GAG staining of cellular origin appeared in a distinctly darker red and could be distinguished very well from background staining (Figure 5.33, A). While collagen I seemed to be produced in a lower amount in the PG-SH top layer, the collagen II signal occurred more evenly distributed throughout both gel layers (Figure 5.33, E, I).

MSCs cultured in the PG-SH part of zonal gels exhibited a more roundish, pericellular signal for GAGs, while cells encapsulated in the top layer showed only moderate amounts of collagen type I, the collagen type II signal appeared stronger. In general, ECM deposition in the HA-SH_{FMZ} layer showed a more stretched shape, and the signals for collagen type I and type II were more regular distributed (Figure 5.33, B–C, F–G, J–K). Fibrin gels, on the other hand, showed the most extensive staining for ECM molecules, but they shrank and were not stable in shape, and it has to be taken into account that cells are more closely packed due to shrinkage (Figure 5.33, D, H, L)

Quantification of DNA amount showed a higher number of cells in the zonal gels compared to fibrin control gels. The determination of total GAG and GAG/DNA showed a significant increase in the zonal gels in comparison to fibrin gels (Figure 5.34).

Hereby, the general feasibility of zonal gels and their suitability for chondrogenic differentiation of MSCs was demonstrated in this pilot experiment. In further experiments, the evaluation needs to be expanded, and zonal gels should be compared to single PG-SH and HA-SH_{FMZ} gels in addition.

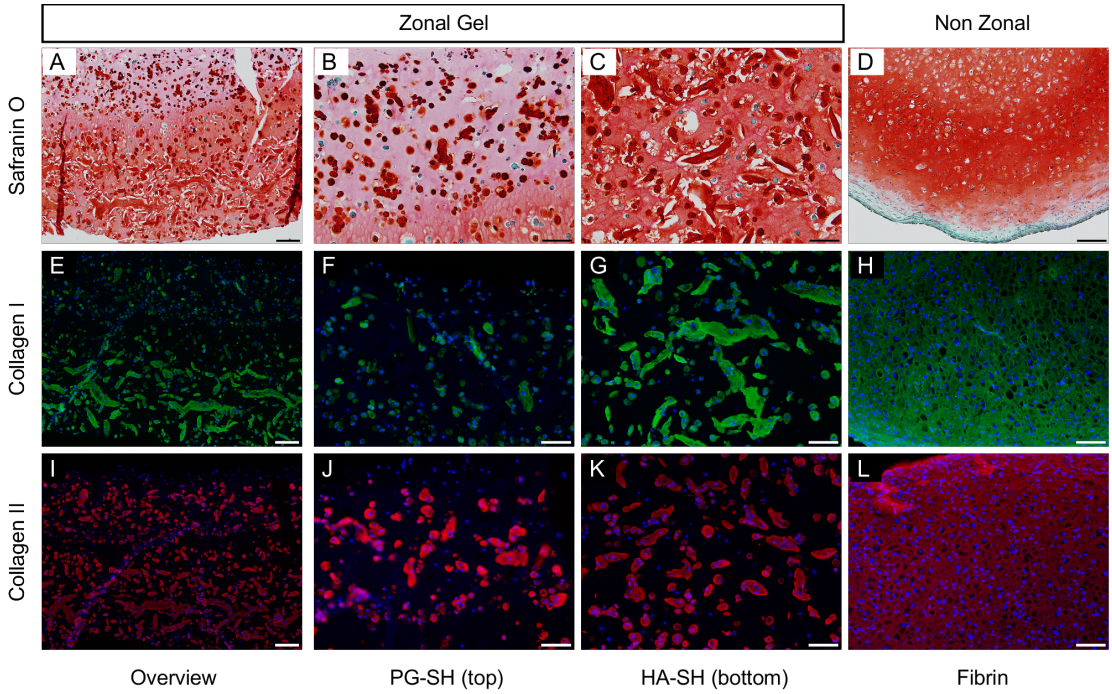

Figure 5.33: Histological and immunohistochemical staining of MSCs encapsulated in zonal hydrogels in overview (A, E, I) and in the specific zones (B–C, F–G, J–K) in comparison to fibrin gels, seeded with 20.0×10^6 MSCs/mL, after 28 days of chondrogenic differentiation. Longitudinal sections were stained for deposition of GAGs with safranin O and collagen I (green) or collagen II (red) to show ECM development. Nuclei (blue) were counterstained with DAPI; scale bars represent 200 µm in the overview images A, E, I, and 100 µm in the all other images.

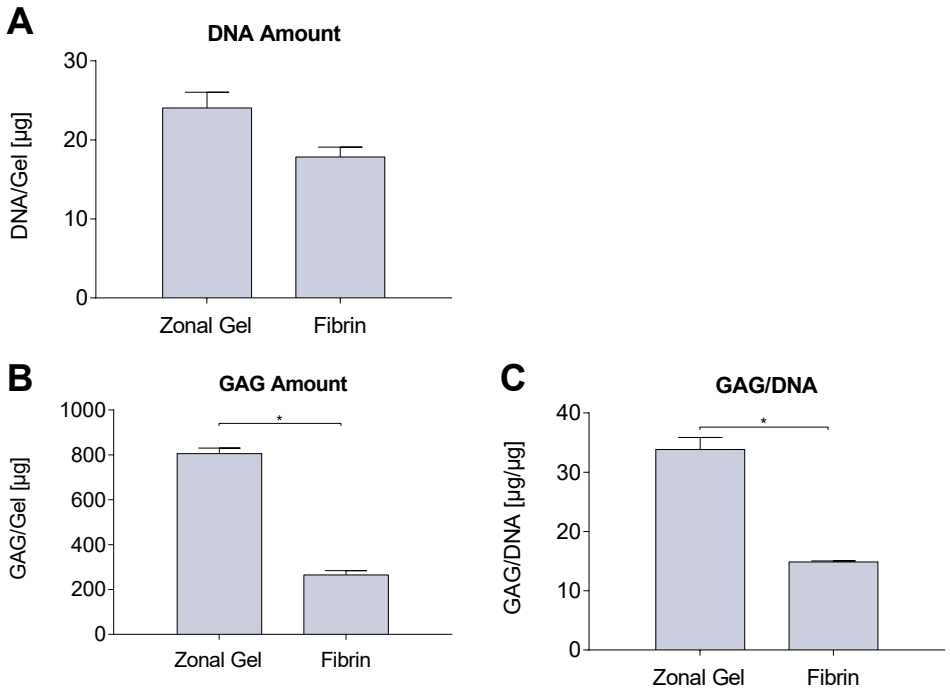

Figure 5.34: Total DNA amount (A), total GAG per gel (B) and normalized to DNA amount (C) of MSCs encapsulated either in zonal or fibrin hydrogels, after 28 days of chondrogenic differentiation. Data are presented as means ± standard deviation (n=3). Statistically significant differences between different gels are denoted with ($\star$) $p<0.05$.

Part IV

Discussion

Chapter 6

Discussion

Novel therapeutic concepts based on cartilage tissue engineering approaches have already proven their regenerative potential in the treatment of severe cartilage defects in patients. However, the vast majority of clinically utilized scaffolding materials is not very cartilage-specific. To achieve improved cartilage regeneration, materials that resemble the natural cartilage ECM and allow cells to form and secrete new cartilaginous tissue while replacing the scaffold material appear desirable. As a result there is a need for innovative materials which are chemically more flexible and highly modifiable for biomimetic functionalization, while at the same time contain low amounts of synthetic polymer.

To address these challenges and limitations, a hydrogel system based on thiolated HA (HA-SH) was set up by initially cross-linking with acrylated PEG derivatives via Michael addition which allowed the formation of a hydrogel under physiological conditions. In a further evolution of the system, acrylated poly(glycidol) (PG-Acr), a multifunctional polymer as an alternative to PEG was introduced. The application of PG-Acr facilitated the incorporation of biomimetic peptides and TGF-β1 into the hydrogels, and allowed us to assess the impact of these modifications on MSC chondrogenesis. Additionally, the usability of a bioinert, pure poly(glycidol) (PG) UV-cross-linked hydrogel system for MSC chondrogenesis was evaluated in the context of biomimetic functionalization. Furthermore, to mimic the zonal organization of native articular cartilage, MSCs were encapsulated in a zonal construct, consisting of two differently composed hydrogels, and chondrogenesis was investigated in a preliminary experiment.

6.1 Hyaluronic Acid Hydrogels Cross-linked with Poly(eythylene glycol) or Poly(glycidol) Derivatives

6.1.1 General Material Suitability for MSC Chondrogenesis

First, the suitability of HA-PEGDA (0.4 %) hydrogels for construct generation and subsequent MSC chondrogenesis was assessed *in vitro*. As far as viability was concerned, no significant differences between a negative control and hydrogel-encapsulated cells cultured in TGF-β1-containing medium were detectable (Figure 5.2). The suitability of the chosen hydrogel formulation for chondrogenic differentiation was demonstrated for the TGF-β1 group by positive staining for cartilage-specific ECM components, like GAG with safranin O and collagen II via IHC (Figure 5.3).

6.1.2 Variation of PEGDA Cross-linker Concentrations

In the next step, towards the optimization of the hydrogel composition, different concentrations of PEGDA were used to cross-link HA-SH. The resulting cell-laden hydrogels were evaluated regarding basic handling characteristics in cell culture, mechanical stability and the impact on chondrogenic differentiation of MSCs. Overall, proliferation and a quantitatively robust chondrogenic differentiation was observed in all hydrogels (Figure 5.5), which is fundamental to MSC chondrogenesis *in vitro* [137]. While gels with low concentrations of PEGDA (0.1% and 0.2%) were unstable in culture 0.4% PEGDA hydrogels provided optimal hydrogel stability. With respect to mechanical stability, handling characteristics and homogeneity of cell distribution, this formulation was superior to the low PEGDA concentrations. These observations correlated well with the storage modulus of the corresponding cell-free HA-SH hydrogel formulations that were cross-linked with PEGDA.

With regards to the quality of chondrogenesis, the 0.4% PEGDA hydrogels also showed that cartilage matrix in these constructs was more evenly distributed in the intercellular space, whereas matrix was mostly restricted to the pericellular area in hydrogels cross-linked with 1.0% and 2.0% PEGDA. These results indicate a better permeability for deposition of cellularly produced ECM components in the 0.4% PEGDA cross-linked hydrogels (Figures 5.4 and 5.6), pointing to an inverse correlation between gel stiffness (storage modulus) and permeability for matrix deposition of hydrogels. The more homogeneous distribution of cartilage-specific molecules, such as type II collagen and aggrecan may further be beneficial for the stabilization of the initially relatively weak hydrogels. Besides construct stabilization, homogeneously distributed ECM may

additionally improve MSC chondrogenesis. Collagen II the major type of collagen present in natural articular cartilage and, through its network-like organization, contributes to the stiffness of cartilage [6]. It is also capable of maintaining MSC chondrogenesis by enhancing the effect of TGF-β1 by sequestering it to the ECM [138, 139]. Also, cell-secreted proteoglycans are known for their capability to bind and immobilize growth factors [140], and may thereby trap TGF-β1 and improve MSC chondrogenesis within the hydrogels.

In comparison to other hydrogel formulations, the maximum stiffness of 762 ± 191 Pa for the 2.0% PEGDA cross-linked hydrogel is still very low compared to other systems such as MeHA with a higher cross-linking density, that reach storage moduli from 3.5 kPa to 60 kPa [141]. Regarding matrix stiffness, different strategies are available to adjust the mechanical properties of hydrogels. Either by altering the amount of macromer [141, 142] or by variation of irradiation time in UV cross-linked hydrogels [141], or by changing the cross-linking density [141, 143], as performed in the optimization experiment using PEGDA concentrations from 0.1% to 2.0% (Section 5.1.2).

6.1.3 Variation of the Hydrogel Cross-linker

After the determination of a suitable PEGDA concentration the effects of 4-arm branched PEGTA on MSC chondrogenesis were investigated. While the number of acrylate groups was kept at the same level (2.4 mM), the concentration of PEGTA was increased up to 0.6% PEGTA because of differences in molecular weight (PEGDA 3400 Da, PEGTA 10 000 Da). This resulted in an increase from 218 ± 38 Pa (0.4% PEGDA) to 1643 ± 469 Pa (0.6% PEGTA) simply by changing the cross-linker design from a 2-arm linear PEG to a branched 4-arm PEG. Experiments by other groups have shown that storage moduli in a range from 1000 Pa to 3000 Pa seemed to be optimal for hydrogel-based *in vitro* chondrogenesis [144–146]. Interestingly, there were no significant differences quantitatively and qualitatively between the 0.4% PEGDA and 0.6% PEGTA cross-linked hydrogels regarding deposition of GAG or collagens despite the change in gel matrix stiffness. In fact, the cell-secreted cartilage-specific ECM molecules were distributed in a similar manner throughout the examined hydrogel sections (Figures 5.9 and 5.10).

To enable the introduction of biomimetic functionalization, the change of cross-linker from 0.6% PEGTA to 0.6% PG-Acr increased the number of functional acrylate groups from 2.4 mM (0.6% PEGTA) to 11.8 mM (0.6% PG-Acr). This increase in binding sites significantly increased the variability of the hydrogel system for further biomimetic functionalization. The stiffness of the material changed to a lower storage modulus and

decreased down to 603 ± 241 Pa for 0.6% PG-Acr, which was comparable to the 2.0% PEGDA hydrogels, 762 ± 191 Pa, while just 30% of cross-linker concentration needed to be used. Regarding the quantity of GAG production, no significant differences could be detected for MSCs cultured in 0.6% PG-Acr or 0.6% PEGTA cross-linked hydrogels. The quality of matrix deposition, on the other hand, was different, as shown for GAG by safranin O staining and IHC for both collagen type I and type II displaying a more evenly distributed matrix in the PG-Acr cross-linked gels. The determination of total collagen mirrored these staining results yielding higher amounts for MSCs encapsulated in 0.6% PG-Acr hydrogels (Figures 5.11 and 5.12). Variations in collagen synthesis in the 0.6% PEGTA cross-linked hydrogels compared to previous experiments with the same formulation may be explained by donor variability in collagen production. It is also possible that the observed differences between 0.6% PEGTA and 0.6% PG-Acr cross-linked gels are a result of differences in stiffness and pore size. Therefore, the influence of hydrogel stiffness on MSC chondrogenesis would be an interesting topic to be further investigated in future experiments. Concerning this, a recent experimental evidence suggests an influence of the employed cross-linker, possibly resulting in different gel structure and pore size, on the quality of MSC chondrogenesis encapsulated in different cross-linked hydrogels [146].

These experiments demonstrate that the developed HA hydrogel system already exhibits a very good permeability for cell-derived ECM molecules. The hydrogel formulation applied here contains a certain amount of degradability because of the particular design of ester bonds that are established during Michael addition (Figure 5.7). A thioether bond in proximity to an acrylate group generates a positive charge on the carbon atom of the acrylate ester group, and in this way increases its susceptibility for nucleophilic hydroxyl anions in early ester hydrolysis [71]. This has been demonstrated for acrylated PEG derivatives that had been reacted with thiolated compounds that esters with neighboring sulfide groups are highly susceptible for hydrolysis [147–149], and thereby enable hydrogel degradation.

As an alternative mechanism, hydrogels may be further modified with MMP-sensitive cross-linkers to enhance degradability, penetrability for cellularly produced ECM, and chondrogenesis of encapsulated MSCs [96, 150–152] and chondrocytes [152, 153]. In more detail, in response to the insertion of MMP-sensitive peptides into a hydrolytically non-degradable MeHA hydrogel, MSCs switched to a more spreaded morphology, matrix distribution was more extensive, and the expression of chondrogenic marker genes was elevated compared to MMP-insensitive hydrogels [150]. Patterson and Hubbell compared a wide range of different MMP-sensitive peptides considering their cleavage rates and

extensively studied the use of MMP-sensitive cross-linkers for the controlled degradation of PEG hydrogels in response to MMPs. They were able to show that it is possible to tune the kinetics of hydrogel degradation as function of MMP type [102], yet this still is a very fast degradation. Due to the relative softness and biodegradability of the employed hydrogel system employed in this work, the incorporation of MMP-sensitive cross-linkers is not required, thus keeping the system more simple and controllable. Since the degradation speed of the developed HA gels is not directly connected to the MMP-production and the activity of surrounding cells and tissues, their specific degradation behavior may be beneficial for *in vivo* applications.

Issues concerning shape stability and resistance to mechanical forces arising during *in vivo* applications could be overcome by the incorporation of mechanical support structures into the hydrogels using either 3D-printed [154, 155] or spun [156, 157] biodegradable reinforcement fibers or structures. Specifically for cartilage tissue engineering approaches the utilization of reinforced hydrogels has already been proven adavantagous with regards to the generation of scaffolds meeting the mechanical properties of native cartilage [158, 159]. The aforementioned supporting structures might be used to improve the mechanical properties and thereby the clinical potential of the developed HA hydrogel system.

6.2 Biomimetic Functionalization of Hyaluronic Acid Hydrogels

With the introduction of PG-Acr as a highly modifiable and multifunctional alternative cross-linker to PEG into the hydrogel system, it now became possible to covalently incorporate peptides and growth factors (TGF-β1) into the hydrogels and to thereby achieve biomimetic functionalization. Sequences that had previously already shown their bioactive potential were included in following experiments to study the effect of peptide modification on MSC chondrogenesis in the developed hydrogel system.

6.2.1 Biomimetic Functionalization with Peptides

Various peptide sequences and their corresponding scrambled controls were incorporated at different concentrations into the HA hydrogels to introduce biomimetic functionalization. The HAV motif, a N-cadherin mimetic sequence, was previously shown to enhance chondrogenic differentiation of MSCs by mimicking cell condensation in MeHA hydrogels [101]. For HAV and the related scrambled motif, concentrations of 1.0 mM and 2.5 mM were used [101]. A concentration of 5.0 mM of the collagen type II binding sequence KLER was reported to enhance chondrogenesis in a PEG hydrogel system [99]. Hence,

KLER and its scrambled sequence were incorporated into the gels. Additonally, a positive impact on MSC chondrogenesis was also demonstrated for the cell adhesion sequence RGD in PEG-based hydrogels, which was also incorporated at a concentration of 1.0 mM [160](Table 5.2).

In general, no significant improvement of MSC chondrogenesis could be seen in response to incorporation of the various peptide sequences, neither qualitatively (Figures 5.14 and 5.15), nor quantitatively (Figures 5.16 and 5.17) independent of the incorporated peptide sequence. Moreover, the obtained results indicated a negative effect of incorporated peptides like 2.5 mM HAV, 5.0 mM KLER and 1.0 mM RGD on proteoglycan production compared to unmodified controls. Additionally, 1.0 mM RGD incorporation significantly decreased collagen production (Figure 5.17). While these results vary from other hydrogel systems, it needs to be pointed out that reports about the effect of RGD on chondrogenesis are inconsistent, with studies showing negative effects on BMSC chondrogenesis in alginate and agarose hydrogels in a dose-dependent manner due to changes in the cytoskeletal organization after integrin-mediated adhesion [161, 162]. Others showed a beneficial effect on chondrogenesis when presented to cells as a cleavable peptide in pure PEG hydrogels [160], or when incorporated in heparin-enriched MMP-degradable starPEG hydrogels [152].

Further, the incorporation of the collagen type II binding sequence from decorin, KLER, neither led to an improvement of MSC chondrogenesis nor an increase in type II collagen deposition or alteration of matrix deposition. In well accordance, a recently published study was also not able to show a chondro-supportive influence on MSCs in response to KLER incorporation into heparin-enriched MMP-degradable starPEG hydrogels [152]. Thus, we and others were not able to detect an induction of chondrogenic differentiation or cartilage-specific ECM deposition of MSCs in response to the presentation of KLER, in contrast to reports in pure PEG hydrogels [99]. This leads to the speculation that maybe the positive impact of KLER becomes just detectable in a less supportive hydrogel system, like a pure PEG gel, while its supportive effect may be covered or be too weak within the chondro-supportive background of heparin and HA.

Subsequently, the incorporation of 2.5 mM of the N-cadherin mimetic peptide HAV into the hydrogels not only decreased GAG content significantly, it tremendously changed the appearance of cell nuclei to a more irregular, less rounded shape, as shown by safranin O staining (Figure 5.14). In comparison to this, the incorporation of 1.0 mM HAV, as well as 1.0 mM and 2.5 mM of its Scr peptide, led to significantly enhanced GAG/DNA and collagen/DNA contents. These observations suggest that the dose of N-cadherin signaling is crucial for the outcome of chondrogenic differentiation *in vitro*. It is known

that N-cadherin expression and signaling is essential for *in vitro* [15, 17, 163] and *in vivo* [15] chondrogenesis. Moreover, the correct temporal expression pattern of N-cadherin was shown to be important during chondrogenesis [163]. Inhibition of N-cadherin signaling in standard pellet cultures led to a complete disruption of condensation and pellet formation [17]. Interestingly, we were not able to detect a positive effect on MSC chondrogenesis upon incorporation of 1.0 mM HAV compared to 1.0 mM of the scrambled motif, as it has been reported by Bian and colleagues for MSCs incorporated in MeHA hydrogels [101]. The improved collagen deposition and in trends towards higher production of GAGs in the 1.0 mM HAV and scrambled sequence group may be due to softening of the hydrogels and differences in mesh size. To follow up on this, the hydrogel structure could be further analyzed, e.g., utilizing scanning electron microscopy (SEM).

An explanation for the discrepancy between the obtained results and reportes in the literature could be that the employed hydrogel system is softer, and therefore can be penetrated better by cell-secreted ECM than other hydrogel networks in connection with peptides [99, 101, 160]. As already discussed above, cells encapsulated in softer gels within a storage moduli range from 1000 Pa to 3000 Pa showed improved chondrogenesis compared to cells encapsulated in stiffer hydrogels (Section 6.1.3 on page 93). Hence, the relative softness in combination with the supportive HA background [73, 164, 165], may outperform the positive effects of incorporated peptides. Additionally, due to the greater permeability, incorporated peptides could be covered by cellularly produced matrix and thus impair peptide mediated effects. This hypothesis could be investigated further by significantly increasing the hydrogel stiffness and network density.

In summary, there were no positive effects of incorporated peptides on MSC chondrogenesis in the per se chondro-supportive HA hydrogel detectable. Most of the reports that showed positive peptide effects were carried out in less-supportive PEG hydrogels [99, 160] or in significantly stiffer MeHA-based hydrogels [101]. It may be more important to design and shape the ideal hydrogel network with regard to network density and matrix stiffness than rather mimic cell-cell interactions, or to offer additional cell adhesion and ECM binding sites. However, further studies elucidating peptide effects and the search for additional not yet utilized peptides, either in stiffer gels or even perhaps in a complete bioinert setting, may on the one hand, help to understand basics in ECM signaling during chondrogenesis, and on the other hand, help to enhance the overall clinical potential of hydrogels in cartilage tissue engineering approaches.

6.2.2 Biomimetic Functionalization with Growth Factors

Another possibility to utilize the high tunability of PG-Acr for biomimetic functionalization could be the covalent binding of a growth factor. Hence, here we exemplarily demonstrated this by the covalent incorporation of TGF-β1 into the HA hydrogels for MSC chondrogenesis. Hence, TGF-β1 was reacted with Traut's reagent at a 4:1 molar ratio of Traut's reagent to TGF-β1 and was subsequently bound to PG-Acr. Finally, various doses of thiolated TGF-β1 (resulting in 10 nM, 50 nM and 100 nM in the final gel) were tethered to the gels (TGF-β1 Traut).

As mentioned in Section 1.4.2 on page 12, a few studies already utilized this technique to incorporate either the latent form of TGF-β1 into HA hydrogels [116], or the active form of TGF-β1 into pure PEG gels [117, 118]. The studies, carried out by McCall et al. [117] and Sridhar et al. [118], served as basis for this study. In all cases, growth factor incorporation showed positive effects on chondrogenesis of MSCs and chondrocytes. However, none of these studies compared the effects and possible differences of the chondrogenic performance of cells following covalent tethering of TGF-β1 with the outcome of locally administered, but not covalently bound TGF-β1.

Moreover, the defined local administration of TGF-β1 may be of vital importance in *in vivo* applications. Besides its very short half-life [166], intra-articular injections of TGF-β1 were shown to cause osteoarthritis-like changes, the formation of osteophytes, and formation of synovial hyperplasia in murine model systems [167–169]. Additionally, TGF-β1 stimulated cells in the synovium to secrete soluble inflammatory mediators, which promoted articular chondrocytes into terminal hypertrophy, as shown by enhanced collagen X production [170]. Furthermore, dysregulation of TGF-β signaling is known to be a supportive factor in tumor development and progression, caused by local high levels of TGF-β [171]. Therefore, it appears important to present growth factors in locally defined areas to prevent activation of unwanted cell sources under *in vivo* conditions. Besides that, the delivery of TGF-β in thermo-reversible hydrogels blended with HA showed synergistic effects on chondrogenic differentiation of chondrocytes in a mouse model [172]. In summary, the previously mentioned points show, on the one hand, the needs for a controlled delivery of TGF-β1, and on the other hand, the possible benefits and potential for a successful implementation of this delivery approach for possible clinical applications.

Therefore, this study aimed to investigate the potential of TGF-β1-modified HA hydrogels to induce MSC chondrogenesis. As mentioned above, various doses of thiolated TGF-β1 (resulting in 10 nM, 50 nM and 100 nM in the final gel) were tethered to the gels

(TGF-β1 Traut). In the following experiments, MSC chondrogenesis of these groups was compared to the chondrogenesis of MSCs encapsulated in hydrogels in which 100 nM of unmodified TGF-β1, and thus, was mixed into without covalent binding (100 nM TGF-β1). A group receiving exogenously delivered TGF-β1, added with every medium change (TGF-β1-Medium) served as a positive control, and a group without TGF-β1 as a negative control (w/o TGF-β1). Since the biological activity of Traut-modified TGF-β1 and its latent form has been shown several times using Smad-reporter cell lines [116–118], no further test was conducted in this matter.

Analysis of MSC chondrogenesis showed clearly a positive effect of covalent binding of TGF-β1 into the hydrogels in a dose-dependent manner. Incorporation of 100 nM TGF-β1 into the gels led to robust chondrogenesis compared to lower doses after 21 days, with clearly increased GAG and collagen content, as shown by biochemical assays (Figure 5.21), histological staining and by IHC of major cartilage ECM molecules (data not shown). When compared to gels receiving equal amounts of TGF-β1 mixed into the gels (100 nM TGF-β1), 100 nM TGF-β1 Traut-modified gels showed a significant improvement on all assessed levels of chondrogenesis (Figures 5.20 to 5.23). Surprisingly, the 100 nM TGF-β1 Traut group even outperformed constructs receiving soluble TGF-β1 with each medium change (standard concentration of 10 ng/mL for *in vitro* chondrogenesis), with regard to proteoglycan content (Figure 5.21). Interestingly, the total amount of administered TGF-β1 over the 21 days of *in vitro* culturing was lower in 100 nM TGF-β1 Traut group (102.4 ng) compared to the TGF-β1-Medium group (135 ng). A previous study has shown for MSCs cultured in PEG gels with 100 nM tethered TGF-β1 that they reached comparable levels of chondrogenesis in relation to control gels cultured in medium containing soluble TGF-β1 [117]. The same research group was able to reproduce the previously obtained results in a follow-up study for encapsulated chondrocytes in a similar PEG gel system. This time, 50 nM tethered TGF-β1 outperformed the standard positive control with soluble TGF-β1 by reaching higher amounts in DNA, GAG and collagen content after 28 days of chondrogenic induction *in vitro* [118]. Another study employing vascular smooth muscle cells encapsulated in PEG gels showed similar trends of increased ECM production upon exposure to tethered TGF-β1 compared to cells cultured with soluble TGF-β1 [173].

MSCs in the 100 nM TGF-β1 Traut group deposited considerably more GAG and aggrecan into the gel matrix compared to gels cultured in TGF-β1 supplemented medium (Figures 5.20 and 5.23). This effect of elevated proteoglycan production was in well agreement with a work from Van Beuningen et al. showing enhanced levels of proteoglycan synthesis upon intra-articular injection of TGF-β1 in a murine model [168]. Conversely,

collagen synthesis was more pronounced in the TGF-β1-Medium group compared to 100 nM TGF-β1 Traut group, which was further confirmed by densitometric quantification of Western Blot analysis in a preliminary trial experiment which needs to be verified in additional experiments (Figure 5.25). Otherwise, collagen type X was present in only small amounts in both groups, indicating a mild chondrocyte hypertrophy [174] after 21 days of *in vitro* chondrogenesis, while mRNA expression levels were still upregulated in all chondrogenically induced groups at later culturing time points (Figure 5.24).

Most interestingly, MSC chondrogenesis in the 100 nM TGF-β1 Traut group was clearly superior compared to the 100 nM TGF-β1 group without covalently incorporated growth factor (Figures 5.22 and 5.23). Biochemical analysis confirmed the histological findings which revealed clearly increased accumulation of proteoglycans and collagens in sections of 100 nM TGF-β1 Traut gels (Figures 5.20 and 5.21).

Analysis of mRNA expression of chondrogenic markers showed comparable patterns for all investigated genes during MSC chondrogenesis. *COL2A1*, *ACAN*, and *SOX9* were upregulated in all chondrogenically induced groups (Figure 5.24, B–D). The expression of *COL2A1* is known to be correlated with the expression of the transcription factor *SOX9*, which is involved in initiating chondrogenic differentiation [21, 22]. At day 21 the 100 nM TGF-β1 Traut gels showed significant upregulation of the three chondrogenic marker genes compared to the other chondrogenically induced groups, indicating that the most robust and prolonged chondrogenesis proceeded in this group (Figure 5.24, B–D).

As already introduced in Section 1.2 on page 4, TGF-β1 is a key regulator of chondrogenesis *in vitro* and *in vivo*. This study successfully showed that covalent incorporation of 100 nM TGF-β1 leads to significant improvement of TGF-β1-dependent chondrogenesis of MSCs. Upon canonical activation by binding of TGF-β1 to type II receptor, type I receptors, mainly ALK-5, are phosphorylated at the transmembrane and the signal is transduced by phosphorylation of Smad2/3 [170, 175]. Following that, the signal is transmitted to the nucleus regulating TGF-β1-dependent gene transcription [176]. This pathway is called Smad-dependent pathway. Alternatively, TGF-β signaling is transmitted by so-called Smad-independent pathways, namely via activating mitogen-activating protein kinases (MAPKs) (ERK, JNK/p38), phosphatidylinositol 3-kinase (PI3K)/Akt and GTPases [170, 175, 177, 178]. Thus, TGF-β signaling is controlled via multiple intracellular mechanisms, particularly by regulation of TGF-β receptor activity. For example, a complex of receptor-bound TGF-β1 undergoes clathrin- or caveolin-1-mediated endocytosis, and can subsequently be degraded [175].

Equally important, it is known that growth factors, like epidermal growth factor receptor (EGFR) ligands, can be bound to ECM molecules or cell membranes and enable

so-called juxtacrine signaling [179, 180]. In accordance with this, there have been several reports about the immobilization of growth factors, like insulin [181, 182], recombinant human BMP-2 [183] and TGF-β1 [173], showing positive effects on cellular behavior upon exposure to these signals. Since for the 100 nM TGF-β1 group qRT-PCR analysis showed a significant upregulation of *ALK-5* expression at later time points (Figure 5.24), we speculate that this might be due to prolonged presentation and thus, enhanced TGF-β1 signaling caused by covalently bound TGF-β1. This enhancement may be due to the inhibition of receptor endocytosis and degradation by covalently bound growth factor. Therefore, we hypothesize that covalently bound TGF-β1 acts similarly in the hydrogel system via a reproduced juxtacrine signaling mechanism since gels into which non-tethered TGF-β1 was just mixed reached significant lower levels of chondrogenesis.

As an alternative future type of application, the modification of TGF-β1 with PG-Acr may result in an effect similar to PEGylation and may thus be used as a surrogate. Since it is known that PEGylation of growth factors and proteins improves solubility, decreased immunogenicity, and most importantly increased stability and half-life time, [184, 185], the modification of TGF-β1 with PG may further improve the potential for *in vivo* applications.

In summary, the potential of covalent TGF-β1 incorporation into PG-Acr cross-linked HA hydrogels for cartilage tissue engineering approaches was demonstrated. The chondrogenic differentiation in the 100 nM TGF-β1 Traut group was significantly improved in comparison to the 100 nM TGF-β1 group without covalent incorporation of TGF-β1. Due to its multifunctionality, PG enables not only the introduction of one growth factor or peptide into a hydrogel in future experiments, but offers the opportunity to cumulate various biological cues, such as, both peptides and growth factors, into hydrogels.

6.3 Biomimetic Functionalization of Pure Poly(glycidol) Hydrogels

The application of pure PG hydrogels allowed us to analyze the effect of a biomimetic peptide without the supportive background of HA in a proof-of-principle experiment. Again, PG served as a multifunctional surrogate for PEG, as commonly used polymer in tissue engineering approaches.

PG is, like PEG, a completely bioinert material without adhesion sites for cells [85, 122, 186]. Thus, we chose the HAV sequence as the biomimetic factor to be incorporated into the pure PG hydrogels. This peptide was selected, because, on the one hand, HAV

is known to mimic N-cadherin-mediated cell-cell contacts [187], and on the other hand, it was shown to be an important factor in the early condensation phase of chondrogenesis [163]. Given that the incorporation of 2.5 mM HAV led to negative effects in HA hydrogels formed by Michael addition (Section 5.2.1 and fig. 5.14), we decided to incorporate 1.0 mM of HAV and its scrambled sequence into PG gels and compared them with unmodified gels.

Analysis of cell viability showed that the highest amount of viable cells could be found in 1.0 mM HAV-modified gels compared to Scr- and unmodified gels (Figure 5.27). This trend was also well reflected in the quantification of DNA amount (Figure 5.30, A). Since pure PEG hydrogels are known for their lack of adhesion sites for cells and have been shown to reduce viability when purely applied [188, 189], this result was expected. In well correlation with the results for cell viability, the most robust chondrogenesis was seen in the 1.0 mM HAV-modified hydrogels.

The strongest staining for GAGs and cartilage-specific ECM molecules such as collagen II and aggrecan was detectable for MSCs encapsulated in HAV-modified gels. On the other hand, when exposed to the scrambled peptide sequence MSCs also showed deposition of ECM, although the signals were much more restricted to pericellular regions after 21 days (Figures 5.28 and 5.29). Biochemical assays verified these observations and showed a significant increase of GAG and collagen in HAV-modified PG gels (Figure 5.30). Yet when compared to overall chondrogenesis and the pattern of matrix distribution in Michael addition-generated HA hydrogels, signals in PG gels were more restricted to pericellular regions, similar to what had been observed for cells encapsulated in pure PEG hydrogels [82, 88, 99, 143].

The improved chondrogenesis of MSCs encapsulated in scrambled-modified gels compared to unmodified gels may be due to some extent of unspecific adherence of cells and ECM components to the scrambled peptide and thereby result in an improved cell survival and chondrogenesis.

As already introduced, the correct expression and signaling patterns via N-cadherin, to mediate information of existing cell-cell contacts, is important for successful *in vitro* [15, 17, 163] and *in vivo* [15] chondrogenesis during the early condensation phase. In this context, it was shown that incorporation of the HAV peptide might have partially compensated the complete absence of biological cues, both in terms of either ECM- or cellular signals, in pure PG gels. A study focusing on the role of Notch and Wnt/β-catenin signaling in MSC chondrogenesis upon encapsulation in pure PEG hydrogels has shown reduced MSC chondrogenesis [190]. It suggested that the disruption of cell-cell contacts due to hydrogel encapsulation impeded chondrogenesis through unidirectional cell-cell

contact-mediated Wnt/β-catenin crosstalk [190]. Additionally, it is known that Wnt signaling plays an important role in cartilage development and degeneration [191], pointing towards the potential of Wnt research to provide insights in cartilage development. Bian and colleagues were able to demonstrate the positive effects of HAV-modification on MSC chondrogenesis in MeHA hydrogels, but the effects were shown against the background of HA signaling and without a further focus on the underlying signaling events, which were causal for the enhanced chondrogenic differentiation of MSCs [101]. In contrast to this, utilization of the pure PG gel system now offers the opportunity to clarify the fundamental mechanisms involved in these processes without the interfering influence of HA. Moreover, it would be easier to elucidate possible effects of clustering of peptides utilizing PG compared to PEG due the multifunctionality of PG [122].

Taken together, the potential of pure PG gels to study the effects of single peptides in a completely bioinert hydrogel environment was demonstrated in a proof-of-principle experiment. Because of its multifunctionality, PG offers the chance to incorporate growth factors in combination with peptides into hydrogels, and may therefore be used as a versatile toolbox to investigate the interplay of different peptides and growth factors in chondrogenesis or during other developmental processes.

6.4 Zonal Gels - Combination of HA Gels and PG Gels

This section of the thesis focused on a feasibility study of zonal gels, as part of the HydroZONES consortium, which targets the development of bioactive zonal hydrogels as scaffolding materials for articular cartilage repair. During the past years, zonal approaches gained significant attention since articular cartilage exhibits a hierarchical organization that fulfills different requirements regarding matrix composition, mechanical properties and cellular organization [127, 128]. Therefore, we combined a cell-laden HA containing bottom layer and a pure PG top layer to a hierarchical gel and evaluated MSC chondrogenesis within these gels in a pilot experiment.

Here, zonal constructs were successfully generated that kept their shape and stayed cohesive during 28 days of *in vitro* chondrogenesis. On the one hand, the preparation of longitudinal sections to assess viability showed a clear zonal organization of the gels, and on the other hand, a large number of viable MSCs (Figure 5.32). Staining for GAGs exhibited a robust chondrogenic differentiation in both zones, but with a lot of background staining in the HA containing bottom layer. The background staining could be explained by the significanlty higher HA-SH content (5.4 wt%) in the thiol-ene cross-linked hydrogels compared to HA-SH (0.8 wt%) in the Michael addition-generated

hydrogels. Additionally, due to the high polymer content in both layers, ECM signals were solely restricted to pericellular regions. This has also been reported several times for cells encapsulated in PEG hydrogels [82, 88, 99, 143] and MeHA hydrogels [141, 142] containing higher polymer amounts. This drawback may either be overcome by utilization of MMP-cleavable cross-linkers, as already discussed in Section 6.1.3 on page 93, or by lowering the polymer content.

Qualitatively, cells in the PG top layer produced more type II collagen compared to type I collagen, while signals for both molecules appeared to be equivalent in the HA bottom layer (Figure 5.33). The relevance of these findings has to be evaluated in future experiments by comparing the chondrogenesis of MSCs encapsulated in zonal gels with single PG-SH and HA-SH gels. In contrast to the zonal gels, ECM deposition of MSCs within fibrin exhibited a more prominent staining throughout the whole hydrogel. This impression, however, resulted from the enormous contraction of fibrin gels during *in vitro* culture, which may in part have led to the effect of a seemingly stronger chondrogenic differentiation in this type of gels (Figure 5.33). Biochemical analysis, on the other hand, demonstrated that MSCs encapsulated in the zonal gels produced significantly higher amounts of GAG.

The specific organization of cartilage and its zonal characteristics were addressed in several studies [192–198]. For instance, one study aimed to resemble the zone-specific matrix characteristics of the superficial, middle and calcified zone by variation of stiffness, organization and amount of reinforcement structures, grade of degradability, growth factor loading, and cell density in separately generated and cultured hydrogels [197]. This example illustrates the complexity of such tissue engineering approaches for an presumably simple tissue like articular cartilage. Each of the mentioned variables in this particular study was and still has to be addressed in more detail to gain more insight into zonal-specific cartilage regeneration and to move a step closer to sufficient tissue engineering-based therapeutic concepts for the treatment of severe cartilage defects.

In summary, the feasibility study for the generation of zonal gels was successful. It was possible to induce chondrogenic differentiation of MSCs in a stable, hierarchical hydrogel consisting of two differently composed zones, generated by the thiol-ene-click reaction. Besides further biomimetic functionalization and variation of the composition of both zones, the combination of chondrocytes together with MSCs may enhance the chondrogenic and clinical potential of the developed gel system, given that co-cultures have clearly been shown beneficial to cartilage formation [199–201].

Part V

Summary

Chapter 7

Summary

Improved treatment options for the degenerative joint disease osteoarthritis (OA) are of major interest, since OA is one of the main sources of disability, pain, and socioeconomic burden worldwide [202]. According to epidemiological data, already 27 million people suffer from OA in the US [23]. Moreover, the WHO expects OA to be the fourth most common cause of disability in 2020 [203], illustrating the need for effective and long-lasting therapy options of severe cartilage defects. Despite numerous clinically available products for the treatment of cartilage defects [62], the development of more cartilage-specific materials is still at the beginning.

Hyaluronic acid (HA) is a major component of the cartilaginous extracellular matrix (ECM) and inherently creates a cell-friendly niche by providing cell attachment and migration sites. Furthermore, it is known that the functional groups of HA are well suited for chemical modification. These characteristics render HA an attractive material for hydrogel-based tissue engineering approaches. Poly(glycidol) (PG) as chemical cross-linker basically features similar chemical characteristics as the widely used poly(ethylene glycol) (PEG), but provides additional side groups at each repeating unit that can be further chemically functionalized. With the introduction of PG as multifunctional cross-linker for HA gels, a higher cross-linking density and, accordingly, a greater potential for biomimetic functionalization may be achieved. However, despite the mentioned potential benefits, PG has not been used for cartilage regeneration approaches so far.

The initial aim of the study was to set up and optimize a HA-based hydrogel for the chondrogenic differentiation of mesenchymal stromal cells (MSCs), using different amounts and variations of cross-linkers. Therefore, the hydrogel composition was optimized by the utilization of different PEG diacrylate (PEGDA) concentrations to cross-link thiol-

modified HA (Glycosil®, HA-SH) via Michael addition. We aimed to generate volume-stable scaffolds that simultaneously enable a maximum of ECM deposition. Histological and biochemical analysis showed 0.4% PEGDA as the most suitable concentration for these requirements (Section 5.1.2).

In order to evaluate the impact of a differently designed cross-linker on MSC chondrogenesis, HA-SH was cross-linked with PEGTA (0.6%) and compared to PEGDA (0.4%) in a next step. Following this, acrylated PG (PG-Acr) as multifunctional cross-linker alternative to acrylated PEG was evaluated. It provides around five times more functional groups when utilized in PG-Acr (0.6%) HA-SH hydrogels compared to PEGTA (0.6%) HA-SH hydrogels, thus enabling higher degrees of biomimetic functionalization. Determination of cartilage-specific ECM components showed no substantial differences between both cross-linkers while the deposition of cartilaginous matrix appeared more homogeneous in HA-SH PG-Acr gels. Taken together, we were able to successfully increase the possibilities for biomimetic functionalization in the developed HA-SH hydrogel system by the introduction of PG-Acr as cross-linker without negatively affecting MSC chondrogenesis (Section 5.1.3).

The next part of this thesis focused extensively on the biomimetic functionalization of PG-Acr (0.6%) cross-linked HA-SH hydrogels. Here, either biomimetic peptides or a chondrogenic growth factor were covalently bound into the hydrogels.

Interestingly, the incorporation of a N-cadherin mimetic (HAV), a collagen type II binding (KLER), or a cell adhesion-mediating peptide (RGD) yielded no improvement of MSC chondrogenesis. For instance, the covalent binding of 2.5 mM HAV changed morphology of cell nuclei and reduced GAG production while the incorporation of 1.0 mM RGD impaired collagen production. These findings may be attributed to the already supportive conditions of the employed HA-based hydrogels for chondrogenic differentiation. Most of the previous studies reporting positive peptide effects on chondrogenesis have been carried out in less supportive PEG hydrogels or in significantly stiffer MeHA-based hydrogels [99, 101, 160]. Thus, the incorporation of peptides may be more important under unfavorable conditions while inert gel systems may be useful for studying single peptide effects (Section 5.2.1).

The chondrogenic factor transforming growth factor beta 1 (TGF-β1) served as an example for growth factor binding to PG-Acr. The utilization of covalently bound TGF-β1 may thereby help overcome the need for repeated administration of TGF-β1 in *in vivo* applications, which may be an advantage for potential clinical application. Thus, the effect of covalently incorporated TGF-β1 was compared to the effect of the same

amount of TGF-β1 without covalent binding (100 nM TGF-β1) on MSC chondrogenesis. It was successfully demonstrated that covalent incorporation of TGF-β1 had a significant positive effect in a dose-dependent manner. Chondrogenesis of MSCs in hydrogels with covalently bound TGF-β1 showed enhanced levels of chondrogenesis compared to hydrogels into which TGF-β1 was merely mixed, as shown by stronger staining for GAGs, total collagen, aggrecan and collagen type II. Biochemical evaluation of GAG and collagen amounts, as well as Western blot analysis confirmed the histological results. Furthermore, the positive effect of covalently bound TGF-β1 was shown by increased expression of chondrogenic marker genes *COL2A1*, *ACAN* and *SOX9*. In summary, covalent growth factor incorporation utilizing PG-Acr as cross-linker demonstrated significant positive effects on chondrogenic differentiation of MSCs (Section 5.2.2).

In general, PG-Acr cross-linked HA hydrogels generated by Michael addition represent a versatile hydrogel platform due to their high degree of acrylate functionality. These hydrogels may further offer the opportunity to combine several biological modifications, such as the incorporation of biomimetic peptides together with growth factors, within one cell carrier.

A proof-of-principle experiment demonstrated the suitability of pure PG gels for studying single peptide effects. Here, the hydrogels were generated by the utilization of thiol-ene-click reaction. In this setting, without the supportive background of hyaluronic acid, MSCs showed enhanced chondrogenic differentiation in response to the incorporation of 1.0 mM HAV. This was demonstrated by staining for GAGs, the cartilage-specific ECM molecules aggrecan and type II collagen, and by increased GAG and total collagen amounts shown by biochemical analysis. Thus, pure PG gels exhibit the potential to study the effects and interplay of peptides and growth factors in a highly modifiable, bioinert hydrogel environment.

The last section of the thesis was carried out as part of the EU project HydroZONES that aims to develop and generate zonal constructs. The importance of zonal organization has attracted increased attention in the last years [127, 128], however, it is still underrepresented in tissue engineering approaches so far. Thus, the feasibility of zonal distribution of cells in a scaffold combining two differently composed hydrogels was investigated. A HA-SH_{FMZ} containing bottom layer was generated and a pure PG top layer was subsequently cast on top of it, utilizing both times thiol-ene-click reaction. Indeed, stable, hierarchical constructs were generated that allowed encapsulated MSCs to differentiate chondrogenically in both zones as shown by staining for GAGs and collagen type II, and

by quantification of GAG amount. Thus, the feasibility of differently composed zonal hydrogels utilizing PG as a main component was successfully demonstrated (Section 5.4).

With the first-time utilization and evaluation of PG-Acr as versatile multifunctional cross-linker for the preparation of Michael addition-generated HA-SH hydrogels in the context of cartilage tissue engineering, a highly modifiable HA-based hydrogel system was introduced. It may be used in future studies as an easily applicable and versatile toolbox for the generation of biomimetically functionalized hydrogels for cell-based cartilage regeneration. The introduction of reinforcement structures to enhance mechanical resistance may thereby further increase the potential of this system for clinical applications.

Additionally, it was also demonstrated that thiol-ene clickable hydrogels can be used for the generation of cell-laden, pure PG gels or for the generation of more complex, coherent zonal constructs. Furthermore, thiol-ene clickable PG hydrogels have already been further modified and successfully been used in 3D bioprinting experiments [204]. 3D bioprinting, as part of the evolving biofabrication field [205], offers the possibilities to generate complex and hierarchical structures, and to exactly position defined layers, yet at the same time alters the requirements for the utilized hydrogels [159, 206–209]. Since a robust chondrogenesis of MSCs was demonstrated in the thiol-ene clickable hydrogel systems, they may serve as a basis for the development of hydrogels as so called bioinks which may be utilized in more sophisticated biofabrication processes.

Chapter 8

Zusammenfassung

Es ist von großem Interesse die Therapieoptionen für die degenerative Gelenkerkrankung Osteoarthrose (OA) zu verbessern, da OA als eine der weltweit häufigsten Ursachen von Bewegungseinschränkungen und Schmerzen gilt und somit eine sozioökonomische Belastung darstellt [202]. Laut epidemiologischen Studien leiden bereits 27 Millionen Menschen in den USA an OA [23]. Darüber hinaus geht die WHO davon aus, dass OA bereits im Jahr 2020 die vierthäufigste Ursache von körperlichen Behinderungen sein wird [203], was die Notwendigkeit für effektive und langanhaltende Therapien von schweren Knorpeldefekten zeigt. Obwohl sich bereits eine Vielzahl von Therapien in klinischer Anwendung für die Behandlung von Knorpeldefekten befindet [62], ist die Entwicklung von knorpelspezifischen Produkten noch nicht weit fortgeschritten.

Hyaluronsäure (HA), als Hauptbestandteil der Extrazellulären Matrix (ECM) von Knorpel, stellt eine generell zytokompatible Umgebung dar, die Zellen von Natur aus Bindungsstellen zur Adhäsion und Fortbewegung bietet. Zudem ist bekannt, dass die funktionellen Gruppen von HA besonders gut für chemische Modifikationen geeignet sind. Aufgrund dieser Eigenschaften wird HA häufig als Material für das hydrogelbasierte *Tissue Engineering* verwendet. Durch die Verwendung von *Poly(glycidol)* (PG) als *Cross-linker* stehen die gleichen chemischen Eigenschaften wie bei der Verwendung des gängigen *Cross-linkers Poly(ethylene glycol)* (PEG) zur Verfügung, allerdings bietet es zusätzliche Seitenketten an jeder Wiederholungseinheit. Durch die Einführung von PG als multifunktionalem *Cross-linker* zur Herstellung von HA-Gelen ergibt sich letztlich eine höhere Vernetzungsdichte und damit auch ein größeres Potenzial für biomimetische Funktionalisierungen. Trotz dieser genannten Vorteile wird PG bisher noch nicht im Bereich der Knorpelregeneration verwendet.

Das erste Ziel dieser Arbeit beinhaltete die Etablierung und Optimierung eines HA-basierten Hydrogels für die chondrogene Differenzierung von Mesenchymalen Stromazellen (MSCs). Hierzu wurden verschiedene Mengen und Derivate von *Cross-linkern* eingesetzt. Zunächst wurde die Hydrogelzusammensetzung mithilfe von verschiedenen PEG-Diacrylat (PEGDA)-Konzentrationen zur Vernetzung von thiolmodifizierter HA (Glycosil®, HA-SH) mittels Michael-Addition optimiert. Das Ziel war hierbei die Herstellung eines volumenstabilen Konstrukts, das gleichzeitig die größtmögliche Ablagerung von ECM erlaubt. Histologische und biochemische Analysen zeigten in Bezug darauf, dass eine Konzentration von 0,4% PEGDA die zuvor genannten Anforderungen am besten erfüllte (Abschnitt 5.1.2).

Um im weiteren Verlauf den Einfluss von verschiedenen *Cross-linkern* auf die chondrogene Differenzierung von MSCs zu untersuchen, wurde die HA-SH vergleichend mit PEGTA (0,6%) und PEGDA (0,4%) vernetzt. Nachfolgend wurde acryliertes PG (PG-Acr) als eine Alternative zu acrylierten PEG-Derivaten evaluiert. Der Vorteil in der Verwendung von PG-Acr (0,6%) im Vergleich zu PEGTA (0,6%) liegt darin, dass es eine ca. fünfmal höhere Anzahl an funktionellen Gruppen bietet, was wiederum ein deutlich höheres Maß an biomimetischer Funktionalisierung ermöglicht. Hierbei zeigte die Untersuchung der knorpelspezifischen ECM-Bestandteile keine grundlegenden Unterschiede zwischen beiden *Cross-linkern*, wobei durch die Verwendung von PG-Acr eine gleichmäßigere Ablagerung von Knorpelmatrix in die entsprechenden Gele zu erkennen war. Zusammenfassend lässt sich feststellen, dass die Möglichkeiten für eine biomimetische Funktionalisierung durch die Verwendung von PG-Acr deutlich erhöht wurden, ohne dabei die Chondrogenese von MSCs negativ zu beeinträchtigen (Abschnitt 5.1.3).

Der nächste Teil dieser Arbeit befasste sich mit der umfangreichen biomimetischen Funktionalisierung von mit PG-Acr (0,6%) vernetzten HA-SH Hydrogelen. Hierzu wurden entweder biomimetische Peptide oder ein chondrogener Wachstumsfaktor kovalent in das Hydrogel eingebunden.

Interessanterweise führte weder das Einbringen des N-Cadherin-mimetischen (HAV), des Kollagen II-bindenden (KLER), noch des Zelladhäsions-vermittelnden (RGD) Peptids zu einer Verbesserung der chondrogenen Differenzierung der MSCs. Beispielsweise führte das kovalente Anbinden von 2,5 mM HAV zu einer Veränderung der Zellkernmorphologie und einer Verringerung der Glykosaminoglykan (GAG)-Produktion, wohingegen das Einbringen von 1,0 mM RGD die Kollagenproduktion hemmte. Diese Ergebnisse könnten möglicherweise darauf zurückzuführen sein, dass die hier verwendeten HA-SH-Hydrogele selbst bereits ausreichend effizient für die chondrogene Differenzierung von MSCs sind.

Im Vergleich dazu wurden die vorherigen Studien, die positive Effekte von Peptiden nachweisen konnten, entweder in neutralen PEG-Hydrogelen oder in wesentlich festeren MeHA-Hydrogelen durchgeführt [99, 101, 160]. Daraus lässt sich folgern, dass die Verwendung von Peptiden gerade unter ungünstigen Bedingungen von Bedeutung sein könnte und ein neutrales Gelsystem für die Untersuchung von einzelnen Peptideffekten geeignet scheint (Abschnitt 5.2.1).

Als nächstes wurde exemplarisch der chondrogene Wachstumsfaktor *Transforming Growth Factor Beta 1* (TGF-β1) kovalent an PG-Acr angebunden. Durch die Verwendung von kovalent gebundenem TGF-β1 könnte somit die Notwendigkeit einer wiederholten Zugabe von TGF-β1 bei *in vivo*-Anwendungen vermieden werden, was wiederum bei einer potentiellen klinischen Anwendung von Vorteil sein könnte. Deshalb wurde der Einfluss von kovalent gebundenem TGF-β1 auf die Chondrogenese von MSCs mit der gleichen Menge ungebundenem TGF-β1 (100 nM TGF-β1) verglichen. Hierbei wurde ein signifikant positiver, dosisabhängiger Effekt von kovalent gebundenem TGF-β1 erfolgreich nachgewiesen. Die Chondrogenese von MSCs in Hydrogelen mit kovalent gebundenem TGF-β1 war dabei der Chondrogenese von MSCs in Hydrogelen, in die TGF-β1 lediglich gemischt wurde, deutlich überlegen. Dies wurde anhand von stärkeren Färbungen für GAGs, Gesamtkollagen, Aggrecan und Kollagen II in den TGF-β1-modifizierten Gelen gezeigt. Darüber hinaus bestätigten sowohl biochemische Analysen des GAG- und Kollagengehalts, als auch Western Blot-Analysen die histologischen Daten. Zusätzlich wurde der positive Effekt von kovalent gebundenem TGF-β1 durch erhöhte Expressionsraten der chondrogenen Markergene *COL2A1*, *ACAN* und *SOX9* nachgewiesen. Zusammenfassend konnte gezeigt werden, dass durch die kovalente Bindung des Wachstumsfaktors TGF-β1 ein signifikant positiver Effekt auf die chondrogene Differenzierung von MSCs entsteht (Abschnitt 5.2.2).

Generell stellen die auf Basis von Michael-Addition hergestellten PG-Acr-HA-SH-Hydrogele aufgrund ihrer hohen Acrylat-Funktionalität eine vielseitige Hydrogelplattform dar. So bieten diese Hydrogele zahlreiche Möglichkeiten für das Einbringen von verschiedensten biologischen Modifikationen wie die kovalente Bindung von biomimetischen Peptiden zusammen mit Wachstumsfaktoren in ein und demselben Zellträger.

Anhand eines *Proof-of-principle*-Experiments wurde die generelle Eignung von reinen PG-Hydrogelen für die Evaluation von einzelnen Peptideffekten demonstriert. Dazu wurden die Hydrogele unter Verwendung der *Thiol-ene-click*-Reaktion hergestellt. In diesem Hydrogelsystem, ohne den unterstützenden Effekt von HA, zeigten MSCs eine verstärkte chondrogene Differenzierung in Anwesenheit von 1,0 mM HAV. Diese ließ

sich anhand von stärkeren Färbungen für GAGs, Aggrecan und Kollagen II nachweisen. Außerdem waren die GAG- und Gesamtkollagen-Werte deutlich erhöht. Hiermit wurde gezeigt, dass sich die vielseitig modifizierbaren, reinen PG-Hydrogele für die Analyse von Peptideffekten und deren Interaktion mit Wachstumsfaktoren eignen (Abschnitt 5.3).

Der letzte Teil dieser Arbeit wurde im Rahmen des EU-Projektes HydroZONES durchgeführt, welches an der Entwicklung und Herstellung von zonalen Konstrukten arbeitet. Der Aspekt der zonalen Organisation von Knorpel rückte in den letzten Jahren verstärkt in den Fokus [127, 128], jedoch findet er im Bereich des *Tissue Engineering* noch immer wenig Beachtung. Deshalb wurde im Folgenden die zonale Verteilung von Zellen innerhalb eines Zellträgers realisiert. Dazu wurden zwei unterschiedlich zusammengesetzte Hydrogele mithilfe der *Thiol-ene-click*-Reaktion hergestellt: eine aus HA-SH_{FMZ} bestehende untere Lage und eine darauf liegende Lage aus reinem PG. Hierbei gelang es stabile, zonale Konstrukte herzustellen, in denen MSCs in beiden Zonen chondrogen differenzierten, was anhand von GAG- und Kollagen II-Färbungen, sowie durch die Quantifizierung des GAG-Gehalts bestätigt wurde. Hiermit konnte ein aus zwei verschiedenen Hydrogelen zusammengesetztes zonales Konstrukt erfolgreich hergestellt werden (Abschnitt 5.4).

Durch den erstmaligen Einsatz des multifunktionalen *Cross-linkers* PG-Acr für das *Tissue Engineering* von Knorpel wurde ein auf Michael-Addition basierendes, vielseitiges HA-SH-Hydrogelsystem etabliert. Das hier vorgestellte Hydrogelsystem besitzt das Potenzial zukünftig als eine einfach anwendbare und vielseitige *Toolbox* zur Herstellung von biomimetischen Hydrogelen für die zellbasierte Knorpelregeneration verwendet zu werden. Vor allem könnte dabei der Einsatz von Stützstrukturen von entscheidender Bedeutung sein, um die mechanische Widerstandskraft der Zellträger zu erhöhen und somit das Potenzial für klinische Anwendungen zu vergrößern.

Zusätzlich wurde gezeigt, dass *Thiol-ene-click*-Hydrogele sowohl zur Herstellung von zellbeladenen, reinen PG-Gelen, als auch zur Herstellung von deutlich komplexeren, zonalen Konstrukten geeignet sind. Diese *Thiol-ene-click*-Hydrogele wurden bereits erfolgreich weiterentwickelt und für *3D-Bioprinting*-Prozesse verwendet [204]. *3D-Bioprinting* ist eine Teildisziplin des sich immer weiter entwickelnden Feldes der Biofabrikation [205]. Die Verwendung in diesem Bereich verändert zwar die Anforderungen an die hierfür verwendeten Hydrogele, ermöglicht es aber gleichzeitig deutlich komplexere sowie hierarchische Strukturen herzustellen und kleinere Lagen noch exakter zu positionieren [159, 206–209]. Da in den hier vorgestellten *Thiol-ene-click*-Hydrogelen eine deutliche chondrogene Differenzierung von MSCs nachgewiesen wurde, ist es vorstellbar, dass sie als Basis

für die Herstellung sogenannter *Bioinks* dienen, welche in zukünftigen, anspruchsvollen Biofabrikationsprozessen Anwendung finden sollen.

Bibliography

1. Hayes, A. J., Hall, A., Brown, L., Tubo, R. & Caterson, B. Macromolecular organization and in vitro growth characteristics of scaffold-free neocartilage grafts. *The Journal of Histochemistry and Cytochemistry* **55,** 853–866 (2007).
2. Tuan, R. S. & Chen, F. H. in *Stem cell and gene-based therapy: frontiers in regenerative medicine* (eds Battler, A. & Leor, J.) 2006th ed., 179–193 (Springer, 2005). ISBN: 978-1-84628-142-6.
3. Zhu, W., Mow, V. C., Koob, T. J. & Eyre, D. R. Viscoelastic shear properties of articular cartilage and the effects of glycosidase treatments. *Journal of Orthopaedic Research* **11,** 771–781 (1993).
4. Schinagl, R. M., Gurskis, D., Chen, A. C. & Sah, R. L. Depth-dependent confined compression modulus of full-thickness bovine articular cartilage. *Journal of Orthopaedic Research* **15,** 499–506 (1997).
5. Sophia Fox, A. J., Bedi, A. & Rodeo, S. A. The basic science of articular cartilage: structure, composition, and function. *Sports Health* **1,** 461–468 (2009).
6. Mendler, M., Eich-Bender, S. G., Vaughan, L., Winterhalter, K. H. & Bruckner, P. Cartilage contains mixed fibrils of collagen types II, IX, and XI. *Journal of Cell Biology* **108,** 191–197 (1989).
7. Kiani, C., Chen, L., Wu, Y. J., Yee, A. J. & Yang, B. B. Structure and function of aggrecan. *Cell Research* **12,** 19–32 (2002).
8. Heinegård, D. & Hascall, V. C. Aggregation of cartilage proteoglycans. 3. Characteristics of the proteins isolated from trypsin digests of aggregates. *The Journal of Biological Chemistry* **249,** 4250–4256 (1974).
9. DeLise, A., Fischer, L. & Tuan, R. Cellular interactions and signaling in cartilage development. *Osteoarthritis and Cartilage* **8,** 309–334 (2000).
10. Goldring, M. B., Tsuchimochi, K. & Ijiri, K. The control of chondrogenesis. *Journal of Cellular Biochemistry* **97,** 33–44 (2006).
11. Grotewold, L. & Rüther, U. Bmp, Fgf and Wnt signalling in programmed cell death and chondrogenesis during vertebrate limb development: the role of Dickkopf-1. *The International Journal of Developmental Biology* **46,** 943–947 (2002).
12. Shum, L., Coleman, C. M., Hatakeyama, Y. & Tuan, R. S. Morphogenesis and dysmorphogenesis of the appendicular skeleton. *Birth Defects Research. Part C* **69,** 102–122 (2003).

13. Tavella, S., Bellese, G., Castagnola, P., Martin, I., Piccini, D., Doliana, R., Colombatti, A., Cancedda, R. & Tacchetti, C. Regulated expression of fibronectin, laminin and related integrin receptors during the early chondrocyte differentiation. *Journal of Cell Science* **110,** 2261–2270 (1997).

14. Shakibaei, M., Zimmermann, B. & Merker, H. J. Changes in integrin expression during chondrogenesis in vitro: an immunomorphological study. *The Journal of Histochemistry and Cytochemistrymistry* **43,** 1061–1069 (1995).

15. Oberlender, S. A. & Tuan, R. S. Expression and functional involvement of N-cadherin in embryonic limb chondrogenesis. *Development* **120,** 177–187 (1994).

16. DeLise, A. M. & Tuan, R. S. Alterations in the spatiotemporal expression pattern and function of N-cadherin inhibit cellular condensation and chondrogenesis of limb mesenchymal cells in vitro. *Journal of Cellular Biochemistry* **87,** 342–359 (2002).

17. Tuli, R., Tuli, S., Nandi, S., Huang, X., Manner, P. A., Hozack, W. J., Danielson, K. G., Hall, D. J. & Tuan, R. S. Transforming growth factor-β-mediated chondrogenesis of human mesenchymal progenitor cells involves N-cadherin and Mitogen-activated protein kinase and Wnt signaling cross-talk. *Journal of Biological Chemistry* **278,** 41227–41236 (2003).

18. Santo, V. E., Gomes, M., Mano, J. & Reis, R. L. Controlled release strategies for bone, cartilage and osteochondral engineering - Part I: Recapitulation of native tissue healing and variables for the design of delivery systems. *Tissue Engineering. Part B,* 1–43 (2012).

19. Gañan, Y., Macias, D., Duterque-Coquillaud, M., Ros, M. a. & Hurle, J. M. Role of TGFβs and BMPs as signals controlling the position of the digits and the areas of interdigital cell death in the developing chick limb autopod. *Development* **122,** 2349–2357 (1996).

20. Johnstone, B., Hering, T. M., Caplan, A. I., Goldberg, V. M. & Yoo, J. U. In vitro chondrogenesis of bone marrow-derived mesenchymal progenitor cells. *Experimental cell research* **238,** 265–272 (1998).

21. Ng, L.-J., Wheatley, S., Muscat, G. E., Conway-Campbell, J., Bowles, J., Wright, E., Bell, D. M., Tam, P. P., Cheah, K. S. & Koopman, P. Sox9 binds DNA, activates transcription, and coexpresses with type II collagen during chondrogenesis in the mouse. *Developmental Biology* **183,** 108–121 (1997).

22. Wright, E., Hargrave, M. R., Christiansen, J., Cooper, L., Kun, J., Evans, T., Gangadharan, U., Greenfield, A. & Koopman, P. The Sry-related gene Sox9 is expressed during chondrogenesis in mouse embryos. *Nature Genetics* **9,** 15–20 (1995).

23. Lawrence, R. C., Felson, D. T., Helmick, C. G., Arnold, L. M., Choi, H., Deyo, R. A., Gabriel, S., Hirsch, R., Hochberg, M. C., Hunder, G. G., Jordan, J. M., Katz, J. N., Kremers, H. M. & Wolfe, F. Estimates of the prevalence of arthritis and other rheumatic conditions in the United States: Part II. *Arthritis & Rheumatism* **58,** 26–35 (2008).

24. Arden, N. & Nevitt, M. Osteoarthritis: Epidemiology. *Best Practice & Research Clinical Rheumatology* **20,** 3–25 (2006).

25. Outerbridge, R. E. Further studies on the etiology of chondromalacia patellae. *The Journal of Bone and Joint Surgery* **46,** 179–190 (1964).

26. Rackwitz, L., Schneider, U., Andereya, S., Siebenlist, S., Reichert, J. C., Fensky, F., Arnholdt, J., Arnhold, J., Löer, I., Grossstück, R., Zinser, W., Barthel, T., Rudert, M. & Nöth, U. [Reconstruction of osteochondral defects with a collagen I hydrogel. Results of a prospective multicenter study]. *Der Orthopäde* **41,** 268–279 (2012).

27. Widuchowski, W., Widuchowski, J. & Trzaska, T. Articular cartilage defects: Study of 25,124 knee arthroscopies. *The Knee* **14,** 177–182 (2007).

28. Schnabel, M., Marlovits, S., Eckhoff, G., Fichtel, I., Gotzen, L., Vécsei, V. & Schlegel, J. Dedifferentiation-associated changes in morphology and gene expression in primary human articular chondrocytes in cell culture. *Osteoarthritis and Cartilage* **10,** 62–70 (2002).

29. Ma, B., Leijten, J., Wu, L., Kip, M., van Blitterswijk, C., Post, J. & Karperien, M. Gene expression profiling of dedifferentiated human articular chondrocytes in monolayer culture. *Osteoarthritis and Cartilage* **21,** 599–603 (2013).

30. Kang, S.-W., Yoo, S. P. & Kim, B.-S. Effect of chondrocyte passage number on histological aspects of tissue-engineered cartilage. *Bio-medical Materials and Engineering* **17,** 269–276 (2007).

31. Zuk, P. A., Zhu, M., Mizuno, H., Huang, J., Futrell, J. W., Katz, A. J., Benhaim, P., Lorenz, H. P. & Hedrick, M. H. Multilineage cells from human adipose tissue: Implications for cell-based therapies. *Tissue Engineering* **7,** 211–228 (2001).

32. Pittenger, M. F. Multilineage potential of adult human mesenchymal stem cells. *Science* **284,** 143–147 (1999).

33. De Bari, C., Dell'Accio, F., Tylzanowski, P. & Luyten, F. P. Multipotent mesenchymal stem cells from adult human synovial membrane. *Arthritis & Rheumatism* **44,** 1928–1942 (2001).

34. Zvaifler, N. J., Marinova-Mutafchieva, L., Adams, G., Edwards, C. J., Moss, J., Burger, J. A. & Maini, R. N. Mesenchymal precursor cells in the blood of normal individuals. *Arthritis Research* **2,** 477–488 (2000).

35. Beane, O. S. & Darling, E. M. Isolation, characterization, and differentiation of stem cells for cartilage regeneration. *Annals of Biomedical Engineering* **40,** 2079–2097 (2012).

36. Hass, R., Kasper, C., Böhm, S. & Jacobs, R. Different populations and sources of human mesenchymal stem cells (MSC): A comparison of adult and neonatal tissue-derived MSC. *Cell communication and Signaling* **9,** 12 (2011).

37. Mueller, M. B., Blunk, T., Appel, B., Maschke, A., Goepferich, A., Zellner, J., Englert, C., Prantl, L., Kujat, R., Nerlich, M. & Angele, P. Insulin is essential for in vitro chondrogenesis of mesenchymal progenitor cells and influences chondrogenesis in a dose-dependent manner. *International Orthopaedics* **37,** 153–158 (2013).

38. Bauer-Kreisel, P., Goepferich, A. & Blunk, T. Cell-delivery therapeutics for adipose tissue regeneration. *Advanced Drug Delivery Reviews* **62,** 798–813 (2010).

39. Wittmann, K., Storck, K., Muhr, C., Mayer, H., Regn, S., Staudenmaier, R., Wiese, H., Maier, G., Bauer-Kreisel, P. & Blunk, T. Development of volume-stable adipose tissue constructs using polycaprolactone-based polyurethane scaffolds and fibrin hydrogels. *Journal of Tissue Engineering and Regenerative Medicine* **10,** E409–E418 (2016).

40. Shao, J., Zhang, W. & Yang, T. Using mesenchymal stem cells as a therapy for bone regeneration and repairing. *Biological Research* **48,** 1–7 (2015).

41. De Bari, C., Dell'Accio, F., Vandenabeele, F., Vermeesch, J. R., Raymackers, J.-M. & Luyten, F. P. Skeletal muscle repair by adult human mesenchymal stem cells from synovial membrane. *The Journal of Cell Biology* **160,** 909–918 (2003).

42. Dezawa, M., Ishikawa, H., Itokazu, Y., Yoshihara, T., Hoshino, M., Takeda, S.-i., Ide, C. & Nabeshima, Y.-i. Bone marrow stromal cells generate muscle cells and repair muscle degeneration. *Science* **309,** 314–317 (2005).

43. Young, R. G., Butler, D. L., Weber, W., Caplan, A. I., Gordon, S. L. & Fink, D. J. Use of mesenchymal stem cells in a collagen matrix for achilles tendon repair. *Journal of Orthopaedic Research* **16,** 406–413 (1998).

44. Chaudhury, S. Mesenchymal stem cell applications to tendon healing. *Muscles, Ligaments and Tendons Journal* **2,** 222–229 (2012).

45. Cheng, L., Qasba, P., Vanguri, P. & Thiede, M. A. Human mesenchymal stem cells support megakaryocyte and pro-platelet formation from CD34(+) hematopoietic progenitor cells. *Journal of Cellular Physiology* **184,** 58–69 (2000).

46. Majumdar, M. K., Thiede, M. a., Haynesworth, S. E., Bruder, S. P. & Gerson, S. L. Human marrow-derived mesenchymal stem cells (MSCs) express hematopoietic cytokines and support long-term hematopoiesis when differentiated toward stromal and osteogenic lineages. *Journal of Hematotherapy & Stem Cell Research* **9,** 841–848 (2000).

47. Robert, H. Chondral repair of the knee joint using mosaicplasty. *Orthopaedics and Traumatology: Surgery and Research* **97,** 418–429 (2011).

48. Brittberg, M., Lindahl, A., Nilsson, A., Ohlsson, C., Isaksson, O. & Peterson, L. Treatment of deep cartilage defects in the knee with autologous chondrocyte transplantation. *New England Journal of Medicine* **331,** 889–895 (1994).

49. Corpus, K. T., Bajaj, S., Daley, E. L., Lee, A., Kercher, J. S., Salata, M. J., Verma, N. N. & Cole, B. J. Long-term evaluation of autologous chondrocyte implantation: Minimum 7-year follow-up. *Cartilage* **3,** 342–350 (2012).

50. Briggs, T. W. R., Mahroof, S., David, L. A., Flannelly, J., Pringle, J., Bayliss, M., Orth, M. & Bayliss, A. M. Histological evaluation of chondral defects after autologous chondrocyte implantation of the knee. *The Journal Of Bone And Joint Surgery* **8585,** 1077–1083 (2003).

51. Peterson, L., Brittberg, M., Kiviranta, I., Akerlund, E. L. & Lindahl, A. Autologous chondrocyte transplantation. Biomechanics and long-term durability. *The American Journal of Sports Medicine* **30,** 2–12 (2002).

52. Guney, A., Yurdakul, E., Karaman, I., Bilal, O., Kafadar, I. H. & Oner, M. Medium-term outcomes of mosaicplasty versus arthroscopic microfracture with or without platelet-rich plasma in the treatment of osteochondral lesions of the talus. *Knee Surgery, Sports Traumatology, Arthroscopy* **24,** 1293–1298 (2016).

53. Bentley, G., Biant, L. C., Vijayan, S., Macmull, S., Skinner, J. a. & Carrington, R. W. J. Minimum ten-year results of a prospective randomised study of autologous chondrocyte implantation versus mosaicplasty for symptomatic articular cartilage lesions of the knee. *The Journal of Bone and Joint Surgery* **94,** 504–509 (2012).

54. Harris, J. D., Siston, R. A., Brophy, R. H., Lattermann, C., Carey, J. L. & Flanigan, D. C. Failures, re-operations, and complications after autologous chondrocyte implantation - a systematic review. *Osteoarthritis and Cartilage* **19,** 779–791 (2011).

55. Macmull, S., Parratt, M. T. R., Bentley, G., Skinner, J. a., Carrington, R. W. J., Morris, T. & Briggs, T. W. R. Autologous chondrocyte implantation in the adolescent knee. *The American Journal of Sports Medicine* **39,** 1723–1730 (2011).

56. Shekkeris, A. S., Perera, J. R., Bentley, G., Flanagan, A. M., Miles, J., Carrington, R. W. J., Skinner, J. A. & Briggs, T. W. R. Histological results of 406 biopsies following ACI/MACI procedures for osteochondral defects in the knee. *Orthopaedic Proceedings* **94-B,** 1–12 (2012).

57. Fickert, S., Gerwien, P., Helmert, B., Schattenberg, T., Weckbach, S., Kaszkin-Bettag, M. & Lehmann, L. One-year clinical and radiological results of a prospective, investigator-initiated trial examining a novel, purely autologous 3-Dimen-sional autologous chondrocyte transplantation product in the knee. *Cartilage* **3,** 27–42 (2012).

58. Buckwalter, J. A., Bowman, G. N., Albright, J. P., Wolf, B. R. & Bollier, M. Clinical outcomes of patellar chondral lesions treated with juvenile particulated cartilage allografts. *The Iowa Orthopaedic Journal* **34,** 44–49 (2014).

59. McCormick, F., Cole, B. J., Nwachukwu, B., Harris, J. D., Adkisson, H. D. & Farr, J. Treatment of focal cartilage defects with a juvenile allogeneic 3-Dimensional articular cartilage graft. *Operative Techniques in Sports Medicine* **21,** 95–99 (2013).

60. Adkisson, H. D., Martin, J. A., Amendola, R. L., Milliman, C., Mauch, K. A., Katwal, A. B., Seyedin, M., Amendola, A., Streeter, P. R. & Buckwalter, J. A. The potential of human allogeneic juvenile chondrocytes for restoration of articular cartilage. *The American Journal of Sports Medicine* **38,** 1324–1333 (2010).

61. Bonasia, D. E., Martin, J. A., Marmotti, A., Amendola, R. L., Buckwalter, J. A., Rossi, R., Blonna, D., Adkisson, H. D. & Amendola, A. Cocultures of adult and juvenile chondrocytes compared with adult and juvenile chondral fragments: in vitro matrix production. *The American Journal of Sports Medicine* **39,** 2355–2361 (2011).

62. Huang, B. J., Hu, J. C. & Athanasiou, K. A. Cell-based tissue engineering strategies used in the clinical repair of articular cartilage. *Biomaterials* **98,** 1–22 (2016).

63. Pietschmann, M. F., Horng, A., Niethammer, T., Pagenstert, I., Sievers, B., Jansson, V., Glaser, C. & Müller, P. E. Cell quality affects clinical outcome after MACI procedure for cartilage injury of the knee. *Knee Surgery, Sports Traumatology, Arthroscopy* **17,** 1305–1311 (2009).

64. Zheng, M.-H., Willers, C., Kirilak, L., Yates, P., Xu, J., Wood, D. & Shimmin, A. Matrix-induced autologous chondrocyte implantation (MACI®): biological and histological assessment. *Tissue Engineering* **13,** 737–746 (2007).

65. Crawford, D. C., Heveran, C. M., Cannon, W. D., Foo, L. F. & Potter, H. G. An autologous cartilage tissue implant NeoCart for treatment of grade III chondral injury to the distal femur: prospective clinical safety trial at 2 years. *The American Journal of Sports Medicine* **37,** 1334–1343 (2009).

66. Barnewitz, D., Endres, M., Krüger, I., Becker, A., Zimmermann, J., Wilke, I., Ringe, J., Sittinger, M. & Kaps, C. Treatment of articular cartilage defects in horses with polymer-based cartilage tissue engineering grafts. *Biomaterials* **27,** 2882–2889 (2006).

67. Clavé, A., Potel, J.-F., Servien, E., Neyret, P., Dubrana, F. & Stindel, E. Third-generation autologous chondrocyte implantation versus mosaicplasty for knee cartilage injury: 2-year randomized trial. *Journal of Orthopaedic Research* **34,** 658–665 (2016).

68. Nicodemus, G. D. & Bryant, S. J. Cell encapsulation in biodegradable hydrogels for tissue engineering applications. *Tissue Engineering. Part B* **14,** 149–165 (2008).

69. Balakrishnan, B. & Banerjee, R. Biopolymer-based hydrogels for cartilage tissue engineering. *Chemical Reviews* **111,** 4453–4474 (2011).

70. Spiller, K. L., Maher, S. A. & Lowman, A. M. Hydrogels for the repair of articular cartilage defects. *Tissue Engineering. Part B* **17,** 281–299 (2011).

71. Zhu, J. & Marchant, R. E. Design properties of hydrogel tissue-engineering scaffolds. *Expert Review of Medical Devices* **8,** 607–626 (2011).

72. Khan, F. & Ahmad, S. R. Polysaccharides and their derivatives for versatile tissue engineering application. *Macromolecular Bioscience* **13,** 395–421 (2013).

73. Zhu, H., Mitsuhashi, N., Klein, A., Barsky, L. W., Weinberg, K., Barr, M. L., Demetriou, A. & Wu, G. D. The role of the hyaluronan receptor CD44 in mesenchymal stem cell migration in the extracellular matrix. *Stem Cells* **24,** 928–935 (2006).

74. Hardwick, C., Hoare, K., Owens, R., Hohn, H. P., Hook, M., Moore, D., Cripps, V., Austen, L., Nance, D. M. & Turley, E. A. Molecular cloning of a novel hyaluronan receptor that mediates tumor cell motility. *The Journal of Cell Biology* **117,** 1343–1350 (1992).

75. Goldberg, V. & Buckwalter, J. Hyaluronans in the treatment of osteoarthritis of the knee: evidence for disease-modifying activity. *Osteoarthritis and Cartilage* **13,** 216–224 (2005).

76. Tan, H., Ramirez, C. M., Miljkovic, N., Li, H., Rubin, J. P. & Marra, K. G. Thermosensitive injectable hyaluronic acid hydrogel for adipose tissue engineering. *Biomaterials* **30,** 6844–6853 (2009).

77. Burdick, J. A. & Prestwich, G. D. Hyaluronic acid hydrogels for biomedical applications. *Advanced Materials* **23,** 41–56 (2011).

78. Smeds, K., Pfister-Serres, A., Miki, D., Dastghieb, K. A., Inoue, M., Hatchell, D. L. & Grinstaff, M. W. Novel Photocrosslinkable Polysaccharides for In Situ Hydrogel Formation. *Journal of Biomedical Materials Research* **54,** 115–121 (2001).

79. Nettles, D. L., Vail, T. P., Morgan, M. T., Grinstaff, M. W. & Setton, L. A. Photocrosslinkable hyaluronan as a scaffold for articular cartilage repair. *Annals of Biomedical Engineering* **32,** 391–397 (2004).

80. Burdick, J. A., Chung, C., Jia, X., Randolph, M. a. & Langer, R. Controlled degradation and mechanical behavior of photopolymerized hyaluronic acid networks. *Biomacromolecules* **6,** 386–391 (2005).

81. Park, S.-H., Park, S. R., Chung, S. I., Pai, K. S. & Min, B.-H. Tissue-engineered cartilage using fibrin/hyaluronan composite gel and its in vivo implantation. *Artificial Organs* **29,** 838–845 (2005).

82. Chung, C. & Burdick, J. A. Influence of three-dimensional hyaluronic acid microenvironments on mesenchymal stem cell chondrogenesis. *Tissue Engineering. Part A* **15,** 243–254 (2009).

83. Lenas, P. & Luyten, F. P. An emerging paradigm in tissue engineering: from chemical engineering to developmental engineering for bioartificial tissue formation through a series of unit operations that simulate the in vivo successive developmental stages. *Industrial and Engineering Chemistry Research* **50,** 482–522 (2011).

84. Caldwell, K. L. & Wang, J. Cell-based articular cartilage repair: The link between development and regeneration. *Osteoarthritis and Cartilage* **23,** 351–362 (2015).

85. Zhu, J. Bioactive modification of poly(ethylene glycol) hydrogels for tissue engineering. *Biomaterials* **31,** 4639–4656 (2010).

86. Pierschbacher, M. D. & Ruoslahti, E. Cell attachment activity of fibronectin can be duplicated by small synthetic fragments of the molecule. *Nature* **309,** 30–33 (1984).

87. Zhu, J., Beamish, J. A., Tang, C., Kottke-Marchant, K. & Marchant, R. E. Extracellular matrix-like cell-adhesive hydrogels from RGD-containing poly(ethylene glycol) diacrylate. *Macromolecules* **39,** 1305–1307 (2006).

88. Salinas, C. N. & Anseth, K. S. The influence of the RGD peptide motif and its contextual presentation in PEG gels on human mesenchymal stem cell viability. *Journal of Tissue Engineering and Regenerative Medicine* **2,** 296–304 (2008).

89. Tashiro, K., Sephel, G. C., Weeks, B., Sasaki, M., Martin, G. R., Kleinman, H. K. & Yamada, Y. A synthetic peptide containing the IKVAV sequence from the A chain of laminin mediates cell attachment, migration, and neurite outgrowth. *Journal of Biological Chemistry* **264,** 16174–16182 (1989).

90. Graf, J., Iwamoto, Y., Sasaki, M., Martin, G. R., Kleinman, H. K., Robey, F. A. & Yamada, Y. Identification of an amino acid sequence in laminin mediating cell attachment, chemotaxis, and receptor binding. *Cell* **48,** 989–996 (1987).

91. Weber, L. M., Hayda, K. N., Haskins, K. & Anseth, K. S. The effects of cell–matrix interactions on encapsulated β-cell function within hydrogels functionalized with matrix-derived adhesive peptides. *Biomaterials* **28,** 3004–3011 (2007).

92. Patel, P. N., Gobin, A. S., West, J. L. & Patrick, C. W. Poly(ethylene glycol) hydrogel system supports preadipocyte viability, adhesion, and proliferation. *Tissue Engineering* **11,** 1498–1505 (2005).

93. Staatz, W. D., Fok, K. F., Zutter, M. M., Adams, S. P., Rodriguez, B. A. & Santoro, S. A. Identification of a tetrapeptide recognition sequence for the $\alpha 2\beta 1$ integrin in collagen. *Journal of Biological Chemistry* **266,** 7363–7367 (1991).

94. Chia, H., Vigen, M. & Kasko, A. Effect of substrate stiffness on pulmonary fibroblast activation by TGF-β. *Acta Biomaterialia* **8,** 2602–2611 (2012).

95. Knight, C. G., Morton, L. F., Onley, D. J., Peachey, A. R., Messent, J., Smethurst, P. A., Danny, S., Farndale, R. W., Michael, J., Knight, C. G., Morton, L. F., Onley, D. J., Peachey, A. R., Messent, A. J., Smethurst, P. A., Tuckwell, D. S., Farndale, R. W. & Barnes, M. J. Identification in collagen type I of an integrin $\alpha 2\beta 1$-binding site containing an essential GER sequence. *The Journal of Biological Chemistry* **273,** 33287–33294 (1998).

96. Mhanna, R., Öztürk, E., Vallmajo-Martin, Q., Millan, C., Müller, M. & Zenobi-Wong, M. GFOGER-modified MMP-sensitive polyethylene glycol hydrogels induce chondrogenic differentiation of human mesenchymal stem cells. *Tissue Engineering. Part A* **20,** 1165–1174 (2014).

97. Lee, H. J., Yu, C., Chansakul, T., Hwang, N. S., Varghese, S., Yu, S. M. & Elisseeff, J. H. Enhanced chondrogenesis of mesenchymal stem cells in collagen mimetic peptide-mediated microenvironment. *Tissue engineering. Part A* **14,** 1843–51 (2008).

98. Scott, J. E. Proteodermatan and proteokeratan sulfate (decorin, lumican/fibromodulin) proteins are horseshoe shaped. Implications for their interactions with collagen. *Biochemistry* **35,** 8795–9 (1996).

99. Salinas, C. N. & Anseth, K. S. Decorin moieties tethered into PEG networks induce chondrogenesis of human mesenchymal stem cells. *Journal of Biomedical Materials Research. Part A* **90,** 456–464 (2009).

100. Blaschuk, O. W., Sullivan, R., David, S. & Pouliot, Y. Identification of a cadherin cell adhesion recognition sequence. *Developmental Biology* **139,** 227–229 (1990).

101. Bian, L., Guvendiren, M., Mauck, R. L. & Burdick, J. a. Hydrogels that mimic developmentally relevant matrix and N-cadherin interactions enhance MSC chondrogenesis. *Proceedings of the National Academy of Sciences* **110,** 10117–10122 (2013).

102. Patterson, J. & Hubbell, J. Enhanced proteolytic degradation of molecularly engineered PEG hydrogels in response to MMP-1 and MMP-2. *Biomaterials* **31,** 7836–7845 (2010).

103. Censi, R., Di Martino, P., Vermonden, T. & Hennink, W. E. Hydrogels for protein delivery in tissue engineering. *Journal of Controlled Release* **161,** 680–692 (2012).

104. Santo, V. E., Gomes, M. E., Mano, J. F. & Reis, R. L. Controlled release strategies for bone, cartilage, and osteochondral engineering - Part I: recapitulation of native tissue healing and variables for the design of delivery systems. *Tissue engineering. Part B* **19,** 308–326 (2013).

105. Santo, V. E., Gomes, M. E., Mano, J. F. & Reis, R. L. Controlled release strategies for bone, cartilage, and osteochondral engineering - Part II: challenges on the evolution from single to multiple bioactive factor delivery. *Tissue Engineering. Part B* **19,** 327–352 (2013).

106. Mathieu, M., Vigier, S., Labour, M. N., Jorgensen, C., Belamie, E. & Noël, D. Induction of mesenchymal stem cell differentiation and cartilage formation by cross-linker-free collagen microspheres. *European Cells & Materials* **28,** 82–97 (2014).

107. Ansboro, S., Hayes, J. S., Barron, V., Browne, S., Howard, L., Greiser, U., Lalor, P., Shannon, F., Barry, F. P., Pandit, A. & Murphy, J. M. A chondromimetic microsphere for in situ spatially controlled chondrogenic differentiation of human mesenchymal stem cells. *Journal of Controlled Release* **179,** 42–51 (2014).

108. Xu, X., Jha, A. K., Duncan, R. L. & Jia, X. Heparin-decorated, hyaluronic acid-based hydrogel particles for the controlled release of bone morphogenetic protein 2. *Acta Biomaterialia* **7,** 3050–3059 (2011).

109. Zhang, Z., Gupte, M. J., Jin, X. & Ma, P. X. Injectable peptide decorated functional nanofibrous hollow microspheres to direct stem cell differentiation and tissue regeneration. *Advanced Functional Materials* **25,** 350–360 (2015).

110. Elisseeff, J., McIntosh, W., Fu, K., Blunk, T. & Langer, R. Controlled-release of IGF-I and TGF-β1 in a photopolymerizing hydrogel for cartilage tissue engineering. *Journal of Orthopaedic Research* **19,** 1098–1104 (2001).

111. Bian, L., Zhai, D. Y., Tous, E., Rai, R., Mauck, R. L. & Burdick, J. a. Enhanced MSC chondrogenesis following delivery of TGF-β3 from alginate microspheres within hyaluronic acid hydrogels in vitro and in vivo. *Biomaterials* **32,** 6425–6434 (2011).

112. Reyes, R., Delgado, A., Solis, R., Sanchez, E., Hernandez, A., Roman, J. S. & Evora, C. Cartilage repair by local delivery of transforming growth factor-β1 or bone morphogenetic protein-2 from a novel, segmented polyurethane/polylactic-co -glycolic bilayered scaffold. *Journal of Biomedical Materials Research. Part A* **102,** 1110–1120 (2014).

113. Tsaryk, R., Gloria, A., Russo, T., Anspach, L., De Santis, R., Ghanaati, S., Unger, R. E., Ambrosio, L. & Kirkpatrick, C. J. Collagen-low molecular weight hyaluronic acid semi-interpenetrating network loaded with gelatin microspheres for cell and growth factor delivery for nucleus pulposus regeneration. *Acta Biomaterialia* **20,** 10–21 (2015).

114. Rocha, P. M., Santo, V. E., Gomes, M. E., Reis, R. L. & Mano, J. F. Encapsulation of adipose-derived stem cells and transforming growth factor-β1 in carrageenan-based hydrogels for cartilage tissue engineering. *Journal of Bioactive and Compatible Polymers* **26,** 493–507 (2011).

115. Mullen, L. M., Best, S. M., Ghose, S., Wardale, J., Rushton, N. & Cameron, R. E. Bioactive IGF-1 release from collagen-GAG scaffold to enhance cartilage repair in vitro. *Journal of Materials Science: Materials in Medicine* **26,** 5325 (2015).

116. Place, E. S., Nair, R., Chia, H. N., Szulgit, G., Lim, E.-h. & Stevens, M. M. Latent TGF-β hydrogels for cartilage tissue engineering. *Advanced Healthcare Materials* **1,** 480–484 (2012).

117. McCall, J. D., Luoma, J. E. & Anseth, K. S. Covalently tethered transforming growth factor beta in PEG hydrogels promotes chondrogenic differentiation of encapsulated human mesenchymal stem cells. *Drug Delivery and Translational Research* **2,** 305–312 (2012).

118. Sridhar, B. V., Doyle, N. R., Randolph, M. A. & Anseth, K. S. Covalently tethered TGF-β1 with encapsulated chondrocytes in a PEG hydrogel system enhances extracellular matrix production. *Journal of Biomedical Materials Research. Part A* **102,** 4464–4472 (2014).

119. Kainthan, R. K., Janzen, J., Levin, E., Devine, D. V. & Brooks, D. E. Biocompatibility testing of branched and linear polyglycidol. *Biomacromolecules* **7,** 703–709 (2006).

120. Imran Ul-Haq, M., Lai, B. F. L., Chapanian, R. & Kizhakkedathu, J. N. Influence of architecture of high molecular weight linear and branched polyglycerols on their biocompatibility and biodistribution. *Biomaterials* **33,** 9135–9147 (2012).

121. Dworak, A., Slomokowski, S., Basinska, T., Gosecka, M., Walach, W. & Trzebicka, B. Polyglycidol - how is it synthesized and what is it used for? *Polimery* **58,** 641–649 (2013).

122. Thomas, A., Müller, S. S. & Frey, H. Beyond poly(ethylene glycol): Linear polyglycerol as a multifunctional polyether for biomedical and pharmaceutical applications. *Biomacromolecules* **15,** 1935–1954 (2014).

123. Singh, S., Topuz, F., Hahn, K., Albrecht, K. & Groll, J. Embedding of active proteins and living cells in redox-sensitive hydrogels and nanogels through enzymatic cross-linking. *Angewandte Chemie - International Edition* **52,** 3000–3003 (2013).

124. Zheng Shu, X., Liu, Y., Palumbo, F. S., Luo, Y. & Prestwich, G. D. In situ crosslinkable hyaluronan hydrogels for tissue engineering. *Biomaterials* **25,** 1339–1348 (2004).

125. Shu, X. Z., Ahmad, S., Liu, Y. & Prestwich, G. D. Synthesis and evaluation of injectable, in situ crosslinkable synthetic extracellular matrices for tissue engineering. *Journal of Biomedical Materials Research. Part A* **79,** 902–912 (2006).

126. Nair, D. P., Podgórski, M., Chatani, S., Gong, T., Xi, W., Fenoli, C. R. & Bowman, C. N. The Thiol-Michael addition click reaction: A powerful and widely used tool in materials chemistry. *Chemistry of Materials* **26,** 724–744 (2014).

127. Klein, T. J., Malda, J., Sah, R. L. & Hutmacher, D. W. Tissue engineering of articular cartilage with biomimetic zones. *Tissue Engineering. Part B* **15,** 143–157 (2009).

128. Klein, T. J., Rizzi, S. C., Reichert, J. C., Georgi, N., Malda, J., Schuurman, W., Crawford, R. W. & Hutmacher, D. W. Strategies for zonal cartilage repair using hydrogels. *Macromolecular Bioscience* **9,** 1049–1058 (2009).

129. Martin, I., Obradovic, B., Freed, L. E. & Vunjak-Novakovic, G. Method for quantitative analysis of glycosaminoglycan distribution in cultured natural and engineered cartilage. *Annals of Biomedical Engineering* **27,** 656–662 (1999).

130. Schmitz, N., Laverty, S., Kraus, V. & Aigner, T. Basic methods in histopathology of joint tissues. *Osteoarthritis and Cartilage* **18,** S113–S116 (2010).

131. Kim, Y.-J., Sah, R. L., Doong, J.-Y. H. & Grodzinsky, A. J. Fluorometric assay of DNA in cartilage explants using Hoechst 33258. *Analytical Biochemistry* **174,** 168–176 (1988).

132. Farndale, R. W., Buttle, D. J. & Barrett, A. J. Improved quantitation and discrimination of sulphated glycosaminoglycans by use of dimethylmethylene blue. *BBA - General Subjects* **883,** 173–177 (1986).

133. Woessner, J. The determination of hydroxyproline in tissue and protein samples containing small proportions of this imino acid. *Archives of Biochemistry and Biophysics* **93,** 440–447 (1961).

134. Hollander, A. P., Heathfield, T. F., Webber, C., Iwata, Y., Bourne, R., Rorabeck, C. & Poole, A. R. Increased damage to type II collagen in osteoarthritic articular cartilage detected by a new immunoassay. *Journal of Clinical Investigation* **93,** 1722–1732 (1994).

135. Simões, A. E. S., Pereira, D. M., Amaral, J. D., Nunes, A. F., Gomes, S. E., Rodrigues, P. M., Lo, A. C., D'Hooge, R., Steer, C. J., Thibodeau, S. N., Borralho, P. M. & Rodrigues, C. M. P. Efficient recovery of proteins from multiple source samples after TRIzol(®) or TRIzol(®)LS RNA extraction and long-term storage. *BMC Genomics* **14,** 181 (2013).

136. Schindelin, J., Arganda-Carreras, I., Frise, E., Kaynig, V., Longair, M., Pietzsch, T., Preibisch, S., Rueden, C., Saalfeld, S., Schmid, B., Tinevez, J.-Y., White, D. J., Hartenstein, V., Eliceiri, K., Tomancak, P. & Cardona, A. Fiji: an open-source platform for biological-image analysis. *Nature Methods* **9,** 676–682 (2012).

137. Dexheimer, V., Frank, S. & Richter, W. Proliferation as a requirement for in vitro chondrogenesis of human mesenchymal stem cells. *Stem Cells and Development* **21,** 2160–9 (2012).

138. Zhu, Y., Oganesian, A., Keene, D. R. & Sandell, L. J. Type IIA procollagen containing the cysteine-rich amino propeptide is deposited in the extracellular matrix of prechondrogenic tissue and binds to TGF-β1 and BMP-2. *Journal of Cell Biology* **144,** 1069–1080 (1999).

139. Bosnakovski, D., Mizuno, M., Kim, G., Takagi, S., Okumura, M. & Fujinaga, T. Chondrogenic differentiation of bovine bone marrow mesenchymal stem cells (MSCs) in different hydrogels: Influence of collagen type II extracellular matrix on MSC chondrogenesis. *Biotechnology and Bioengineering* **93,** 1152–1163 (2006).

140. Hildebrand, A., Romarís, M., Rasmussen, L. M., Heinegård, D., Twardzik, D. R., Border, W. A. & Ruoslahti, E. Interaction of the small interstitial proteoglycans biglycan, decorin and fibromodulin with transforming growth factor β. *Biochemical Journal* **302,** 527–534 (1994).

141. Bian, L., Hou, C., Tous, E., Rai, R., Mauck, R. L. & Burdick, J. A. The influence of hyaluronic acid hydrogel crosslinking density and macromolecular diffusivity on human MSC chondrogenesis and hypertrophy. *Biomaterials* **34,** 413–21 (2013).

142. Erickson, I. E., Huang, A. H., Sengupta, S., Kestle, S., Burdick, J. A. & Mauck, R. L. Macromer density influences mesenchymal stem cell chondrogenesis and maturation in photocrosslinked hyaluronic acid hydrogels. *Osteoarthritis and Cartilage* **17,** 1639–1648 (2009).

143. Bryant, S. J., Chowdhury, T. T., Lee, D. A., Bader, D. L. & Anseth, K. S. Crosslinking density influences chondrocyte metabolism in dynamically loaded photocrosslinked poly(ethylene glycol) hydrogels. *Annals of Biomedical Engineering* **32,** 407–417 (2004).

144. Wang, L.-S., Du, C., Toh, W. S., Wan, A. C., Gao, S. J. & Kurisawa, M. Modulation of chondrocyte functions and stiffness-dependent cartilage repair using an injectable enzymatically crosslinked hydrogel with tunable mechanical properties. *Biomaterials* **35,** 2207–2217 (2014).

145. Park, J. S., Chu, J. S., Tsou, A. D., Diop, R., Tang, Z., Wang, A. & Li, S. The effect of matrix stiffness on the differentiation of mesenchymal stem cells in response to TGF-β. *Biomaterials* **32,** 3921–3930 (2011).

146. Maturavongsadit, P., Bi, X., Metavarayuth, K., Luckanagul, J. A. & Wang, Q. Influence of Cross-Linkers on the in Vitro Chondrogenesis of Mesenchymal Stem Cells in Hyaluronic Acid Hydrogels. *ACS Applied Materials & Interfaces* **9,** 3318–3329 (2017).

147. Hudalla, G. A., Eng, T. S. & Murphy, W. L. An approach to modulate degradation and mesenchymal stem cell behavior in poly(ethylene glycol) networks. *Biomacromolecules* **9,** 842–849 (2008).

148. Metters, A. & Hubbell, J. Network formation and degradation behavior of hydrogels formed by Michael-Type addition reactions. *Biomacromolecules* **6,** 290–301 (2005).

149. Rydholm, A. E., Anseth, K. S. & Bowman, C. N. Effects of neighboring sulfides and pH on ester hydrolysis in thiol-acrylate photopolymers. *Acta Biomaterialia* **3,** 449–455 (2007).

150. Feng, Q., Zhu, M., Wei, K. & Bian, L. Cell-mediated degradation regulates human mesenchymal stem cell chondrogenesis and hypertrophy in MMP-sensitive hyaluronic acid hydrogels. *PLOS ONE* **9,** e99587 (2014).

151. Bahney, C. S., Hsu, C.-W., Yoo, J. U., West, J. L. & Johnstone, B. A bioresponsive hydrogel tuned to chondrogenesis of human mesenchymal stem cells. *The FASEB Journal* **25,** 1486–96 (2011).

152. Hesse, E., Freudenberg, U., Niemietz, T., Greth, C., Weisser, M., Hagmann, S., Binner, M., Werner, C. & Richter, W. Peptide-functionalized starPEG/heparin hydrogels direct mitogenicity, cell morphology and cartilage matrix distribution in vitro and in vivo. *Journal of Tissue Engineering and Regenerative Medicine.* <`http://doi.wiley.com/10.1002/term.2404`> (2017).

153. Sridhar, B. V., Brock, J. L., Silver, J. S., Leight, J. L., Randolph, M. A. & Anseth, K. S. Development of a cellularly degradable PEG hydrogel to promote articular cartilage extracellular matrix deposition. *Advanced Healthcare Materials* **4,** 702–713 (2015).

154. Cha, C., Soman, P., Zhu, W., Nikkhah, M., Camci-Unal, G., Chen, S. & Khademhosseini, A. Structural reinforcement of cell-laden hydrogels with microfabricated three dimensional scaffolds. *Biomaterials Science* **2,** 703–709 (2014).

155. Agrawal, A., Rahbar, N. & Calvert, P. D. Strong fiber-reinforced hydrogel. *Acta Biomaterialia* **9,** 5313–5318 (2013).

156. Coburn, J. M., Gibson, M., Monagle, S., Patterson, Z. & Elisseeff, J. H. Bioinspired nanofibers support chondrogenesis for articular cartilage repair. *Proceedings of the National Academy of Sciences* **109,** 10012–10017 (2012).

157. Bosworth, L. A., Turner, L.-A. & Cartmell, S. H. State of the art composites comprising electrospun fibres coupled with hydrogels: a review. *Nanomedicine: Nanotechnology, Biology and Medicine* **9,** 322–335 (2013).

158. Visser, J., Melchels, F. P., Jeon, J. E., van Bussel, E. M., Kimpton, L. S., Byrne, H. M., Dhert, W. J., Dalton, P. D., Hutmacher, D. W. & Malda, J. Reinforcement of hydrogels using three-dimensionally printed microfibres. *Nature Communications* **6,** 6933 (2015).

159. Melchels, F. P. W., Blokzijl, M. M., Levato, R., Peiffer, Q. C., de Ruijter, M., Hennink, W. E., Vermonden, T. & Malda, J. Hydrogel-based reinforcement of 3D bioprinted constructs. *Biofabrication* **8,** 035004 (2016).

160. Salinas, C. N. & Anseth, K. S. The enhancement of chondrogenic differentiation of human mesenchymal stem cells by enzymatically regulated RGD functionalities. *Biomaterials* **29,** 2370–2377 (2008).

161. Connelly, J. T., Garcia, A. J. & Levenston, M. E. Inhibition of in vitro chondrogenesis in RGD-modified three-dimensional alginate gels. *Biomaterials* **28,** 1071–1083 (2007).

162. Connelly, J. T., García, A. J. & Levenston, M. E. Interactions between integrin ligand density and cytoskeletal integrity regulate BMSC chondrogenesis. *Journal of Cellular Physiology* **217,** 145–54 (2008).

163. Tavella, S., Raffo, P., Tacchetti, C., Cancedda, R. & Castagnola, P. N-CAM and N-Cadherin expression during in vitro chondrogenesis. *Experimental Cell Research* **215,** 354–362 (1994).

164. Wu, S.-C., Chang, J.-K., Wang, C.-K., Wang, G.-J. & Ho, M.-L. Enhancement of chondrogenesis of human adipose derived stem cells in a hyaluronan-enriched microenvironment. *Biomaterials* **31,** 631–640 (2010).

165. Wu, S.-C., Chen, C.-H., Chang, J.-K., Fu, Y.-C., Wang, C.-K., Eswaramoorthy, R., Lin, Y.-S., Wang, Y.-H., Lin, S.-Y., Wang, G.-J. & Ho, M.-L. Hyaluronan initiates chondrogenesis mainly via CD44 in human adipose-derived stem cells. *Journal of Applied Physiology* **114,** 1610–8 (2013).

166. Wakefield, L. M., Winokur, T. S., Hollands, R. S., Christopherson, K., Levinson, A. D. & Sporn, M. B. Recombinant latent transforming growth factor β1 has a longer plasma half-life in rats than active transforming growth factor β1, and a different tissue distribution. *Journal of Clinical Investigation* **86,** 1976–1984 (1990).

167. Van Beuningen, H. M., Glansbeek, H. L., Van Der Kraan, P. M. & Van Den Berg, W. B. Osteoarthritis-like changes in the murine knee joint resulting from intra-articular transforming growth factor-β1 injections. *Osteoarthritis and Cartilage* **8,** 25–33 (2000).

168. Van Beuningen, H. M., Glansbeek, H. L., van der Kraan, P. M. & van den Berg, W. B. Differential effects of local application of BMP-2 or TGF-β1 on both articular cartilage composition and osteophyte formation. *Osteoarthritis and Cartilage* **6,** 306–317 (1998).

169. Van Beuningen, H. M., van der Kraan, P. M., Arntz, O. J. & van den Berg, W. B. In vivo protection against interleukin-1-induced articular cartilage damage by transforming growth factor-β1: age-related differences. *Annals of the Rheumatic Diseases* **53,** 593–600 (1994).

170. Shen, J., Li, S. & Chen, D. TGF-β signaling and the development of osteoarthritis. *Bone Research* **2,** 14002 (2014).

171. Massagué, J. TGFβ in cancer. *Cell* **134,** 215–230 (2008).

172. Na, K., Kim, S., Woo, D. G., Sun, B. K., Yang, H. N., Chung, H. M. & Park, K. H. Synergistic effect of TGFβ-3 on chondrogenic differentiation of rabbit chondrocytes in thermo-reversible hydrogel constructs blended with hyaluronic acid by in vivo test. *Journal of Biotechnology* **128,** 412–422 (2007).

173. Mann, B. K., Schmedlen, R. H. & West, J. L. Tethered-TGF-β increases extracellular matrix production of vascular smooth muscle cells. *Biomaterials* **22,** 439–444 (2001).

174. Schmid, T. M. & Linsenmayer, T. F. Immunohistochemical Localization of Short Chain Cartilage Collagen (Type-X) in Avian-Tissues. *Journal of Cell Biology* **100,** 598–605 (1985).

175. Huang, F. & Chen, Y.-G. Regulation of TGF-β receptor activity. *Cell & Bioscience* **2,** 1–10 (2012).

176. Miyazawa, K., Shinozaki, M., Hara, T., Furuya, T. & Miyazono, K. Two major Smad pathways in TGF-β superfamily signalling. *Genes to Cells* **7,** 1191–1204 (2002).

177. Zhang, Y. E. Non-Smad pathways in TGF-β signaling. *Cell Research* **19,** 128–139 (2009).

178. Derynck, R. & Zhang, Y. E. Smad-dependent and Smad-independent pathways in TGF-β family signalling. *Nature* **425,** 577–584 (2003).

179. Gilbert, S. *Developmental Biology. Juxtacrine Signaling.* 2000. <`https://www.ncbi.nlm.nih.gov/books/NBK10072/`> (2016).

180. Singh, A. B. & Harris, R. C. Autocrine, paracrine and juxtacrine signaling by EGFR ligands. *Cellular Signalling* **17,** 1183–1193 (2005).

181. Ito, Y., Kondo, S., Chen, G. & Imanishi, Y. Patterned artificial juxtacrine stimulatiom of cells by covalently immobilized insulin. *FEBS Letters* **403,** 159–162 (1997).

182. Ito, Y. & Imanishi, Y. Artificial juxtacrine stimulation for tissue engineering. *Journal of Biomaterials Science, Polymer Edition* **9,** 879–890 (1998).

183. Liu, H. W., Chen, C. H., Tsai, C. L. & Hsiue, G. H. Targeted delivery system for juxtacrine signaling growth factor based on rhBMP-2-mediated carrier-protein conjugation. *Bone* **39,** 825–836 (2006).

184. Jevševar, S., Kunstelj, M. & Porekar, V. G. PEGylation of therapeutic proteins. *Biotechnology Journal* **5,** 113–128 (2010).

185. Zhu, G., Chen, G., Shi, L., Feng, J., Wang, Y., Ye, C., Feng, W., Niu, J. & Huang, Z. PEGylated rhFGF-2 Conveys Long-term Neuroprotection and Improves Neuronal Function in a Rat Model of Parkinson's Disease. *Molecular Neurobiology* **51,** 32–42 (2014).

186. Groll, J., Ademovic, Z., Ameringer, T., Klee, D. & Moeller, M. Comparison of coatings from reactive star shaped PEG-stat-PPG prepolymers and grafted linear PEG for biological and medical applications. *Biomacromolecules* **6,** 956–962 (2005).

187. Williams, G., Williams, E.-J. & Doherty, P. Dimeric versions of two short N-cadherin binding motifs (HAVDI and INPISG) function as N-cadherin agonists. *The Journal of Biological Chemistry* **277,** 4361–4367 (2002).

188. Nuttelman, C., Tripodi, M. & Anseth, K. Synthetic hydrogel niches that promote hMSC viability. *Matrix Biology* **24,** 208–218 (2005).

189. Salinas, C. N. & Anseth, K. S. The influence of the RGD peptide motif and its contextual presentation in PEG gels on human mesenchymal stem cell viability. *Journal of Tissue Engineering and Regenerative Medicine* **2,** 296–304 (2008).

190. Chen, A. X., Hoffman, M. D., Chen, C. S., Shubin, A. D., Reynolds, D. S. & Benoit, D. S. W. Disruption of cell-cell contact-mediated notch signaling via hydrogel encapsulation reduces mesenchymal stem cell chondrogenic potential. *Journal of Biomedical Materials Research. Part A* **103,** 1291–1302 (2014).

191. Staines, K. A., Macrae, V. E. & Farquharson, C. Cartilage development and degeneration: a Wnt Wnt situation. *Cell Biochemistry and Function* **30,** 633–642 (2012).

192. Hwang, N. S., Varghese, S., Lee, H. J., Theprungsirikul, P., Canver, A., Sharma, B. & Elisseeff, J. Response of zonal chondrocytes to extracellular matrix-hydrogels. *FEBS Letters* **581,** 4172–4178 (2007).

193. Schuurman, W., Gawlitta, D., Klein, T. J., ten Hoope, W., van Rijen, M. H. P., Dhert, W. J. A., van Weeren, P. R. & Malda, J. Zonal chondrocyte subpopulations reacquire zone-specific characteristics during in vitro redifferentiation. *The American Journal of Sports Medicine* **37,** 97S–104S (2009).

194. Nguyen, L. H., Kudva, A. K., Guckert, N. L., Linse, K. D. & Roy, K. Unique biomaterial compositions direct bone marrow stem cells into specific chondrocytic phenotypes corresponding to the various zones of articular cartilage. *Biomaterials* **32,** 1327–1338 (2011).

195. Thorpe, S. D., Nagel, T., Carroll, S. F. & Kelly, D. J. Modulating gradients in regulatory signals within mesenchymal stem cell seeded hydrogels: a novel strategy to engineer zonal articular cartilage. *PLOS ONE* **8,** e60764 (2013).

196. Di Luca, A., Szlazak, K., Lorenzo-Moldero, I., Ghebes, C. A., Lepedda, A., Swieszkowski, W., Van Blitterswijk, C. & Moroni, L. Influencing chondrogenic differentiation of human mesenchymal stromal cells in scaffolds displaying a structural gradient in pore size. *Acta Biomaterialia* **36,** 210–219 (2016).

197. Moeinzadeh, S., Pajoum Shariati, S. R. & Jabbari, E. Comparative effect of physicomechanical and biomolecular cues on zone-specific chondrogenic differentiation of mesenchymal stem cells. *Biomaterials* **92,** 57–70 (2016).

198. Zhu, D., Tong, X., Trinh, P. & Yang, F. Mimicking cartilage tissue zonal organization by engineering tissue-scale gradient hydrogels as 3D cell niche. *Tissue Engineering. Part A* **94305,** ten.TEA.2016.0453 (2017).

199. Wu, L., Leijten, J. C., Georgi, N., Post, J. N., van Blitterswijk, C. A. & Karperien, M. Trophic effects of mesenchymal stem cells increase chondrocyte proliferation and matrix formation. *Tissue Engineering. Part A* **17,** 1425–1436 (2011).

200. Wu, L., Prins, H.-J., Helder, M. N., van Blitterswijk, C. A. & Karperien, M. Trophic Effects of Mesenchymal Stem Cells in Chondrocyte Co-Cultures are Independent of Culture Conditions and Cell Sources. *Tissue Engineering Part A* **18,** 1542–1551 (2012).

201. Nazempour, A. & Van Wie, B. J. Chondrocytes, mesenchymal stem cells, and their combination in articular cartilage regenerative medicine. *Annals of Biomedical Engineering* **44,** 1325–1354 (2016).

202. Glyn-Jones, S., Palmer, A. J. R., Agricola, R., Price, A. J., Vincent, T. L., Weinans, H. & Carr, A. J. Osteoarthritis. *The Lancet* **386,** 376–387 (2015).

203. Woolf, A. D. & Pfleger, B. Burden of major musculoskeletal conditions. *Bulletin of the World Health Organization* **81,** 646–656 (2003).

204. Stichler, S., Jungst, T., Schamel, M., Zilkowski, I., Kuhlmann, M., Böck, T., Blunk, T., Teßmar, J. & Groll, J. Thiol-ene clickable poly(glycidol) hydrogels for biofabrication. *Annals of Biomedical Engineering* **45,** 273–285 (2017).

205. Groll, J., Boland, T., Blunk, T., Burdick, J. A., Cho, D.-W., Dalton, P. D., Derby, B., Forgacs, G., Li, Q., Mironov, V. A., Moroni, L., Nakamura, M., Shu, W., Takeuchi, S., Vozzi, G., Woodfield, T. B. F., Xu, T., Yoo, J. J. & Malda, J. Biofabrication: reappraising the definition of an evolving field. *Biofabrication* **8,** 013001 (2016).

206. Daly, A. C., Critchley, S. E., Rencsok, E. M. & Kelly, D. J. A comparison of different bioinks for 3D bioprinting of fibrocartilage and hyaline cartilage. *Biofabrication* **8,** 045002 (2016).

207. Shim, J.-H., Jang, K.-M., Hahn, S. K., Park, J. Y., Jung, H., Oh, K., Park, K. M., Yeom, J., Park, S. H., Kim, S. W., Wang, J. H., Kim, K. & Cho, D.-W. Three-dimensional bioprinting of multilayered constructs containing human mesenchymal stromal cells for osteochondral tissue regeneration in the rabbit knee joint. *Biofabrication* **8,** 014102 (2016).

208. O'Connell, C. D., Di Bella, C., Thompson, F., Augustine, C., Beirne, S., Cornock, R., Richards, C. J., Chung, J., Gambhir, S., Yue, Z., Bourke, J., Zhang, B., Taylor, A., Quigley, A., Kapsa, R., Choong, P. & Wallace, G. G. Development of the Biopen: a handheld device for surgical printing of adipose stem cells at a chondral wound site. *Biofabrication* **8,** 015019 (2016).

209. Mouser, V. H. M., Abbadessa, A., Levato, R., Hennink, W. E., Vermonden, T., Gawlitta, D. & Malda, J. Development of a thermosensitive HAMA-containing bio-ink for the fabrication of composite cartilage repair constructs. *Biofabrication* **9,** 015026 (2017).

Part VI

Appendix

Appendix

A.1 Abbreviations

2D	Two-dimensional
3D	Three-dimensional
ACAN	Aggrecan
ACI	Autologous chondrocyte implantation
ANOVA	Analysis of variance
APS	Ammonium persulfate
ASC	Adipose-derived stem cell
ALK-5	TGF-β receptor 1
bFGF	Basic fibroblast growth factor (FGF-2)
BMP	Bone morphogenetic protein
BMSC	Bone marrow-derrived mesenchymal stem cell
BCA	Bicinchoninic acid
BSA	Bovine serum albumin
Calcein-AM	Calcein acetoxymethyl ester
CD	Cluster of differentiation
cDNA	Copy/complementary deoxyribonucleic acid
CMP/PEODA	Collagen mimetic peptide-conjugated poly(ethylene oxide) diacrylate
Col I	Collagen type I
Col II	Collagen type II
Col X	Collagen type X
CS	Chondroitin sulphate
DAB	p-dimethylamino-benzaldehyde
DAPI	4',6-diamidino-2-phenylindole
DMEM	Dulbecco's Modified Eagle's Medium

DMEM/F-12	Dulbecco's Modified Eagle's Medium/Ham's F-12
DMMB	Dimethylmethylene blue
DMSO	Dimethyl sulfoxide
DNA	Deoxyribonucleic acid
ECM	Extracellular matrix
EDTA	Ethylenediaminetetraacetic acid
EGF	Epidermal growth factor
ERK	Extracellular signal-regulated kinase
EthD	Ethidium homodimer III
FBS	Fetal bovine serum
FGF	Fibroblast growth factor
FGF-2	Fibroblastic growth factor-2
GAG	Gylcosaminoglycan
GAPDH	Glyceraldehyde-3-phosphate dehydrogenase
GDF	Growth differentiation factor
GTP	Guanosine-5'-triphosphate
HA	Hyaluronic acid
HA-SH	thiolated/thiol-modified hyaluronic acid
HEPES	4-(2-hydroxyethyl)-1-piperazineethanesulfonic
HRP	Horseradish peroxidase
IGF	Insulin-like growth factor
IHC	Immunohistochemistry
ITS	Insulin, transferin, selenium
JNK	C-Jun N-terminal kinases
KS	Keratan sulphate
MACI	Matrix-induced autologous chondrocyte implantation
MAPKs	Mitogen-activated protein kinases
MeHA	Methacrylated hyaluronic acid
MMP	Matrix metalloproteinase
mRNA	Messenger ribonucleic acid
MSC	Mesenchymal stromal/stem cells
OA	Osteoarthritis
P2	Second passage cells
P3	Third passage cells
P(AGE/G)	Allyl-modified poly(glycidol)
PBS	Phosphate-buffered saline

PBT	Poly(butylene terephthalate)
PEG	Poly(ethylene glycol)
PEGDA	Poly(ethylene glycol) diacrylate
PEGTA	Poly(ethylene glycol) tetraacrylate
PEGDM	Poly(ethylene glycol) dimethacrylate
PEOT	Poly(ethylene oxideterephthalate)
PG	Poly(glycidol)
PG-Acr	Poly(glycidol)-acrylate
PG-SH	thiolated/thiol-modified poly(glycidol)
PHEMA	Poly(2-hydroxyethyl methacrylate)
PHPMA	Poly(2-hydroxypropyl methacrylate)
PI3K	Phosphatidylinositol 3 kinase
PMMA	Poly(methyl methacrylate)
PNIPAm	Poly(nisopropylacrylamide)
PS	Penicillin-streptomycin
PVA	Poly(vinyl alcohol)
qRT-PCR	Quantitative real-time polymerase chain reaction
RNA	Ribonucleic acid
rpm	Revolutions per minute
RT	Room temperature
SD	Standard deviation
SDS-PAGE	Sodium dodecyl sulfate polyacrylamide gel electrophoresis
SEM	Scanning electron microscopy
Sox9	Sex determining region Y-box 9
TEMED	Tetramethylethylenediamine
TGF-β1	Transforming growth factor beta 1
TGF-β	Transforming growth factor beta
TNF-α	Tumor necrosis factor alpha
TRIS	Tris(hydroxymethyl)aminomethan
UV	Ultraviolet
VEGF	Vascular endothelial growth factor
WB	Western blot

A.2 Curriculum Vitae

A.3 Publications and Conference Contributions

Journal Articles

1. Stichler, S., Jungst, T., Schamel, M., Zilkowski, I., Kuhlmann, M., **Böck, T.**, Blunk, T., Tessmar, J., Groll, J. Thiol-ene clickable poly(glycidol) hydrogels for biofabrication. Annals of Biomedical Engineering **1**, 273-285. ISSN: 0090-6964 (2017).

2. Bertlein, S., Brown, G., Lim, K.S., Jungst, T., **Böck, T.**, Blunk, T., Tessmar, J., Hooper, G., Woodfield, T.B.F., Groll, J., Thiol-ene clickable gelatin as platform bioink for 3D bioprinting and digital light processing. Submitted to Advanced Materials.

3. Stichler, S.*, **Böck, T.***, Paxton, N., Bertlein, S., Levato, R., Schill, V., Smolan, W., Malda, J., Tessmar, J., Blunk, T., Groll, J., Double printing of hyaluronic acid / poly(glycidol) hybrid hydrogels for cartilage regeneration. *Equally contributing authors. Submitted to Biofabrication.

4. **Böck, T.***, Schill, V.*, Krähnke, M., Tessmar, J., Blunk, T.$^{+}$, Groll, J.$^{+}$, TGF-β1-modified hyaluronic acid / poly(glycidol) hydrogels for chondrogenic differentiation of human mesenchymal stromal cells. *Equally contributing authors, $^{+}$corresponding authors. To be submitted to Macromolecular Bioscience.

Oral Presentations

1. **Böck, T.**, Schill, V., Stichler, S., Krähnke, M., Steinert, A., Tessmar, J., Blunk, T., Groll, J. Chondromimetic polyglycidol-based hydrogels for MSC chondrogenesis. 4th International Conference Strategies in Tissue Engineering 2015, Würzburg, Germany.

2. **Böck, T.**, Schill, V., Krähnke, M., Gilbert, F., Steinert, A., Tessmar, J., Blunk, T., Groll, J. Maßgeschneiderte biomimetische und bioaktive Hydrogele für die Knorpelregeneration mit mesenchymalen Stammzellen. Deutscher Kongresses für Orthopädie und Unfallchirurgie (DKOU) 2014, Berlin, Germany.

3. **Böck, T.**, Schill, V., Krähnke, M., Steinert, A. Tessmar, J., Blunk, T., Groll, J. Tailored hyaluronic acid-based hydrogels for cartilage regeneration. 11th World Congress of the International Cartilage Repair Society (ICRS) 2013, Izmir, Turkey.

Poster Presentations

1. **Böck, T.**, Schill, V., Stichler, S., Krähnke, M., Steinert, A., Tessmar, J., Blunk, T., Groll, J. Chondromimetic peptide- and growth factor-modified polyglycidol-based hydrogels for MSC chondrogenesis. PO11-633. Deutscher Kongresses für Orthopädie und Unfallchirurgie (DKOU) 2015, Berlin, Germany.

2. Krähnke M., **Böck T.**, Meffert R., Blunk T. Impact of hypoxia on extracellular matrix-modulating enzymes during chondrogenesis of bone marrow-derived stromal cells. 19. Chirurgische Forschungstage der Deutschen Gesellschaft für Orthopädie und Unfallchirurgie (DGOU) 2015, Würzburg, Germany.

3. Schill, V., Stichler, S., **Böck, T.**, Teßmar, J., Blunk, T., Groll J., Polyglycidol/hyaluronic acid based hydrogels. P020. 4th International Conference Strategies in Tissue Engineering 2015, Würzburg, Germany.

4. Schill, V., **Böck, T.**, Teßmar, J., Blunk, T., Groll J., Polyglycidol/Hyaluronsäure-basierte Hydrogele für das Tissue Engineering. P64. Jahrestagung der Deutschen Gesellschaft für Biomaterialien (DGBM) 2015, Freiburg, Germany.

5. **Böck, T.**, Schill, V., Stichler, S., Krähnke, M., Steinert, A., Tessmar, J., Blunk, T., Groll, J. Versatile polyglycidol-based hydrogel platform for MSC chondrogenesis. P53. 12th World Congress of the International Cartilage Repair Society (ICRS) 2015, Chicago, United States of America.

6. Krähnke, M., Heusler, E., **Böck, T.**, Blunk, T., Meinel, L. Multifunktionale osteochondrale Implantate - Chondrogene und osteogene Differenzierung von mesenchymalen Stammzellen in biphasischen Seidenfibroin-Implantaten. Deutscher Kongresses für Orthopädie und Unfallchirurgie (DKOU) 2014, Berlin, Germany.

7. **Böck, T.**, Schill, V., Krähnke, M., Gilbert, F., Steinert, A., Tessmar, J., Blunk, T., Groll, J. Biomimetic hyaluronic acid-based hydrogels for cartilage regeneration. Eureka - 9th International Symposium organized by the students of the GSLS 2014, Würzburg, Germany.

8. **Böck, T.**, Schill, V., Krähnke, M., Gilbert, F., Steinert, A., Tessmar, J., Blunk, T., Groll, J. Tailored hyaluronic acid-based hydrogels with varying crosslinker concentration for cartilage regeneration – chondrogenic differentiation of mesenchymal stem cells. PP-358. World Conference on Regenerative Medicine 2013, Leipzig, Germany.

9. Krähnke, M., Heusler, E., **Böck, T.**, Blunk, T., Meinel, L. Towards engineering osteochondral implants – chondrogenic and osteogenic differentiation of mesenchymal stem cells in silk fibroin scaffolds. PP-066. World Conference on Regenerative Medicine 2013, Leipzig, Germany.

A.4 Acknowledgments

An erster Stelle möchte ich mich ganz besonders herzlich bei Herrn Prof. Dr. Torsten Blunk dafür bedanken, dass er mir die Möglichkeit gab, meine Doktorarbeit in seiner Arbeitsgruppe anzufertigen. Bei Fragen und Problemen hatte er stets ein offenes Ohr, er nahm sich gerne die Zeit für Gespräche und vermittelte mir in fachlichen Diskussionen viele interessante Aspekte. Mit Gesprächen über die aktuellen Geschehnisse rund um den Fußball sorgte er in Mittagspausen aber auch für Ablenkung vom Laboralltag. Außerdem möchte ich mich bei ihm dafür bedanken, dass er es mir ermöglichte an zahlreichen wissenschaftlichen Konferenzen und Meetings teilzunehmen und ich dadurch viele wertvolle Eindrücke gewinnen konnte.

Bei Herrn Prof. Dr. Rainer Meffert bedanke ich mich für die freundliche Aufnahme in seiner Klinik.

Herrn Prof. Dr. Norbert Schütze danke ich für die Betreuung meiner Arbeit als Zweitgutachter.

Herrn Dr. Jörg Teßmar danke ich für die Bereitschaft als Gutachter in meinem Promotionskomitee zur Verfügung zu stehen. Ganz besonders möchte ich mich aber für seine Hilfsbereitschaft und die Unterstützung bei der Erstellung meiner Arbeit bedanken.

Herrn Prof. Dr. Thomas Dandekar danke ich für die Bereitschaft zum Prüfungsvorsitz.

Dem IZKF Würzburg danke ich für die Förderung des Projektes, die mir die Promotion im Labor der Unfallchirurgie erst ermöglichte.

Bei Herrn Prof. Dr. Jürgen Groll möchte ich mich für die enge und intensive Kooperation mit seinem Lehrstuhl (FMZ), sowie für das Bereitstellen der an seinem Institut entwickelten Materialien bedanken. Darüber hinaus danke ich ihm für die Möglichkeit an dem EU-Projekt HydroZONES mitzuwirken, wodurch ich wertvolle Erfahrungen in einem internationalen Forschungsprojekt sammeln konnte.

Simone Stichler und Verena Schill danke ich für die gute Zusammenarbeit, das Bereitstellen ihrer synthetisierten Materialien und für ihre Geduld und Hilfe bei den chemischen Fragen eines Biologen.

Ganz besonders möchte ich mich natürlich bei meinen Mitstreitern im Labor und Büro für die hervorragende Stimmung und Unterstützung während meiner Doktorarbeit bedanken. Martin ist nicht nur der beste Zimmerpartner auf Konferenzreisen, den man sich vorstellen kann, sondern auch sonst immer zur Stelle, wenn man ihn braucht. Sei es beim Kung Fu oder nur um meinen musikalischen Horizont zu erweitern. Vielen Dank für die gemeinsame Zeit! Nane, Miri und Oli danke ich ganz besonders herzlich für ihre Unterstützung und für die vielen schönen und lustigen Momente in und abseits des Labors. Es war wirklich immer schön mit euch! Rasmus und Wiebke danke ich für die angenehme und freundschaftliche Zusammenarbeit bei uns im Labor.

Ein großes Dankeschön geht an Katha: Für die schöne Zeit zusammen im Labor und auch außerhalb, aber auch für deine Ratschläge und Korrekturen während des Schreibens dieser Arbeit.

Bei Sabine Müller-Morath möchte ich mich ganz besonders für ihre stete und wertvolle Unterstützung im Labor bedanken.

Renate Wahn danke ich für die freundliche und gute Labornachbarschaft und die willkommenen Einladungen zur Espressopause.

Allen anderen nicht namentlich genannten Mitarbeitern des Labors und der Klinik danke ich für ihre Hilfsbereitschaft und das angenehme Arbeitsklima.

Dem Sekretariat um Melanie Riechwald, Juliane Neumann und Brigitte Hofmann danke ich für ihre Hilfe bei allen organisatorischen Angelegenheiten.

Zuletzt möchte ich meiner Familie und meinen Freunden von ganzem Herzen für ihre Unterstützung danken. Mein besonderer Dank gilt dabei Lena, die mich immer wieder motivierte, für die nötige Ablenkung außerhalb des Labors sorgte und auch sonst einfach die beste Freundin ist, die man sich vorstellen kann.

A.5 Affidavit

I hereby confirm that my thesis entitled *Multifunctional Hyaluronic Acid / Poly(glycidol) Hydrogels for Cartilage Regeneration Using Mesenchymal Stromal Cells* is the result of my own work. I did not receive any help or support from commercial consultants. All sources and/or materials applied are listed and specified in the thesis.

Furthermore, I confirm that this thesis has not yet been submitted as part of another examination process neither in identical nor in similar form.

Place, Date	Signature

A.6 Eidesstattliche Erklärung

Hiermit erkläre ich an Eides statt, die Dissertation *Multifunktionale Hyaluronsäure / Poly(glycidol) Hydrogele für die Knorpelregeneration mit Mesenchymalen Stromazellen* eigenständig, d.h. insbesondere selbständig und ohne Hilfe eines kommerziellen Promotionsberaters, angefertigt und keine anderen als die von mir angegebenen Quellen und Hilfsmittel verwendet zu haben.

Ich erkläre außerdem, dass die Dissertation weder in gleicher noch in ähnlicher Form bereits in einem anderen Prüfungsverfahren vorgelegen hat.

Ort, Datum	Unterschrift